A REVIEW OF SOUTHERN AFRICAN KIMBERLITES AND EXPLORATION TECHNIQUES

by

Louis Johannes Venter

B.Sc. (Hons.) (RAU)

A dissertation submitted in partial fulfilment of the requirements for the degree of

MASTER OF SCIENCE

(Exploration Geology)

in the Department of Geology, Rhodes University,

P.O. Box 94, Grahamstown, 6140,

South Africa,

December 1998

ABSTRACT

The dissertation reviews the present knowledge regarding diamonds, from its formation in the lithospheric upper mantle at depths between 150 and 300 km, to its final valuation in terms of US$/carat by diamantaires in London, Antwerp, Tel Aviv and New York. The dissertation is divided into two complimentary sections.

Section one focuses on the formation, emplacement, occurrence and characteristics of kimberlites and, when present, their associated trace amounts of diamonds. The section follows a logical sequence from the regional tectonic-, local structural- and geodynamic controls on kimberlite formation and emplacement to the characteristics of individual kimberlite morphology, mineralogy, petrography and geochemistry. Finally, the environment of diamond formation, resorption and the characteristics that have led to the marketability of diamonds are discussed.

Section two reviews the current exploration techniques used in locating diamondiferous kimberlites and the subsequent economic evaluation of these kimberlites. A brief history of known Southern African kimberlite occurrences, grades, tonnages, tectonic settings, ages and regional structural controls is given. The prospective countries mentioned are Angola, Botswana, Lesotho, South Africa, Swaziland, Tanzania and Zimbabwe.

Exploration techniques considered are ; the application of a landscape analysis and investigation of the surface processes active in a given area, indicator mineral sampling (with reference to their mineralogy and exploration significance), remote sensing techniques (subdivided into satellite imagery and aerial photography), geophysical techniques (including the magnetic-, gravity-, electrical-, radiometric- and seismic methods as well as heat flow models), geochemical techniques, petrographic- and electron beam techniques as well as geobotanical- and geobiological techniques.

Finally, a brief summary of current evaluation techniques employed on diamondiferous kimberlite deposits is presented. The review covers kimberlite sampling methods, sample processing, diamond grade distributions (with reference to the experimental variogram model, statistical methods used in grade distribution calculations as well as block definition and local grade estimation). Stone size distributions, including microdiamond counts and value estimation, are also discussed.

ACKNOWLEDGEMENTS

I would like to express my gratitude to Gold Fields of South Africa Limited for financial assistance towards the Master's degree. I also thank my fellow colleagues for their dedication and hard work as it influenced and motivated me during the two years. The Council for Geoscience have also been accommodating during the last few months of the course, which is appreciated. Thanks to H.L. Doig, R. Esterhuizen, D.M. Erasmus and S.J. Hill who proof read all, or some parts, of the dissertation with some constructive comments thereon. I thank my family and friends for their support and encouragement during the time. After two years of labour my view on the subject of geology is aptly described by Jerome K. Jerome (with apology). " What I want is rest. Rest and a complete change. The overstrain upon my brain has produced a general depression throughout the system. Change of scene, and absence of the necessity of thought, will restore the mental equilibrium". I hope.

CONTENTS Page

CONTENTS Page

CONTENTS Page

CONTENTS Page

LIST OF FIGURES

LIST OF FIGURES

LIST OF FIGURES

LIST OF TABLES

APPENDICES

Appendix I ; Diamond descriptions.

Appendix II ; Indicator mineral descriptions.

1. Southern African kimberlites.

1.1. Introduction.

Diamonds are recovered from primary kimberlite and lamproite deposits and their erosional colluvial-, eluvial-, alluvial- and marine placer derivatives. The search for diamonds in Southern Africa is mainly focused on kimberlite exploration with subordinate alluvial- and marine placer exploration. Kimberlite pipes and fissures account for 60% of the world's diamond production by value (Oldenziel, 1997), therefore primary deposits that have the potential for long-lived and large-scale mining are attractive exploration targets (Levinson *et al.*, 1992). Jennings (1995) argues that a kimberlite diamond mine can be very profitable with annual revenues possibly exceeding a billion dollars and, *in situ* reserves worth as much as US$ 50 billion. Significant discoveries in Southern Africa have been large primary deposits that could be turned into long-term mines with secure and consistent production (Atkinson, 1989). As only 2% of all discovered kimberlite occurrences in Southern Africa have ever been economic it remains a high risk exploration commodity.

Diamond exploration depends on adequate and long-term finance and exploration persistence, coupled with technical expertise in diamond exploration techniques, including heavy mineral sampling and processing, interpretation of indicator mineral chemistry, geotectonic-, structural-, geophysical-, petrographical- and geochemical knowledge of kimberlites (Jennings, 1995). For the purposes of this dissertation only kimberlite exploration will be considered as the writer believes that the potential for locating large, economic primary deposits in Southern Africa remains significant. The Southern African countries considered are Angola, Botswana, Lesotho, South Africa, Swaziland, Tanzania, and Zimbabwe. These countries were selected because they occur over on-craton positions, distinguished by stable and cool Archaean crust, which is a fundamental requirement in kimberlite exploration.

1.2. Regions identified as Archaean cratons (Archons).

Diamondiferous kimberlites are confined to regions of Precambrian, preferably Archaean, cratons, in other words regions that have continental crust older than 2500 Ma (Fig.1), (Clifford, 1966).

Cratons are extensive, stable continental areas comprising a shield, or exposed core of a craton, and overlying platform sequences mostly consisting of sediments and, in places, associated volcanics. Cratons are characterised by thick lithospheric crust and low geothermal gradients and provide the source area for diamondiferous mantle material. In North America seismic tomography has been used to establish the location of these Archaean crustal rocks. The roots of cratons are characterised by high shear wave velocities because of the less dense material and cooler temperatures compared to the juxtaposed asthenosphere (Helmstaedt & Gurney, 1995).

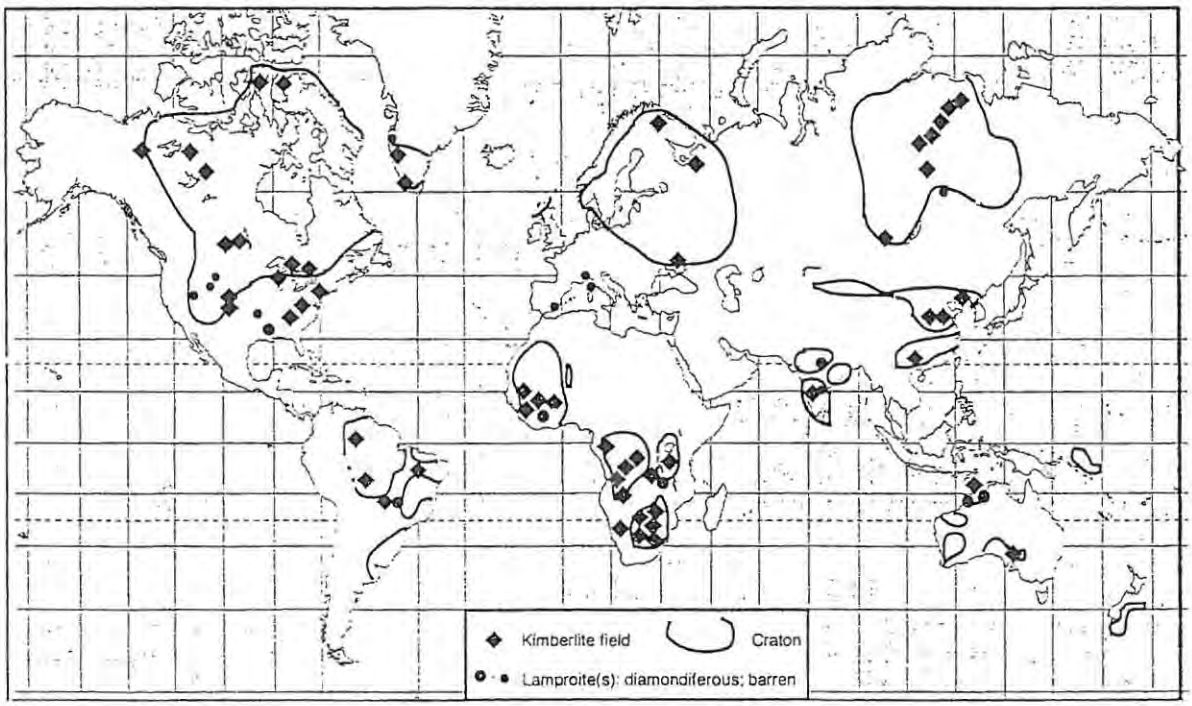

Fig. 1 ; World-wide Archaean cratonic areas and associated diamondiferous kimberlites and lamproites, from Nixon (1995).

The Kalahari-, Tanzanian- and Central African cratons form the cornerstones of Southern African geology (Fig.2). The Kalahari craton consists of two Archaean nuclei, the Kaapvaal and Zimbabwe cratons, which are seperated by the Archaean Limpopo Mobile Belt (LMB). As the LMB was initiated in the Middle to Late Archaean (at about 3000 Ma), and stabilised by 2500 Ma, it prompted the acceptance of the term Kalahari craton (Light, 1982).

The Kalahari craton underlies most of Zimbabwe, the central and northern part of South Africa, Lesotho, Swaziland and eastern Botswana. The Tanzanian craton underlies northwestern Tanzania and the southern parts of Kenya and Uganda. The Central African craton underlies most of Angola and the southern and central parts of Gabon, Cameroon and the Democratic Republic of the Congo.

Haggerty (1986) and Helmstaedt & Gurney (1995) suggest that diamonds form and are preserved where refractive, relatively cool and reduced, low-density lithospheric roots have remained insulated against reheating and tectonic reworking during plate motion. These lithospheric roots, predominantly peridotitic, are marked by convex downward-deflected isotherms and a corresponding convex upward expansion of the diamond stability field (Fig.3a and 3b).

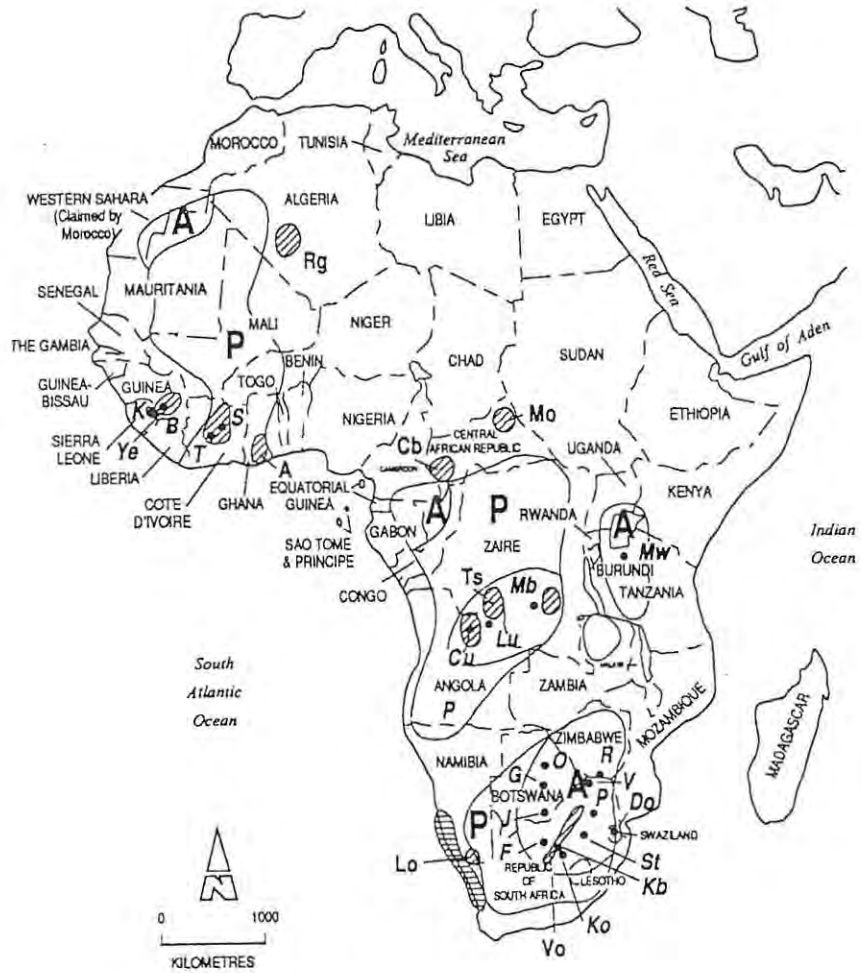

Fig. 2 ; The African cratons with associated kimberlite, alluvial- and marine placer occurrences. (A) Akwatia/ Birrim, Ghana, (B) Banankoro, Guinea, (Cb) Carnot/Berberati, Central African Republic, (Cu) Cuango, Angola, (Do) Dokolwayo, Swaziland, (F) Finsch, South Africa, (G) Gope, Botswana, (J) Jwaneng, Botswana, (Kb) Kimberley, South Africa, (Ko) Kofficfontein, South Africa, (Lo) Lower Orange River, South Africa/Namibia, (Lu) Luanda, Angola, (Mb) Mbuji Maye, Zaire, (Mo) Mokka Quada, Central African Republic, (Mw) Mwadui, Tanzania, (O) Orapa, Botswana, (P) Premier, South Africa, (R) River Ranch, Zimbabwe, (Rg) Reggan, Algeria, (S) Seguela, Ivory Coast, (St) Star, South Africa, (T) Tortiya, Ivory Coast, (Ts) Tsikapa, Zaire, (V) Venetia, South Africa, (Vo) Vaal/Orange Rivers, South Africa, (Ye) Yengema, Sierra Leone, from Janse & Sheahan (1995).

In the model proposed by Helmstaedt & Gurney (1995) a distinction is made between "mantle-root-friendly" structures (for example horizontally intruded dyke swarms and thin-skinned thrust belts), and "mantle-root-destructive" structures (for example mantle plumes, rifts and collision zones). The diamond potential of an area is thus complimented by mantle-root-friendly structures.

(a)

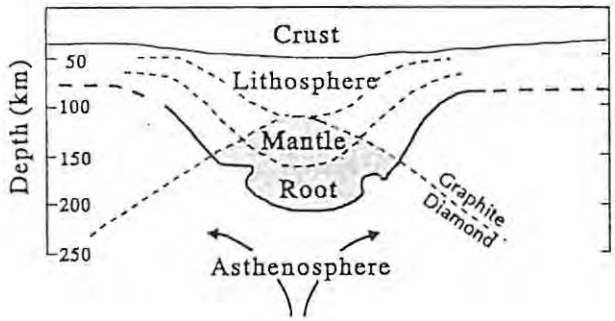

(b)

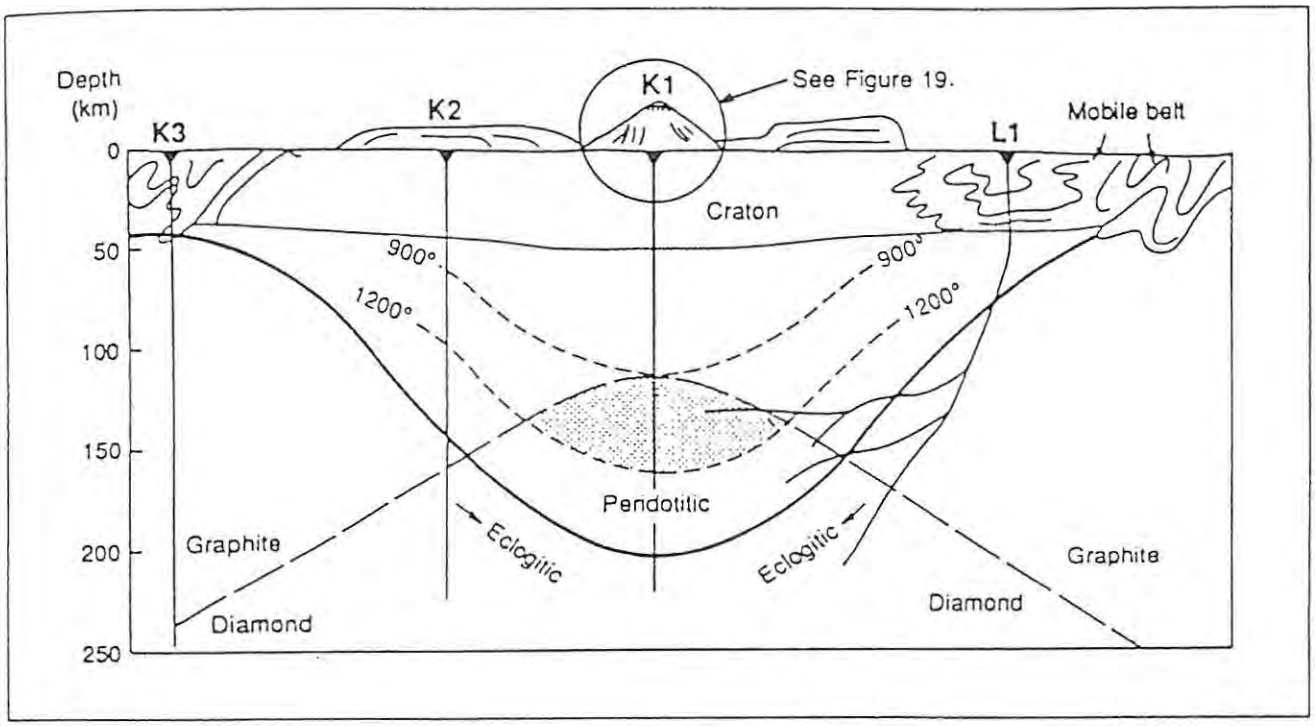

Fig. 3 ; (a) Simplified model of a diamondiferous lithospheric or mantle root, showing the positions of the lithosphere, mantle, mantle root and asthenosphere (after Haggerty, 1986), from Helmstaedt & Gurney (1995). (b) The stable carton and subcratonic areas are as much as 200 km thick (solid line) and are bounded by mobile belts. The downward deflected dashed lines are the approximate shape of the 900° and 1200°C isotherms within the root and the diamond stability field is convex upward. The K1 kimberlite pipe is likely to have P-type diamonds as it sampled diamonds from the shaded area at the keel of the craton. Pipe K2 may have E-type diamonds and pipe K3 will be barren. L1 is the possible location of lamproite pipes, from Kirkley *et al.* (1991).

Griffin & Ryan (1995) show that diamonds are only stable in the mantle above a temperature and pressure given by the intersection between the local geotherm and the diamond-graphite equilibrium, also known as the "diamond window" (Fig.4).

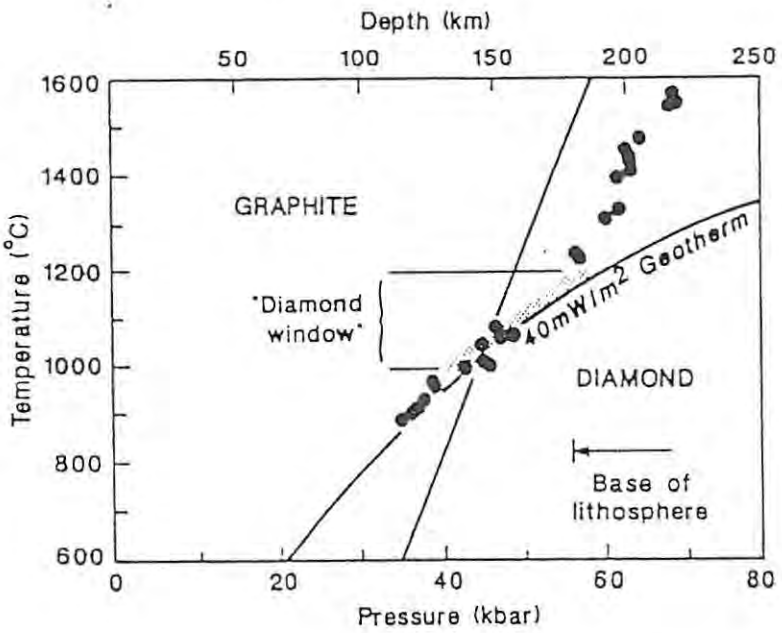

Fig. 4 ; Xenolith-derived geotherm for Northern Lesotho, showing the position of the "kink", the inferred base of the lithosphere, the diamond-graphite equilibrium and the "diamond window", from Griffin & Ryan (1995).

The diamond window is also confirmed by the chemical compositions of coexisting minerals in mineral inclusions in diamonds and mineral assemblages in diamond-bearing xenoliths. These chemical compositions suggest that most diamonds were stable at pressures corresponding to depths of 150 to 200 km and temperatures generally not exceeding 1200^0 C (Boyd & Gurney, 1986).

However, unusually high pressures, corresponding to depths of more than 300 km, were inferred from the diamonds of the Monastery kimberlite (South Africa), where inclusions of high silica (majoritic) garnets are thought to represent pyroxene solid-solution in garnets (Moore & Gurney, 1985). Most diamonds are believed to have come from the lithospheric portion of the upper mantle, though high pressure inclusions in some diamonds, such as shown by Monastery, suggest that a proportion could be derived from the asthenosphere.

The boundary between the rigid lithospheric mantle and underlying asthenospheric mantle, generally accepted as between 200 and 250 km depth, acts as a major discontinuity which seperates mechanically and chemically distinct regions of the mantle. The lithospheric mantle is depleted in basaltic components and is believed to consist of lherzolite and harzburgite, with or without the presence of spinel and garnet, as well as dunite (Table I and Fig.5).

This discontinuity is also a potential site for the underplating of subducted material. Scattered throughout this laterally and vertically heterogeneous assemblage are eclogitic rocks, which may represent basaltic magmas crystallised at high pressure or remnants of ancient subducted oceanic basaltic rocks. The asthenospheric mantle is believed to be relatively homogeneous and to consist of convecting mantle material. This material has the potential to generate mid-oceanic ridge-type basalts which are "fertile" in contrast to the "barren" lithospheric mantle (Mitchell, 1991).

Table I ; Rock nomenclature used throughout the dissertation, adapted from Kirkley *et al.* (1991) and Fipke *et al.* (1995).

ROCK TYPE	DEFINITION
Ultramafic rock	Applied to a rock with less than 42 wt.% SiO2 and predominantly composed of the ferro-magnesian minerals pyroxene and olivine. When these minerals occur together the rock is termed peridotite, but each may constitute a rock on its own - dunite (olivine) and pyroxenite (pyroxene). Refer to fig.5.
Peridotite	A class of ultramafic rocks consisting predominantly of olivine, with or without other ferromagnesian minerals. Peridotite is a general term that includes the more specific rock types dunite, hartzburgite, lherzolite and wehrlite, based on the relative proportions of olivine, orthopyroxene and clinopyroxene. Refer to fig.5.
Lherzolite	A variety of peridotite consisting predominantly of olivine, orthopyroxene and clinopyroxene. Other minor phases may be present (e.g. garnet and spinel). It is by far the dominant rock type constituting the upper mantle. Very common xenolith in kimberlite.
Pyroxenite	An ultramafic rock consisting predominantly of clino- and orthopyroxene.
Eclogite	Typically a coarse-grained bimineralic rock consisting of pyrope-almandine garnet and omphacite clinopyroxene. Accessory minerals may include rutile, kyanite, coesite, sanidine, graphite and diamond.
Glimmerite	An ultramafic rock consisting almost entirely of the micas phlogopite and/or biotite.
MARID suite	Distinctive group of nodules which are olivine-free and consist of varying proportions of mica (phlogopite), amphibole (K-richterite), rutile, ilmenite and diopside (hence the acronym MARID)

Diamond preservation over billions of years requires that the mantle be held at low oxygen fugacities for long periods of time. This is only possible by the long-term development of continental cratons. Passage of oxidised fluids of CO_2 and H_2O would result in the oxidation of diamond to CO_2 or its conversion to graphite (Mitchell, 1991). The formation and preservation of diamonds in the Archaean is demonstrated by the presence of diamonds in the Witwatersrand conglomerates. It implies that kimberlite intrusions were active, and that diamond were available for sampling, from at least 2600 Ma. Known kimberlites show a range of emplacement ages from 1180 Ma for Premier (South Africa) to 20 to 25 Ma for the Ellendale intrusions (Western Australia), (Haggerty, 1986 ; Gurney, 1989). The Archaean age of most diamonds has also been proven by isotope-dating of diamond inclusions.

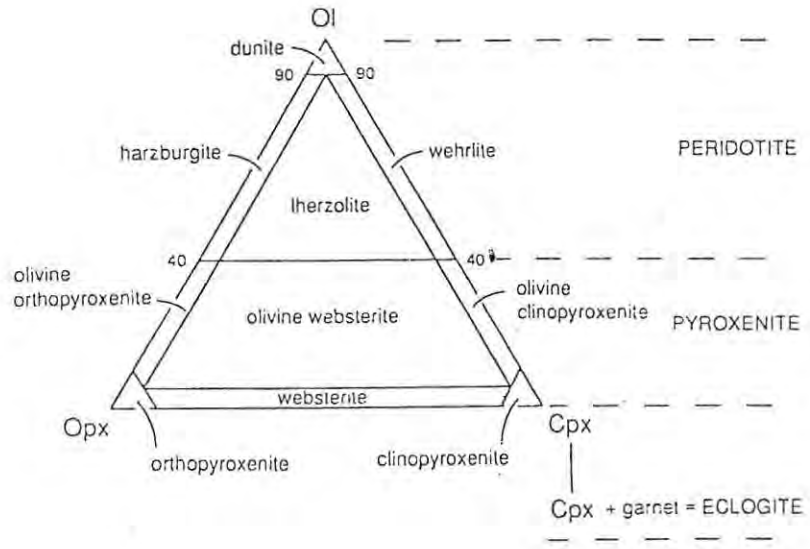

Fig. 5 ; Classification of peridotites and pyroxenites as recommended by the International Union of Geological Sciences. Modal proportions are in volume percent, from Kirkley *et al.* (1991).

1.3. Regional tectonic-, local structural- and geodynamic controls.

1.3.1. Regional tectonic controls.

Diamondiferous kimberlites are restricted to ancient Archaean cratons (Janse, 1966), whilst non-diamondiferous (barren) kimberlites occur in the adjacent mobile belts of younger Precambrian rocks. Kimberlite fields are commonly situated along linear or arcuate trends related to the presence of major crustal fracture zones or lineaments. Major regional faults, shear zones and fractures, which extend to the base of a craton, act as conduits for the ascent of mantle-derived magmas through the lower lithosphere (Mitchell, 1991).

Sedimentary cover sequences, often kilometers thick, obscure any direct structural relationship between the citing of the pipe and an underlying basement structure. These deep structures often give rise to fractures, fold warps or monoclinal flexures in the sedimentary veneer or to basement highs and arches which have been confirmed by deep crustal seismic reflection studies (White *et al.*, 1995).

The distribution of alkaline intrusives, including kimberlites, along major linear to arcuate fracture zones has been attributed to continental drift over stationary hot spots, although other geodynamic controls (refer to section 1.3.3.) have been presented by Helmstaedt (1993). Radiometric ages of kimberlites in Southern Africa show that the peak of intrusive activity occurred in the Cretaceous, which was a period of crustal extension with Africa separating from South America. Long-lived, deep-crustal continental crust lineaments, with associated fracture patterns and circular features, can be delineated by geological mapping, satellite images, aerial photographs and geophysical techniques. Transcurrent or extensional fractures, such as continental rifts or linear grabens, are the most suitable structural features (Clement & Reid, 1989).

In Angola, linear zones of alkaline intrusives, including both carbonatites and kimberlites, are related to the on-land extension of oceanic transform fracture zones (Marsh , 1973 ; Sykes, 1978). Sykes (1978) proposed that these extension fracture zones may reactivate old continental structures. An example of such an on-craton extension structure is the Lucapa Corridor in Angola (Fig.6).

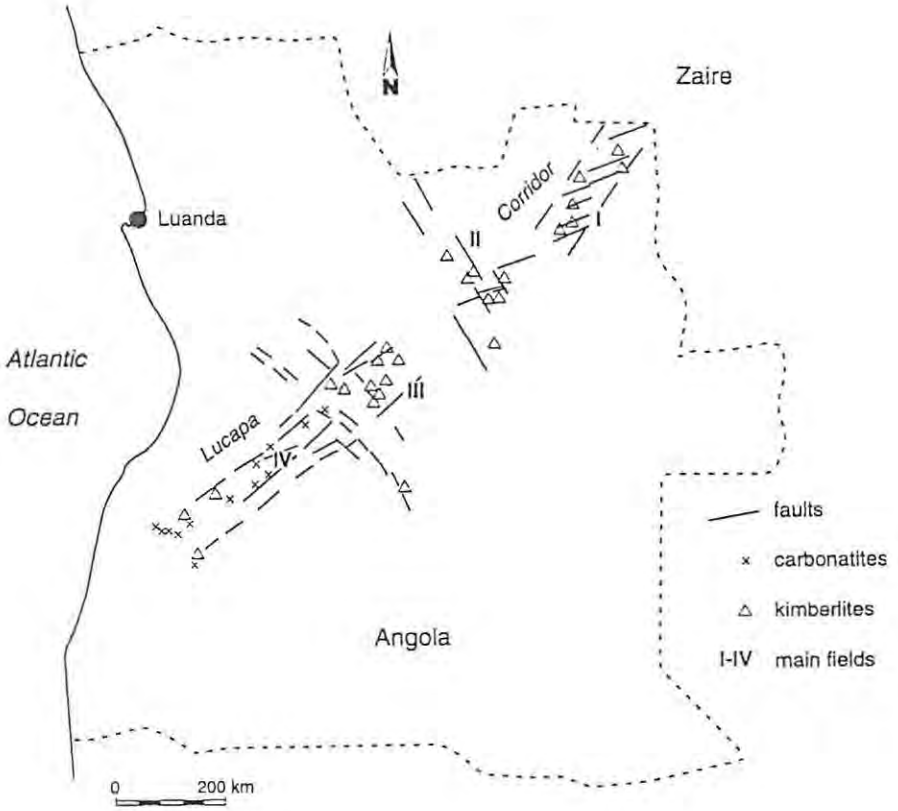

Fig. 6 ; Kimberlites and carbonatites associated with the Lucapa Corridor in Angola. The main diamond Provinces are marked I-IV (adapted from Reis, 1972 and De Boorder, 1982), from White *et al.* (1995).

Cretaceous-aged kimberlite pipes intrude over a strike length of 1600 km within the Central African craton. The basement fault and fracture corridor trends southwest to northeast and varies from 50 to 90 km in width (De Boorder, 1982). The off-craton southwest extension of the corridor links up with the transforms of the Mid Atlantic Ridge. The transform faults have dextral offsets totaling 300 km (Sykes, 1978).

Carbonatites occur on the southwestern margin of the craton. In the northeastern portion of the corridor local basement development, associated with diamondiferous kimberlites, is known as the Lucapa Graben. The intrusives appear to be associated with features in the overlying cover sediments that relate to deep seated basement structures. Four Cretaceous kimberlite provinces (I-IV) have been delineated along the structure. The province nearest to the Atlantic (IV) is mainly carbonatitic and non-diamondiferous, with the number of carbonatites increasing from Province III to IV.

On the Kaapvaal craton in South Africa two types of kimberlites have been recognised based on their isotopic and petrographic differences. The Group I and Group II kimberlites both occur within a wide northeast trending belt from Sutherland to Pretoria (Fig.7).

Group I kimberlites have a wide age-range, with important intrusions at 1600 Ma, 1200 Ma, 500 Ma and between 100 and 70 Ma. The younger Group II kimberlites intruded between 200 and 110 Ma. The successive nature of kimberlite intrusives over a wide range in time complicates the structural interpretation of kimberlites as there are at least four periods of kimberlite emplacement (White *et al.*, 1995).

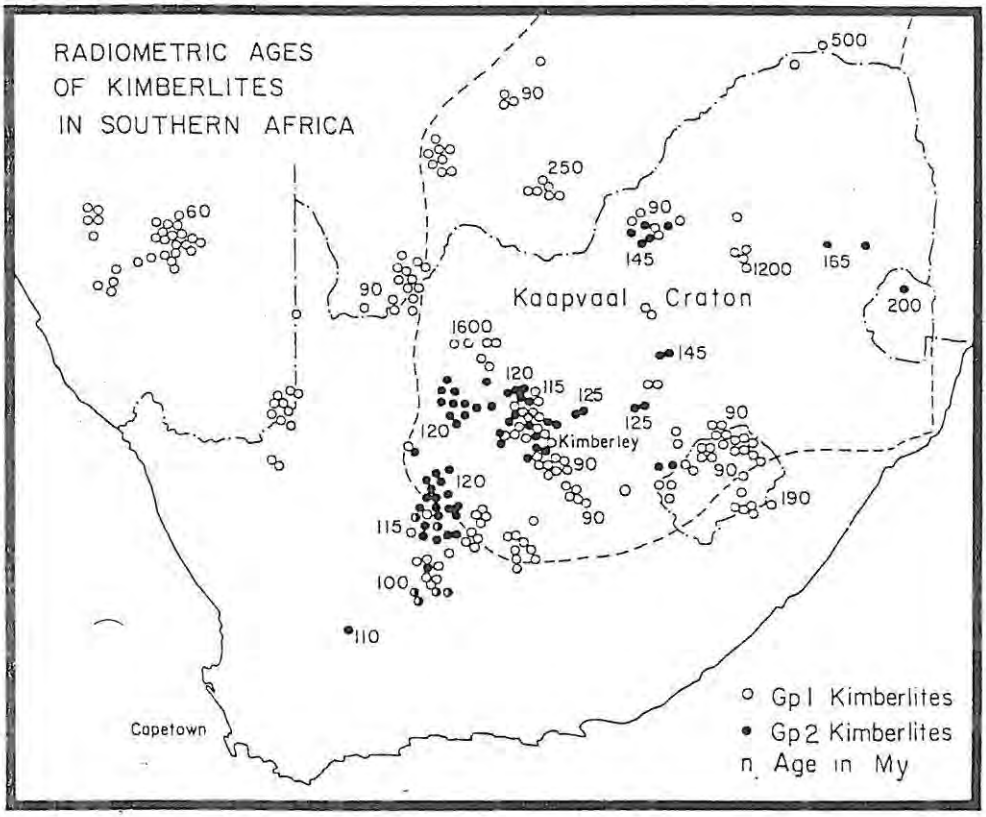

Fig. 7 ; The distribution of Group I and Group II kimberlites in Southern Africa. Note : (1) Many of the circles represent clusters of several complexes and, (2) age data for only selected occurrences are included to represent a range of ages typical of Southern African kimberlites, from Skinner (1989).

Both types of kimberlites may be diamondiferous but are restricted to the Kalahari Craton, including those at Venetia within the Archaean Limpopo Mobile Belt. Carbonatites, nephelinites, melilites and non-diamondiferous kimberlites occur off the craton, in and towards the Cape Fold Belt (White *et al.*, 1995).

The South African kimberlites follow a northeast trending zone that mirrors the trend of the Ventersdorp Graben, as proposed by Clendenin *et al.* (1988). The position and structure of the Graben was identified through gravity-, magnetic- and seismic studies. Clendenin *et al.* (1988) argue that the graben is located on a major lithospheric scale shear, corresponding to the central graben axis, that dips to the west. In this model, the kimberlites are preferentially located from the shelf area, where the basement is least affected, into the graben axis (Fig.8).

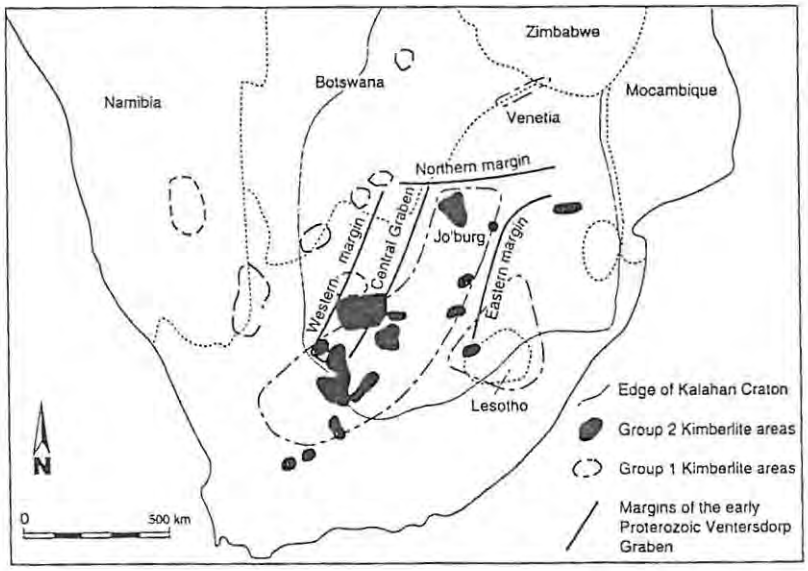

Fig. 8 ; Main kimberlite fields in South Africa in relation to the Ventersdorp Graben, with the distribution of Group I and Group II types also indicated. The transcrustal fault associated with it corresponds to the Central Graben line (based on the data from Skinner *et al.*, 1992 and Clendenin *et al.*, 1988), from White *et al.* (1995).

White *et al.* (1995) divided the important structural environments into two types, either those associated with kimberlite emplacement younger than Mesozoic age or emplacement older than Mesozoic age (Table II).

Table II ; The structural kimberlite emplacement controls based on their ages relative to the Mesozoic, adapted from White *et al.* (1995).

KIMBERLITE EMPLACEMENT	STRUCTURAL CONTROLS
Younger than Mesozoic (250 Ma)	(a) The landward extension of transform faults onto pre-existing mobile belts or basement faults and, (b) Linear grabens. Example : Angolan kimberlites.
Older than Mesozoic (250 Ma)	(a) Deep-seated basement mobile zones or fracture and fault zones and, (b) Linear grabens or aulacogens, particularly those above a deep-seated mobile zone. Example : South African kimberlites.

1.3.2. Local structural controls.

Kimberlites tend to occur in clusters, with several clusters grouped together termed a field. The number of pipes and dykes in any one cluster can vary from 1 to 50. As an example the Kimberley cluster, which has five main diamondiferous pipes that occur within a diameter of 10 km, is 40 km in diameter including the outlying dykes. The Orapa cluster, in Botswana, also shows a diameter of about 40 km. The surface expression of an individual pipe is small and rarely exceeds 1 km in diameter. Dykes are usually less than 1 m wide and occur in swarms of parallel intrusions (Janse, 1985).

In the Lucapa Corridor two important subsidiary trends other than the main northeast lineament have been identified. These are a northwest to north-northwest, and an east-northeast fault and fracture trend, respectively. The conjugate fault and fracture sets crosscut the Lucapa Corridor in four main areas, termed Provinces I, II, III and IV. The Lucapa Corridor has east-northeast inflexions which produced the main kimberlite field in northeast Angola, Province I, and part of Province IV. These areas, in which the east-northeast subsidiary structures dominate, give rise to local grabens (Reis, 1972). The Provinces I and III occur where the conjugate corridors cut the Lucapa Corridor and where the east-northeast trends are present (White *et al.*, 1995).

De Boorder (1982) presented a detailed structural analysis of Province III of the Lucapa Corridor. Fig. 9(a) is a summary of the local structural controls for kimberlites in the Lucapa Corridor. Kimberlites and carbonatites are concentrated where a north-northeast trending conjugate zone intersects the main Lucapa Corridor and produced an area of tensile fractures. The fracture pattern corresponds to the internal R-shear for a dextral sense of displacement. In both shears, the internal structure fit a Riedel geometry in which R-shears and R'-shears indicate a dextral sense of displacement, as shown in Fig.9(b).

The carbonatites have a similar relationship to the main corridors but spread to the southwest along the Lucapa Corridor. A cluster occurs where an internal conjugate crosscuts the main trend. The economic pipes are situated where the Lucapa Corridor is still within the Congo Craton boundary. As the corridor enters the Pan African West Congo Mobile Belt, Province IV, the number of kimberlites decrease and carbonatites, nepheline syenites and alkaline extrusives become predominant (White *et al.*, 1995).

Dawson (1970) noted the importance of the intersection of major fractures in the Kaapvaal Craton (South Africa) and that intersecting trends are important in Tanzania. Within cratons with no directly visible major regional mobile zone or linear graben, it is often the intersection of major fractures that form a favourable site, such as the Kalahari Craton and Tanzanian Craton. In the case of the Kalahari Craton a major regional graben structure may affect at least part of the kimberlite distribution, but sedimentary cover obscures the basement structures (White *et al.*, 1995).

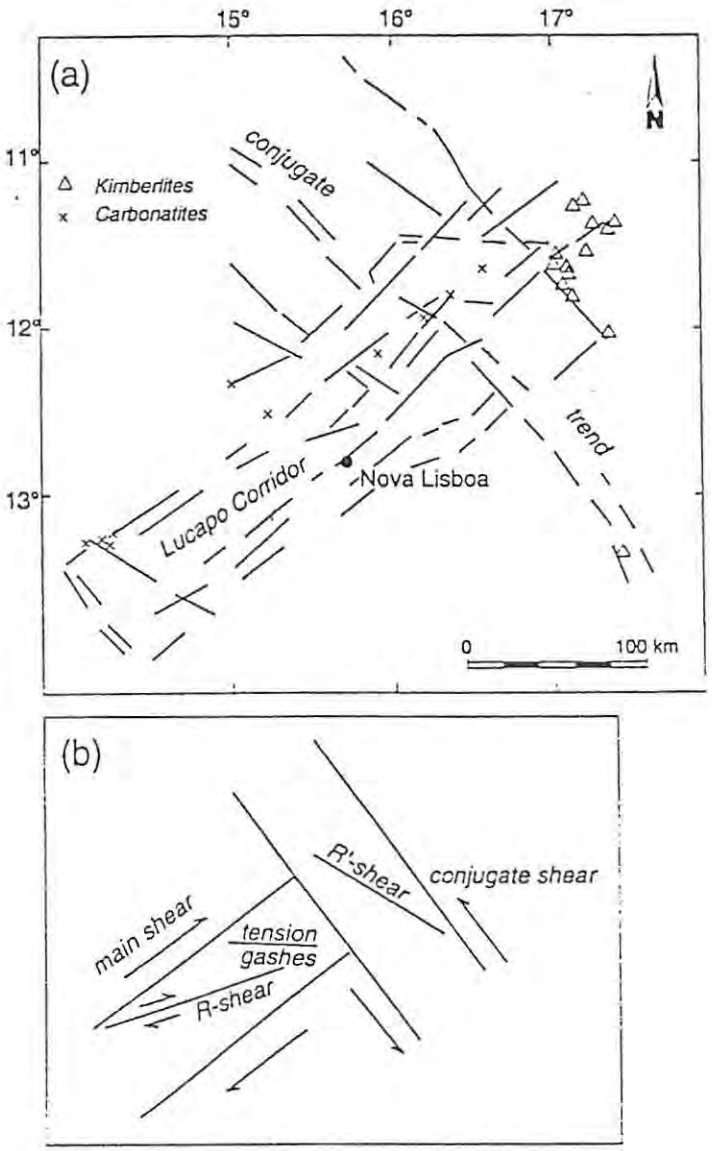

Fig. 9 ; (a) Details of the structural controls of Province III along the Lucapa Corridor, from De Boorder (1982). The kimberlites cluster where a major conjugate corridor cuts the Lucapa Corridor. A cluster of carbonatites have formed in the southwest where an internal conjugate fault has developed with in the Lucapa Corridor. (b) The internal faults show a Riedel geometry, from White *et al.* (1995).

Kimberlite emplacement in Southern Africa is attributed to uplift of the Kaapvaal Craton with attendant downwarping and faulting around its periphery. Dawson (1970) proposes that the Kimberley district lies at the intersection of northeast-southwest, northwest-southeast and east-west fracture trends (Fig.10). Foliation in basement granite-gneiss in the Kimberley area is known to trend east-west, whereas the northeast and northwest trends are inferred to correspond with deep-seated basement structures.

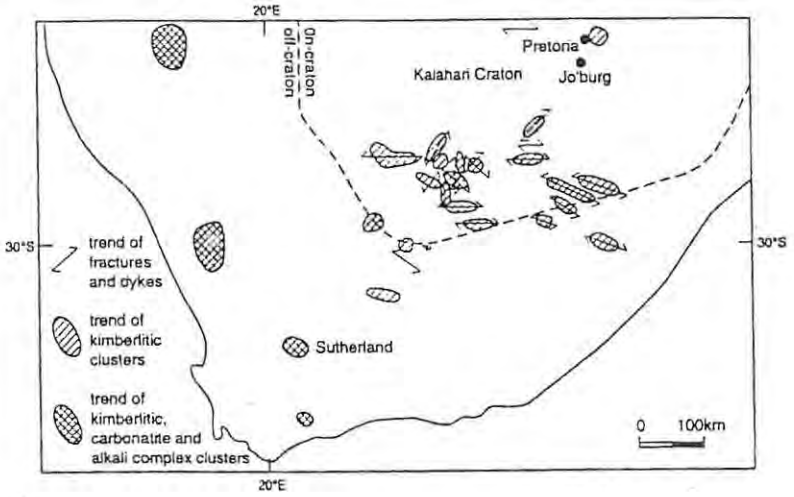

Fig. 10 ; Trends of kimberlite and carbonatite fields in South Africa along with fracture and dyke trends (based on data from Dawson, 1970), from White *et al.* (1995).

Dawson (1970) recorded that the kimberlites are associated with fractures and dykes that have the same trends. They are northeast-southwest, northwest-southeast, east-west and north-south. In addition, kimberlites outside the Sutherland-Pretoria Belt have a west-northwest to east-southeast trend. Clusters of kimberlites follow all of the above trends (White *et al.*, 1995).

Kimberlite intrusions are associated with areas of intersection of orthogonal structures, such as intersecting dyke trends. These conjugate mobile zones, fault or fracture corridors and linear grabens are characterised by major transfer zones which often extend out of the basin as old deep structures into the bordering basement. Intrusives that occur along fault corridors and mobile zones are controlled by internal and splay structures such as dilational tension gashes, R-shears or faults and internal conjugates (White *et al.*, 1995).

The association of kimberlite emplacement at intersecting fracture trends has been noted at the Kimberley pipe which lies at the intersection of northeast-soutwest and northwest-southeast dykes. The kimberlites also follow fracture or bedding trends in the Karoo sediments or the east-west foliation trend in the underlying gneisses (Dawson, 1970). Magnetic- and gravity data support the presence of northwest and northeast trending lineaments (Skinner *et al.*, 1992), which most likely reflect basement structures. Northeast trends probably reflect major basin faults within the Ventersdorp Graben and the northwest trends orthogonal transfer faults in the basement which spread outside the confines of the Graben. The conjugate fracture set within a major lineament or graben-setting reflect transcurrent and/or extensional movement favourable for kimberlite emplacement (White *et al.*, 1995).

In South Africa the kimberlites along the Ventersdorp Graben follow the trends of fractures and dykes, which often form the feeders into the pipes themselves. The dykes and fractures are parallel or orthogonal to the graben trend or follow an oblique north-south or east-west orientation (Dawson, 1970). Away from the graben they follow an east-west trend or west-northwest trend. The dykes trending parallel to the basin axis do not exist outside of the outline of the Ventersdorp Graben (Fig.8).

In Lesotho west-northwest and east-southeast striking kimberlite dykes are aligned parallel to earlier Karoo dolerite dykes and apparently intruded parallel to the same fracture zones (Dawson, 1970). In northern Lesotho the kimberlites are grouped into the Highlands (eastern) region and the Lowlands (western) region. Erosion in the Highlands region has not been sufficiently extensive for removal of all of the diatreme facies rock, and kimberlites occur as dykes, blows, root zones and diatremes. Erosion has been more extensive in the Lowlands region and diatremes are absent, with the hypabyssal facies characterised by swarms of sub-parallel dykes (Fig.11a and b).

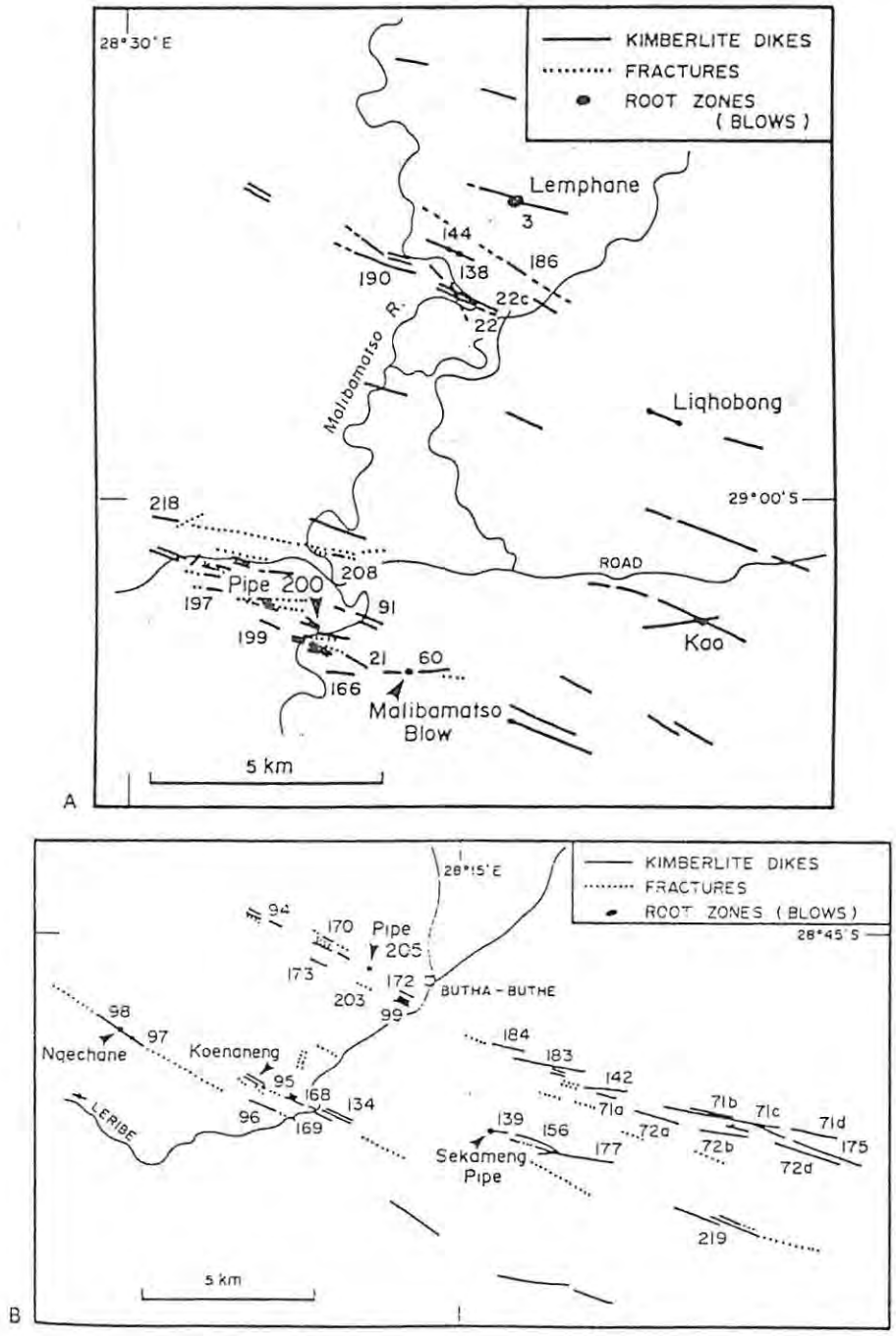

Fig. 11 ; Distribution of kimberlite dykes and blows in (a) the Malibamatso River region of the Lesotho Highlands and, (b) the Buthe-Buthe region of the Lesotho Lowlands, from Mitchell (1986).

1.3.3. Geodynamic controls.

Gurney (1990) summarises the important factors controlling kimberlite emplacement as a convecting lower mantle below the 650 km discontinuity, a ductile asthenosphere which is the source of a variety of basalt and kimberlite, continental lithosphere which may be very old in places and oceanic lithosphere which may persist for some time, but is invariably recycled into the asthenosphere by subduction processes.

It has been mentioned that on a continental-scale, deep penetrating faults or shear zones are necessary to tap the lithospheric-asthenospheric mantle boundary source. Geodynamic controls that influence the spatial and temporal distribution of kimberlite emplacement can be triggered by regional uplifts above upwelling convection currents, mantle diapirs, mantle hot spots, rifting of continents, flat-dipping subduction zones, non-laminar flow above subduction zones and transform faults (Helmstaedt, 1993).

The eruption process of kimberlite pipes, starts of at depths of at least 120 km and the hot and high pressure magma ascends at a rate of 20 to 30 km/hour and steadily accelerates under the effect of rapidly expanding gases. On reaching the surface, a violent reaction occurs with the overlying water table, which results in a large explosion (Miller, 1995). The presence of a gas phase may either be ascribed to the interaction of groundwater with the rising magma (phreatomagmatic) or juvenile water exsolved from the magma itself together with other volatiles, particularly CO_2, or both (Nixon, 1995).

During the kimberlite magma emplacement hydraulic wedging and fracturing, explosive brecciation, spalling, slumping, rock bursting, magmatic stoping and intrusion brecciation occurs through the lithospheric crust. The final stage of kimberlite intrusions are explosive, due to either phreatomagmatic fluid separation with depressurisation or by encountering phreatic fluids near surface, producing crater facies rocks and authigenic brecciation (Clement & Reid, 1989).

The alkaline and kimberlite intrusives associated with mobile zones, faults and/or fracture corridors of the Atlantic side of Africa were emplaced when old, lithospheric structures underwent renewed strike-slip movements, or were reactivated as transcurrent zones as a result of the final phases of movements associated with the opening of the Atlantic during the Cretaceous. The alkali intrusives associated with linear grabens are thought to represent aborted continental rifting. Where the kimberlite intrusions were off-craton, they are barren and are accompanied by carbonatites or alkaline volcanic ring structures (Marsh, 1973 ; Sykes, 1978).

1.4. Kimberlite morphology, mineralogy, petrography and geochemistry.

1.4.1. Kimberlite morphology.

Primary kimberlite deposits occur as pipes or irregular fissures, expressed as dykes and to a lesser extent sills. The size and surface plan views of some well known Southern African kimberlites are shown in Fig.12.

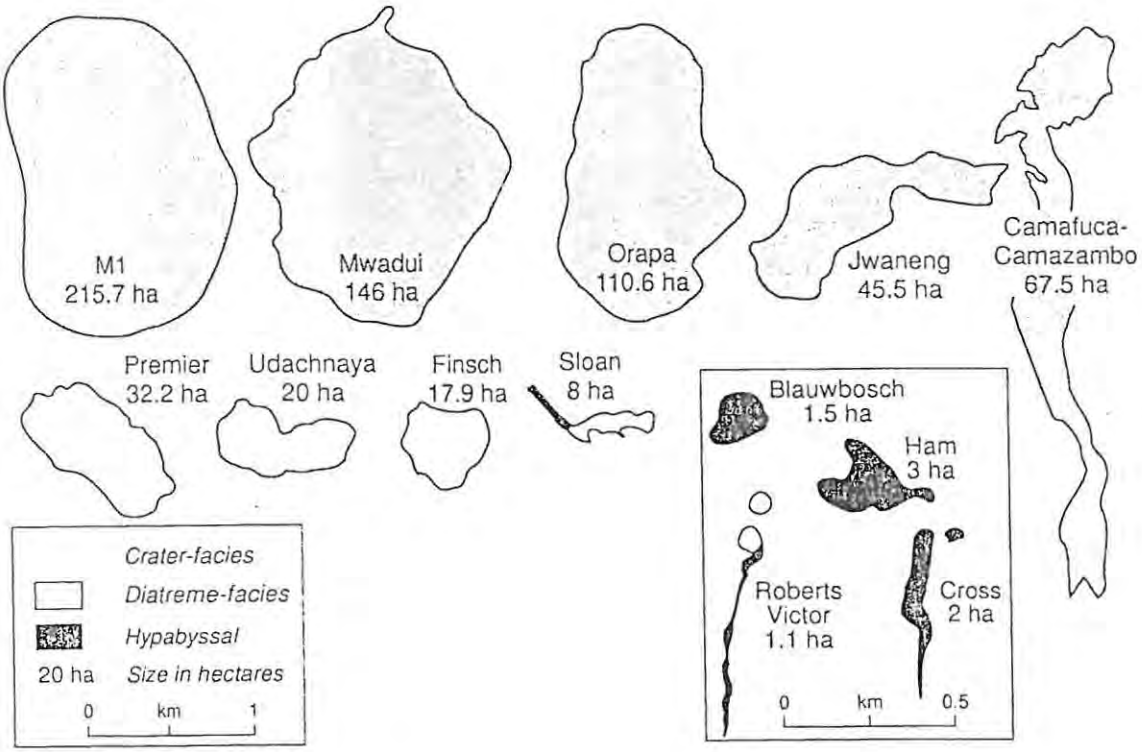

Fig. 12 ; Kimberlite plan views, from Scott-Smith (1992).

Fissures are vertical to near-vertical structures varying from a few centimetres to tens of metres in width. Near surface expansions, or "blows", can be up to 50 m in diameter (Oldenziel, 1997). A kimberlite pipe has a typical carrot-shaped morphology and was subdivided by Hawthorn (1975) into a distinctive hypabyssal-, diatreme- or crater facies (Fig.13).

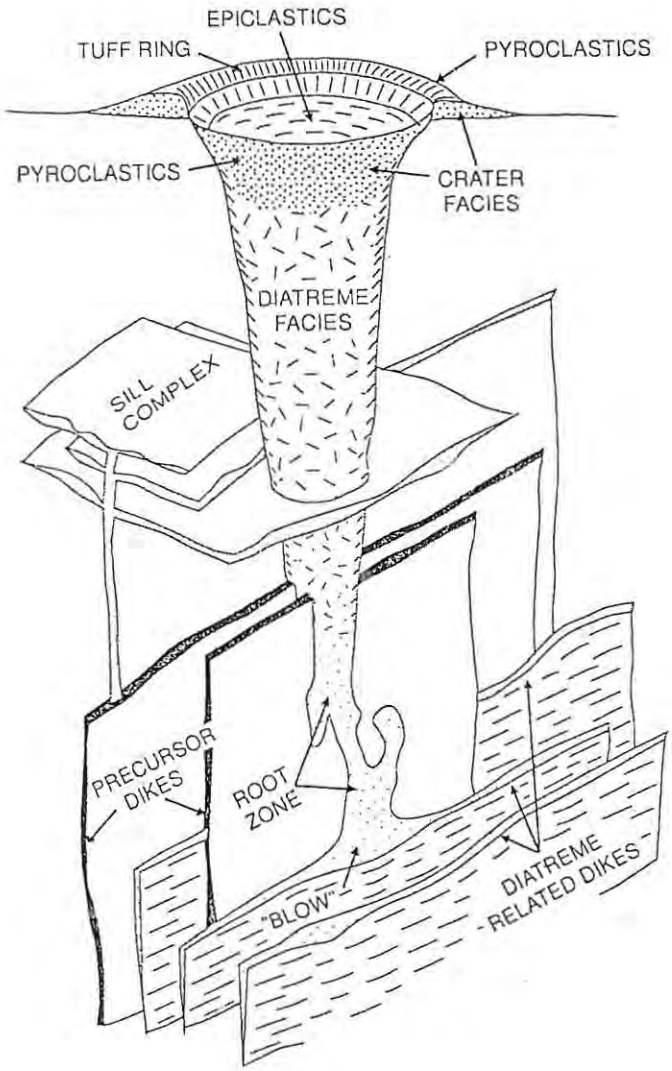

Fig. 13 ; Model of an idealised kimberlite system, illustrating the relationship between crater, diatreme and hypabyssal facies (not to scale). The hypabyssal facies include sills, dykes, root zone and "blow", from Mitchell (1986).

1.4.1.1. Hypabyssal facies.

The hypabyssal facies has an irregular morphology at depth and along strike. Rapid changes in dip and strike of pipe contacts, blocky or serrated edges, intrusion contact breccias and subsurface dome-like or irregular appendages (dykes and sills) are characteristic. Generally, the root zone has a vertical extent of about 0.5 km and occurs about 2 to 3 km below surface. The root zones are narrow and merge into feeder dykes at depth becoming less than 60 cm wide. All pipes are rooted in dykes or are situated near dyke intersections.

The characteristic pinch-and-swell and *en echelon* lenses of dykes are related to host rock lithology. The complexity of the dyke pattern increases from basement granites, to competent dolomites to weathered shales, and generally follow pre-existing structural weaknesses in the country rock.

The internal structure is further complicated by the successive intrusive relationship of different dyke swarms or composite intrusions. Internal contacts vary from sharp to gradational to brecciated, especially along contacts. Dykes are typically < 1 m wide but can be up to 3 m wide in places. They may be up to several kilometres in length, with only local fissure widening and development of small blows (Mitchell, 1986). Sills are less common, but can be up to 5 m thick and laterally extensive (Scott-Smith, 1996).

Dykes in the Swartruggens, Star and Barkly West districts (South Africa) consist of a succession of *en echelon* lenses with a combined strike length of 3 to 7 km. Each lens is rarely more than 60 cm wide and 100 m long. The lenses pinch out at both ends, sometimes very abruptly, and narrow (< 1 cm) stringers of kimberlite or calcite generally lead to another lens that is off-set laterally by 5 to 10 m (Gurney *et al.*, 1991).

1.4.1.2. Diatreme facies.

The diatreme facies have a characteristic steep-sided vertical and regular cylindrical or conical shape of up to 2 km with steep, marginal dips that range from 75 to 85^0. The diatreme contact with the country rock may be joint-bounded, smooth or striated (Clement & Reid, 1989). Structural- and contact metasomatic or metamorphic effects are rare. Updoming or concentric and radial fracturing of the overlying or surrounding host does not occur (Mitchell, 1986).

The diatreme facies develops 2 to 3 km below the surface, is 1 to 2 km in vertical extent, and contains the bulk of the kimberlite pipe. In plan view the diatreme is circular to ellipsoid in shape. The constant dip and downward-tapering shape leads to a regular decrease in the plan view area of the kimberlite with depth.

1.4.1.3. Crater facies.

The crater facies is roughly circular, basin-shaped with shallow-dipping contacts of between 25 and 70^0, but may have multiple and overlapping craters. The oval basin-like structures range between 50 and 1500 m in diameter and from 150 to 300 m in depth. Crater facies rocks have been divided into lavas, pyroclastic- and epiclastic (resedimented) rocks formed at the surface by volcanic-sedimentary processes. Well-bedded, poorly consolidated sediments with chaotic debris-flow deposits and pyroclastics are characteristic. Tuff rings and cones have been described in Mali and Tanzania but not in Southern Africa. Epiclastic rocks were produced by the fluviatile reworking and deposition of pyroclastic kimberlites in crater lakes (maars) formed above diatremes. The epiclastic succession consists of overlapping alluvial fans interbedded with lake-bottom deposits. Kimberlite magmas rarely form lavas, but produce small volumes of pyroclastics that are confined to craters and thinly bedded tuff rings or small cones (Mitchell, 1989).

Orapa consists of two lobes that intruded through basalt, with the northern lobe incorporating large (up to 9.6 m) xenoliths (mostly basalt) in the crater, representing a deep-seated high-energy, gas-charged catastrophic eruption. The crater consists of infilled, simple, grossly layered, primary pyroclastic flow kimberlite. The crater grades down into monotonous diatreme facies rocks (Scott-Smith, 1996). Olive- green serpentinised kimberlite showing no sedimentary features occurs below 90 m and is considered to be primary. Harder but still serpentinised greenish kimberlite is present to a depth of at least 300 m (Baldock *et al.*, 1976).

The southern lobe's crater facies consists of lithic breccia abruptly underlain by diatreme facies at 450 m depth. The main crater infill consists of matrix-supported volcaniclastic breccia with occasional bedded and graded layers, deposited by mass flow processes shortly after eruption. The second type of crater infill, comprising the largest and upper part of the diatreme, consists of later talus and debris flow deposits. The talus deposits are steeply dipping (up to 30^0) and include coarse lithic breccias and bedded deposits composed of kimberlite material.

Near the margins the debris flows consist of channelised country-rock-rich breccias that grade laterally into finer grained mudflows. Slump folding and compaction structures are present. The center of the crater is infilled with kimberlite shales and grits that host a variety of plant and insect fossils deposited in a long-lived crater lake (Baldock *et al.*, 1976 ; Scott-Smith, 1996).

1.4.2. Kimberlite mineralogy and petrography.

Kimberlites are petrographically complex in that they are hybrid rocks containing mantle-derived xenoliths and xenocrysts, as well as a variety of primary phases which crystallised from the host magma and which may have been derived from several mantle sources (Scott-Smith, 1996). Table III summarises some petrographic terms used in the following paragraphs.

Table III ; Kimberlite petrographic terms, adapted from Fipke *et al.* (1995) and Mitchell (1986).

PETROGRAPHIC TERM	DEFINITION
Megacryst	A suite of discrete single crystals commonly found in kimberlites. By definition > 2 cm in longest dimension but can be up to 20 cm in size. The suite commonly consists of some or all of the following phases : olivine, ilmenite, garnet, clinopyroxene, orthopyroxene and zircon.
Macrocryst	Non-genetic term to include both phenocrysts and xenocrysts, usually in the size range 0.5 to 15 mm. They are fragments of megacrysts.
Xenocryst	Fragment of a crystal enclosed by a magma but not genetically related to it.
Xenolith	Rock enclosed by a magma but not genetically related to it.
Phenocryst	Relatively larger crystal set in a fine-grained groundmass of a porphyritic rock. Phenocrysts form during the early crystallisation history of the rock in which they are found.

Two distinct petrographic varieties of kimberlites occur in Southern Africa. Ilmenite-bearing Group I kimberlites are the most common type and occur in all Southern African countries. Ilmenite-poor, micaceous Group II kimberlites only occur in South Africa and Swaziland (Smith *et al.*, 1985). The distribution of Group I and Group II kimberlites are shown in Fig.7.

The following petrographic characteristics of Group I kimberlites is a summary of definitions by Clement *et al.* (1984), Dawson (1971, 1985), Skinner (1989), Mitchell (1989, 1991, 1995), Nixon (1995) and (Scott-Smith, 1996).

Group I kimberlites are rare, volatile-rich (dominantly CO_2), potassic, ultramafic rocks with a distinctive inequigranular texture due to the presence of macrocrysts, or sometimes megacrysts, set within a fine grained matrix. Xenoliths of well-rounded fragments of upper-mantle derived ultramafic rocks, such as peridotite and eclogite, may be present. Usually extreme disaggregation of mantle-derived material produces the characteristic macrocryst suite of minerals, including forsteritic olivine, phlogopite, Cr- poor titanian pyrope- garnet, almandine- pyrope, picro (magnesian)-ilmenite, chromian spinel, enstatite (orthopyroxene) and Cr-poor, commonly subcalcic to calcic, diopside (clinopyroxene).

Minerals which have crystallised from the kimberlite magma prior to emplacement comprise both the megacryst and macrocryst assemblages (refer to Table III). Furthermore, macrocrysts incorporate both phenocrysts and xenocrysts. Olivine macrocrysts (commonly about 25 modal %) are a characteristic constituent in all but fractionated kimberlites.

When olivine macrocrysts are fresh, features such as internal deformation (seen as undulose extinction, kink bands and recrystallisation), are observed. This indicates that the macrocrysts are xenocrysts derived from pre-existing rocks. The other minerals belonging to the macrocryst suite are usually quantitatively insignificant, typically forming < 1% of the mode of a rock, but four, namely ilmenite, garnet, chromian diopside and phlogopite are commonly visually conspicuous. Minerals, such as relatively Fe-rich olivine, Ti-enstatite, Ti-pyrope garnet, phlogopite and ilmenite may be regarded as high-temperature phenocrysts.

Megacrysts (discrete nodules) are single crystals, sometimes weighing several kilograms. The megacrystic suite is dominated by magnesian ilmenite, Cr-poor Fe-Ti-rich pyrope garnet, diopside, olivine and enstatite, which have relatively chrome-poor compositions (< 2 wt.% Cr_2O_3) and rarer zircon. Compositions of megacrysts suggest that they represent a series of crystals precipitated from differentiating magmas. The grains are usually anhedral and are typically rounded or ovoid. In addition, subhedral and euhedral grains can occur, but much of this morphology is imposed by resorption.

Minerals that have crystallised more or less *in situ* to form the volatile-rich, fine-grained matrix comprise a second generation of euhedral olivine which occurs together with one or more of the following primary minerals ; monticellite, phlogopite, perovskite, spinel (chromite-magnetite solid solutions), apatite, rutile, hornblende, augite and serpentine. Many kimberlites contain late stage poikilitic micas of barian phlogopite. Nickeliferous sulphides and rutile are common accessory minerals.

The replacement of early formed olivine, phlogopite, monticellite and apatite by deuteric serpentine, talc and carbonates (mostly calcite, with subordinate dolomite and magnesite) is common. Evolved members of the group may be devoid of, or poor in, macrocrysts and/or are composed essentially of second generation olivine, calcite, serpentine and magnetite, together with minor phlogopite, apatite and perovskite. Kimberlites do no contain primary diopside.

When present diopside is a secondary phase, the crystallisation of which is induced by the assimilation of siliceous xenoliths.

Diamonds only occur as a rare constituents in kimberlites produced from the disaggregation of Archaean peridotite and Proterozoic eclogite xenoliths (Gurney, 1990).

Mitchell (1995) defines Group II kimberlites (orangeites) as "a clan of ultrapotassic peralkaline volatile-rich (dominantly H_2O) rocks, characterised by the presence of phlogopite macrocrysts and microphenocrysts together with groundmass micas which vary in composition from phlogopite to tetraferriphlogopite. Rounded olivine macrocrysts and euhedral primary olivines are common, but not always major constituents.

Characteristic groundmass phases include diopside, commonly zoned and mantled by titanian aegirine, spinels ranging in composition from Mg-chromite to Ti-magnetite, Sr- and REE-rich perovskite, Sr-rich apatite, REE-rich phosphates (monazite, daqingshanite), potassian barian titanites belonging to the hollandite group, potassium triskaidecatitanites ($K_2Ti_{13}O_{27}$), Nb-rutile and Mn-ilmenite. These are set in a mesostasis which may contain calcite, dolomite, ancylite and other rare earth carbonates, witherite, norsethite and serpentine.

Evolved members of the group contain groundmass sanidine and potassium richterite. Zirconium silicates (wadeite, zircon, kimzeyitic garnets) are common as late stage groundmass minerals. Barite is a common secondary or deuteric minerals. Orangeites may be distinguished from kimberlites by the absence of monticellite, magnesian ulvospinel and micas belonging to the barian phlogopite-kinoshitalite series".

A characteristic of the groundmass is the absence of ilmenite. Primary apatite is a common accessory mineral, monticellite is rare and amphibole (antophyllite) has been recorded. Abundant serpentine/clay pseudomorphs after melilite has been described by Skinner (1989).

All kimberlite facies are hosts to a wide range of foreign rock fragments, including fragments of near-surface country rock as well as rocks from the earth's upper mantle.

Fipke *et al.* (1995) have classified mantle-derived xenoliths as ;

(1) the peridotite-pyroxenite suite,
(2) eclogites,
(3) megacrysts,
(4) metasomatised peridotites and,
(5) glimmerites and MARID-suite rocks (refer to Table I).

Mantle xenoliths are commonly rounded, probably due to chemical dissolution at the margins of the fragments. Eclogites and peridotites are the predominant xenoliths found to contain diamonds. The fragmentation of xenoliths explains the ocurrence of diamond xenocrysts, and other single crystals, e.g. garnet, chromite, etc., in the kimberlite rocks (Kirkley *et al.*, 1991).

Peridotite is a general term for a coarse-grained ultramafic rock comprised predominantly of olivine with or without other mafic (high in Fe and Mg) minerals, such as pyroxenes. Garnet and spinel frequently occur in small amounts. It is believed to be the most common and abundant rock type in the mantle. Most peridotitic diamonds are formed in garnet-bearing harzburgite, with minor amounts formed in lherzolite (Gurney, 1989).

Given the upper mantle abundance of peridotite, relatively few xenoliths remain because of a extremely efficient disaggregation process. Low T garnet-spinel peridotites (lherzolites, harzburgites, dunites including some pyroxenites) with coarse "granular" textures represent the most common type of xenolith derived from the lithospheric mantle. Some of the clinopyroxene-deficient harzburgites and dunites within this group contain sub-calcic garnet (Cr pyrope) and have very depleted Mg/Fe and Cr/Al ratios (Nixon, 1995).

Eclogites are coarse-grained ultramafic rocks consisting of granular aggregate of red-garnet (almandine- pyrope) and green pyroxene (jadeitic clinopyroxene or a solid solution between jadeite and diopside), with minor amounts of rutile, kyanite, corundum, coesite, diamond, graphite, orthopyroxene, olivine, amphibole, scapolite, sillimanite, phlogopite, ilmenite and sulphides. Eclogites are indicative of high-pressure and high-temperature environments, which occur in deep crustal metamorphic regions below continents and probably represent solid-state transformation of previously existing rock, probably basalt. Eclogites are less common than peridotites. Some eclogites were incorporated into the intruding kimberlite directly from the Earth's crust and these xenoliths grade into garnet granulites and amphibolites (Nixon, 1995).

"Glimmerites" consist of dominantly phlogopite with varying amounts of amphibole, olivine, ilmenite, rutile and clinopyroxene. The granulite assemblage consists of basic clinopyroxene, garnet, plagioclase, and/or orthopyroxene (O'Reilly, 1985).

MARID group rocks are thought to have crystallised from magmas resulting from metasomatism and consist of mica (low NiO, Cr_2O_3 and Al_2O_3 phlogopite), amphibole (K-richterite), rutile, diopside and rare zircon (Nixon, 1995).

1.4.2.1. Hypabyssal facies.

Clement (1982), Clement & Skinner (1979, 1985) and Clement *et al.* (1984) developed two kimberlite classification schemes. The first classification scheme is based on the relative abundances of five primary minerals, namely diopside, monticellite, phlogopite, calcite and serpentine and only uses the hypabyssal facies mineralogy (Table IV).

The hypabyssal facies kimberlite is "kimberlite" *senso stricto*, and is considered the best available representation of the direct crystallisation product of kimberlite magma. Olivine was not used because it is always an abundant mineral, and distinction between olivine derived from kimberlite magma and xenocrystic magma is also problematic.

In typical hypabyssal kimberlites the olivine phenocrysts account for approximately 25 modal % of the rock. Together with the macrocrysts, olivine typically forms at least 50% of a kimberlite. Olivine phenocrysts have compositions within the range Fo_{85} to Fo_{95}. Phlogopite phenocrysts may occur, but are not all that common.

Table IV ; Mineralogical classification of hypabyssal facies kimberlites, from Skinner (1998).

KIMBERLITE						
STAGE 1	STAGE 2					STAGE 3
ESSENTIAL MINERAL	POTENTIAL CHARACTERIZING ACCESSORY MINERALS					OPAQUE MINERALS
DIOPSIDE	Monticellite	Phlogopite	Calcite	Serpentine	Apatite	Qualify as opaque mineral - rich if opaque minerals = 2/3 modal % of essential mineral
MONTICELLITE	Diopside	Phlogopite	Calcite	Serpentine	Apatite	
PHLOGOPITE	Diopside	Monticellite	Calcite	Serpentine	Apatite	
CALCITE	Diopside	Monticellite	Phlogopite	Serpentine	Apatite	
SERPENTINE	Diopside	Monticellite	Phlogopite	Calcite	Apatite	

Monticellite is a common groundmass mineral and may dominate the groundmass. Monticellite crystallises after spinel and perovskite, but before the late-stage calcite and serpentine. Groundmass micas can be common with relatively high Al_2O_3 and low TiO_2 and the dominant evolutionary trend is one of Al enrichment, with decreasing FeO and TiO_2 (Mitchell, 1995). Spinel and perovskite are usually abundant and are early formed phases in the groundmass. Apatite is typically a late-stage crystallising, fine-grained accessory mineral and is often more abundant and coarser grained in calcite-rich kimberlites (Scott-Smith, 1996).

Serpentine and carbonate are common late-stage primary groundmass minerals that predominate in many kimberlites. Rutile is either of mantle-derived xenocrystic origin or a replacement phase of perovskite. The most common mode of occurrence is as inclusions in the phenocrystal olivine. Primary groundmass clinopyroxene is rare, however, pseudoprimary clinopyroxene is common and has a low TiO_2, Al_2O_3 and Na_2O content. Quartz, sanidine, plagioclase, leucite, nepheline, abundant melilite, kalsilite, andradite-garnet, potassic richterite (or other amphiboles) and barite are typically not associated with kimberlites (Scott-Smith, 1996).

The second classification scheme is a textural-genetic classification scheme that incorporates all three facies, namely crater-, diatreme- and hypabyssal facies (Fig.14).

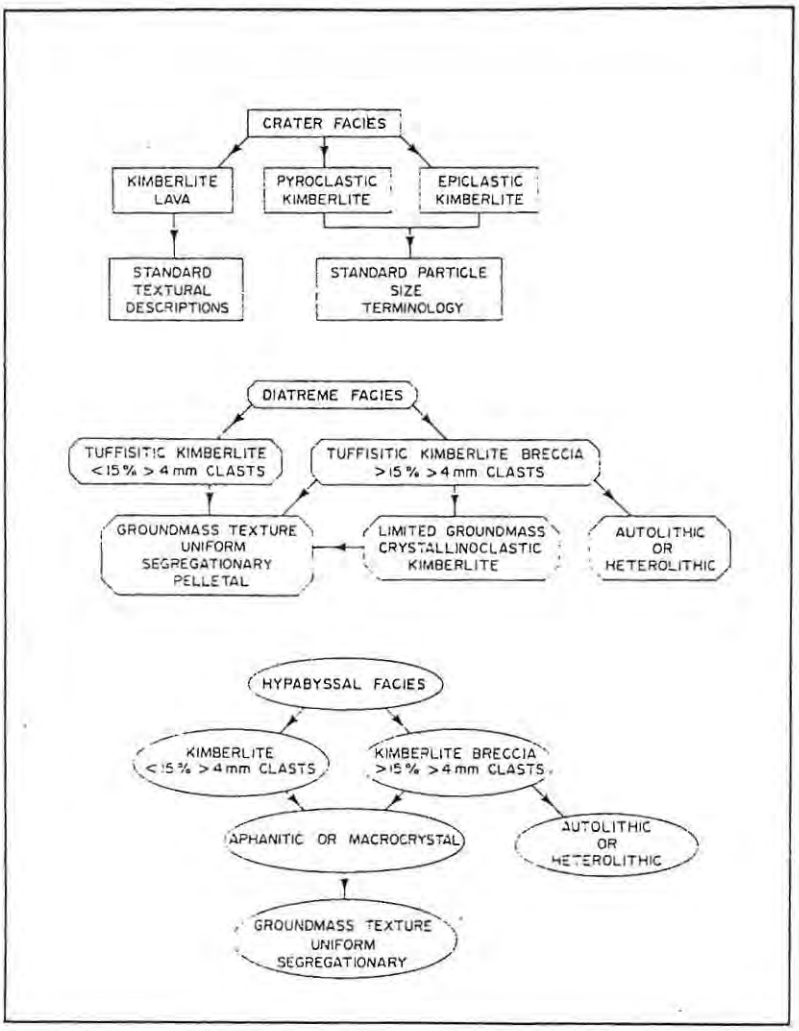

Fig. 14 ; Textural-genetic classification of kimberlites, (adapted from Clement & Skinner, 1979, 1985 and Clement, 1982), from Mitchell (1986).

As the hypabyssal facies formed by the crystallisation of volatile-rich magma, these rocks show igneous, usually porphyritic, textures and the effects of magmatic differentiation. Root zones are characteristically complex due to multiple intrusions. The repeated injections occurred before the previous magma had time to crystallise completely (Mitchell, 1989).

Hypabyssal groundmass may be described as uniform or segregational (Fig.14). Hypabyssal kimberlites contain crystals, and commonly xenoliths, set in a finer-grained matrix formed from the products of the relatively slow crystallisation of the host magma. The volatile-rich constituents, mainly present as primary serpentine and carbonate (plus apatite and mica), can segregate leading to a non-uniform texture described as segregationary (Clement & Skinner, 1985). Sometimes the early silicate-rich constituents form globules set in a volatile-rich matrix and is termed globular segregationary.

1.4.2.2. Diatreme facies.

Diatreme facies rocks were subdivided by Clement & Skinner (1985) into tuffisitic kimberlites (TK) and tuffisitic kimberlite breccias (TKB) depending on the abundance of clasts (Fig.14). Where the abundance of > 4 mm autolithic or heterolithic clasts exceed 15 vol.% it is classified as TKB. Breccias are described in terms of autolithic breccias (being fragments of an earlier generation of kimberlite found within a younger kimberlite) or heterolithic breccias (which contain fragments of country rock and autolithic clasts).

The diatremes mostly consist of several varieties of tuffisitic kimberlite breccia (TKB) that differ with respect to size, shape and type of xenoliths present. The xenolith suite consists of angular clasts derived from local country rock and lesser quantities of rounded lower crustal and mantle-derived xenoliths (Mitchell, 1989). Very large blocks of country rock xenoliths, that range from 50 to 300 m, are termed "floating reefs" in South Africa. Most of the xenoliths are less than 20 cm. The reefs subside into the diatreme and can occur up to 1000 m below their original stratigraphic level (Scott-Smith, 1996).

A characteristic feature of diatreme facies kimberlites is the presence of rounded peridotite and eclogite nodules and a variety of macrocrysts which formed at mantle depths. The macrocrysts consist of forsterite-rich olivine, chrome and titanian pyrope, magnesio-chromite, chrome diopside, enstatite, almandine-pyrope, omphacite, rutile, kyanite, picroilmenite and zircon (Smith, 1985).

Groundmass variation, ranging from limited groundmass to abundant groundmass, has also been used as a classification criteria. Abundant groundmass has been subdivided into uniform- or segregationary-textured types. The groundmass mostly consists of microlitic diopside (clinopyroxene) and serpentine, which represent the quench products of the remaining interstitial volatile-rich fluid phase. The diopside microlites are characteristic of the diatreme facies and are commonly replaced by secondary minerals. Carbonate is typically absent, reflecting total degassing of CO_2 during diatreme formation (Scott-Smith, 1996).

Spherical-to-elliptical lapilli-sized clasts of kimberlite has been termed pelletal lapilli and may vary between 1 to 30 mm in size (Clement & Skinner, 1985). These lapilli usually have a core of euhedral pseudomorphed olivines, or less commonly phlogopite. The peletal lapilli represent droplets of liquid or magma that develop during the rapid degassing of CO_2.

The relatively permeable TKB's of the diatreme facies are susceptible to alteration by groundwater infiltration, therefore serpentine, calcite, clays, silica and zeolites are common secondary mineral phases. The secondary minerals occur as veinlets and replacement products (Scott-Smith, 1996).

1.4.2.3. Crater facies.

The crater facies consists of a combination of volcanic- and sedimentary rock types (Fig.14). Pyroclastic kimberlite represents the explosive ejecta, such as kimberlite tuff or agglomerate deposited around or within the crater, whilst epiclastic rock is pyroclastic kimberlite which has been reworked by fluvial processes and redeposited in the crater, for example kimberlitic sandstone, shale and conglomerate (Gurney *et al.*, 1991).

The crater facies macrocrysts are set in a matrix consisting of varying proportions of the five major mineral components mentioned in Table IV. These components consist of serpentine, calcite, phlogopite, diopside and monticellite, by which the kimberlite is named, for example calcite-phlogopite kimberlite (Clement & Skinner, 1985). A second generation of small, sub- to euhedral olivine crystals are also present. Apatite, perovskite and opaque oxides (ilmenite in the Group I kimberlites and spinels) occur as abundant or accessory groundmass phases.

1.4.3. Kimberlite geochemistry.

Diamond is a stable polymorph of carbon at depths exceeding 150 km but below 300 km in depth. The less than 300 km depth is inferred from the absence of the high-density polymorph of olivine, namely β-olivine. The 150 to 300 km depth range lies within the garnet-lherzolite zone of the upper mantle. Kimberlite geochemistry is constrained by the mineralogical- and chemical characteristics of its source rock in the upper mantle. Therefore, the geochemistry of the magmatic components of kimberlite now located on the Earth's surface gives some indication of the original source rock chemistry.

The bulk rock chemistry of kimberlites show a wide range of compositions. The diversity in kimberlite types reflect the different source materials which are tapped within the upper mantle and has led to the classification of two distinctive kimberlite types in Southern Africa. Smith (1983) classifies kimberlites into Group I kimberlites, which are depleted in LREE and Rb (and derived from an asthenospheric source), and Group II kimberlites, which are enriched in LREE and Rb (and derived from a lithospheric source), relative to the bulk earth composition. For general kimberlite classification the hypabyssal facies is accepted as a direct reflection of kimberlite *senso stricto*.

1.4.3.1. Group I kimberlites.

The following description of Group I hypabyssal facies kimberlite is a summary from data by Smith *et al.* (1985), Skinner (1989, 1998), Scott-Smith (1996) and Mitchell (1991) ;

Group I kimberlites (most between 70 and 114 Ma, but includes kimberlites ranging up to 1600 Ma) are characterised by a monticellite- serpentine- calcite assemblage and are derived from fragments of upper mantle xenoliths, megacrysts and primary phenocryst and groundmass minerals. They are characterised by the megacrystic suite, especially Mg-ilmenite (3 to 23 wt % MgO, but typically > 8 wt % MgO), Cr-poor (0 to 3 wt % Cr_2O_3) titanian pyrope and subcalcic diopside, Ti-poor (< 2 wt % TiO_2) phlogopites as phenocrysts or macrocrysts and groundmass and, spinels that range in composition from titanian magnesian aluminous chromites to magnesian ulvospinel-magnetite solid solutions.

Group I kimberlites are distinctly richer in TiO_2, CaO, H_2O, CO_2 and V_2O_5, and low in K_2O, SiO_2, LREE and LREE/HREE compared to Group II kimberlites. Absent from Group I kimberlites are aluminous diopside and augite, andraditic garnets, feldspars, amphiboles, leucite, nepheline and melilite. Mantle-derived xenocrysts of magnesian aluminous chromite, Cr-diopside and Cr-pyrope are common.

Group I kimberlites are subdivided into centrally located, on-craton Group 1A kimberlites and near craton margins, or off-craton Group 1B kimberlites. Group IB kimberlites have higher total Fe, as well as higher TiO_2, P_2O_5, CaO, CO_2 and H_2O contents and lower MgO and SiO_2 relative to Group IA. In terms of trace elements, Group IB kimberlites have somewhat higher V, Cu, Zn, Pb, Nb, Zr and Y contents than Group IA. Group IB kimberlites are thought to be derived from shallower sources characterised by steeper geothermal gradients, compared to Group IA.

1.4.3.2. Group II kimberlites.

Group II kimberlites or orangeites (110 to 200 Ma) are a suite of micaceous kimberlites that have only been recognised in South Africa. They consist primarily of rounded olivine macrocrysts set in a matrix of macrocrysts and microphenocrysts of phlogopite and diopside, together with spinel (titanian magnesian chromite to ulvospinel- magnetite), perovskite and calcite. K-Ba-V titanates are characteristic accessory phases.

The megacrystic suite is notably absent from Group II kimberlites. Magnesian ulvospinel and monticellite are absent and perovskite is rare. Phlogopite-rich Group II kimberlites generally have high SiO_2 and Al_2O_3, together with high K_2O and low TiO_2. Rb and Ba follow K_2O in Group II kimberlites. Group II kimberlites have higher LREE abundances and LREE/HREE enrichment compared to the kimberlites of Group I.

1.4.3.3. Major element geochemistry.

Even uncontaminated kimberlites show considerable compositional variation in SiO_2, CaO, MgO, CO_2 and H_2O content. The Al_2O_3 and Na_20 contents of kimberlites are extremely low relative to other mafic and alkaline mafic rocks. Difficulties in interpreting bulk compositions include widespread deuteric and secondary alteration, and xenolith contamination by crustal material. Representative average kimberlite compositions for some Southern African examples are given in Table V.

Variable olivine contents in kimberlites is observed in the wide range of MgO contents, which range from 12 to 25 wt % MgO. High proportions of SiO_2, K_2O, Al_2O_3, Rb and Ba are linked to high proportions of phlogopite and high TiO_2, FeO, Fe_2O_3 and V indicate high proportions of groundmass opaque minerals. CaO/CO_2 and MgO abundances reflect modal proportions of calcite and olivine (Mitchell, 1986 ; Skinner, 1998).

Major element abundances have been defined using diatreme and hypabyssal facies kimberlite. Hypabyssal kimberlites have few crustal xenoliths and have retained their volatiles. Clement (1982) formulated a contamination index (C.I.) to evaluate the effects of crustal contamination and weathering ;

$$C.I. = (SiO_2 + Al_2O_3 + Na_2O)/(MgO + 2K_2O)$$

Contamination-free fresh phlogopite and/or diopside-rich kimberlites have C.I.'s of 1 to 1.5. Any analyses with C.I.'s above 1.5 should not be used for the interpretation or comparison of major element data. The index is a measure of the proportions of clay minerals and tectosilicates relative to olivine and phlogopite (Mitchell, 1986 ; Skinner, 1998).

Table V ; Average compositions of some Southern African kimberlites.

	(1)	(2)	(3)	(4)	(5)	(6)	(7)	(8)	(9)	(10)
SiO2	35.2	31.1	32.53	30.42	28.63	25.19	16.9	3.41	38.9	36.12
TiO2	2.32	2.03	1.38	2.95	1.07	1.89	0.93	12.23	1.67	1.45
Al2O3	4.4	4.9	2.12	3.09	2.01	2.87	0.79	7.81	3.97	4.38
Cr2O3	-	-	0.23	0.15	-	-	-	0.1	0.31	-
Fe2O3	-	-	5.10	5.08	4.02	3.72	7.04	19.66	3.57	6.8
FeO	9.8	10.5	3.78	6.28	5.38	6.72	3.47	12.12	-	2.68
MnO	0.11	0.1	0.15	0.18	0.14	0.22	0.24	0.43	0.15	0.22
MgO	27.9	23.9	31.35	25.14	34.02	29.69	16.6	11.93	19.92	22.82
CaO	7.6	10.6	7.59	9.72	11.92	13.59	26.4	17.15	7.06	8.33
Na2O	0.32	0.31	0.05	0.08	0.2	0.01	-	0.26	0.28	0.29
K2O	0.98	2.1	1.63	2.15	0.05	0.15	0.02	0.09	4.68	5.04
P2O5	0.7	0.7	0.54	1.17	0.27	2.2	1.36	2.42	1.34	1.46
CO2	3.3	7.1	4.46	5.30	8.99	12.83	19.23	9.45	-	3.8
H2O+	7.4	5.9	7.59	6.25	2.75	1.15	5.13	2.34	-	4.89
H2O-	-	-	0.44	0.64	0.23	-	0.28	0.3	-	1.28

Sources.

(1) Kimberlite (Dawson, 1967).

(2) Micaceous kimberlite (Dawson, 1967).

(3) Dike 202, Malibamatso River, Lesotho (Gurney & Ebrahim, 1973).

(4) Pipe 200, Lesotho (Gurney & Ebrahim, 1973).

(5) Olivine-magnetite-perovskite cumulate, Benfontein, South Africa (Dawson & Hawthorne, 1973).

(6) Composite sample of Benfontein sill, South Africa (Dawson & Hawthorne, 1973).

(7) Magnetite-calcite-serpentine dyke, Premier, South Africa (Robinson, 1975).

(8) Magnetite perovskite cumulate, Benfontein South Africa (Dawson & Hawthorne, 1973).

(9) Swartruggens Main Dyke, South Africa (Skinner & Scott, 1979).

(10) New Elands dyke, South Africa (Dawson, 1972).

Contamination by crustal rocks results in the addition of SiO_2, Al_2O_3 and Na_2O to kimberlites. Weathering to mixtures of chlorite, montmorillonite and serpentine, and in extreme cases to lateritic assemblages, leads to increased SiO_2 and Al_2O_3 as soluble cations (such as Mg^{2+}) are removed. Uncontaminated rocks show compositions of low Al_2O_3 (0 to 5%) and widely variable SiO_2 (25 to 35%) contents (Mitchell, 1986, 1989).

1.4.3.4. Trace element geochemistry.

Compatible elements.

Compatible elements (with solid/liquid distribution coefficients > 1, for example Cr, Ni and Co) are preferentially incorporated into the early phases crystallising from the magma. The abundances of compatible elements are directly related to the modal proportions of olivine and inversely related to the degree of crustal contamination. More evolved kimberlites, which generally have lower proportions of olivine, are relatively depleted in compatible elements. Compatible element abundances are similar to those of ultramafic rocks and are hosted primarily by olivine (Ni, Co and Sc), spinels (Cr, Ni, Cu, Co, Sc, V and Zn), perovskite (Sc), sulphides (Cu and Ni), diopside (Cr, Sc, V and Ni) and phlogopite (Cr and Sc) (Mitchell, 1989; Skinner, 1998). The mean contents of some compatible elements of kimberlites are compared to those melilites and basalts in Fig.15.

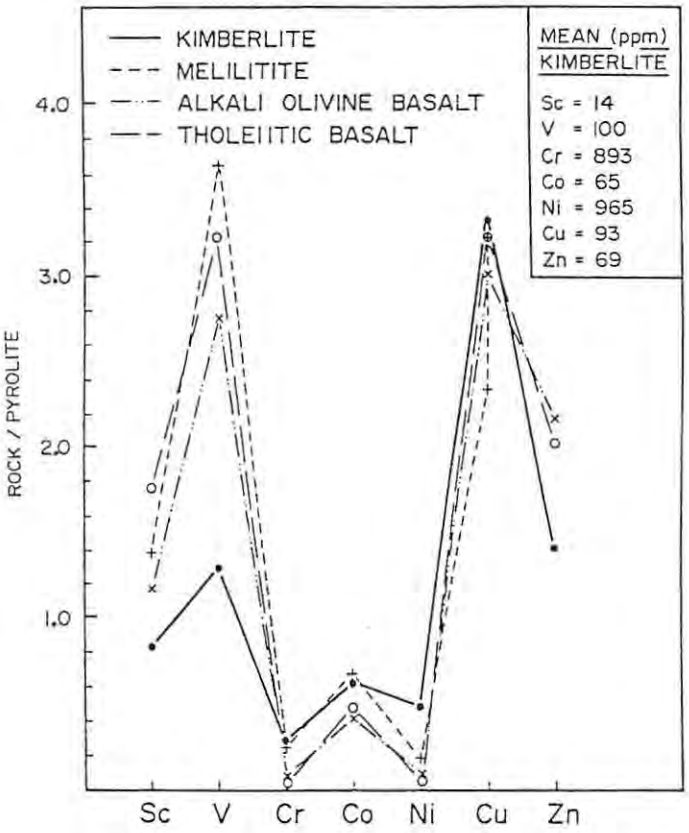

Fig. 15 ; Mean contents of some compatible elements in kimberlites compared to melilites and basalts, from Mitchell (1986).

Incompatible elements.

Incompatible elements (with solid/liquid distribution coefficients = 0, for example Nb, Ta, Zr, Hf, U, Th and REE) are not removed from the liquid until the later stages of crystallisation of the groundmass. However, some incompatible elements do behave compatibly into the relatively early phases, for example Ba in phlogopite and Sr in apatite (Scott-Smith, 1996 ; Skinner, 1998). Incompatible elements and their characteristic hosts include Ba in phlogopite, Sr in apatite, perovskite, diopside and carbonates, Zr, Hf, Nb and Ta in perovskite and macrocrystal ilmenite, U and Th in perovskite and apatite, Rb in phlogopite and REE in perovskite, apatite and carbonates.

REE, and to a lesser extent the other incompatible elements, abundances have been found useful because their abundance and distribution patterns are not substantially modified by fractional crystallisation and places a constraint on the nature of the source region of the kimberlite. All kimberlites have La/Yb ratios significantly greater than other mantle-derived undersaturated potassic lavas. The La/Yb ratios of micaceous kimberlites are generally higher than those of other varieties (Mitchell, 1989 ; Skinner, 1998).

Smith *et al.* (1985) have shown that Groups I and II kimberlites have broadly similar incompatible element enrichment but that they are geochemically distinct. Group II kimberlites have higher contents of P, Rb, Ba and lower Ti and Nb than Group I. The mean contents of some incompatible elements of kimberlites are compared to those of nepheline melilitite and tholeiitic basalts in Fig.16.

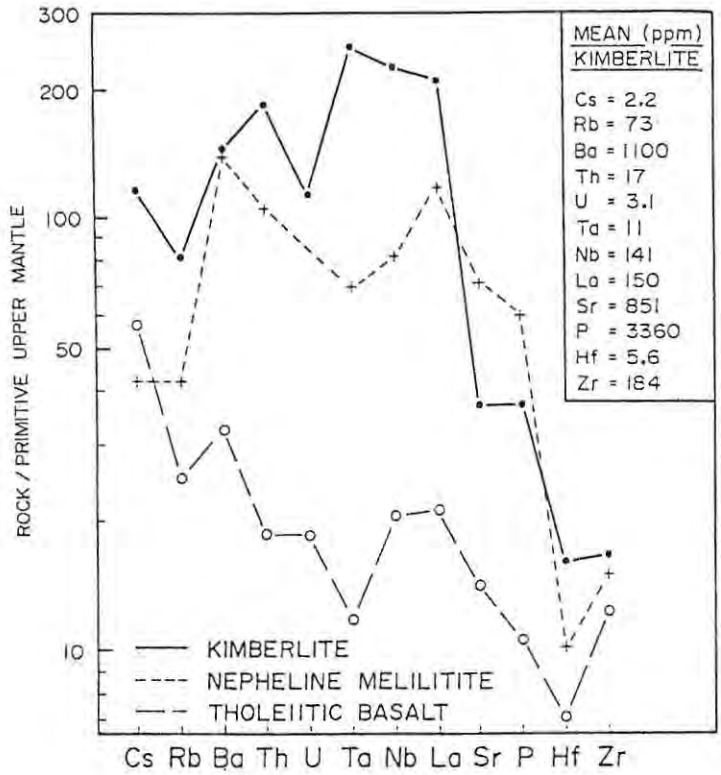

Fig. 16 ; Mean contents of some incompatible elements in kimberlites compared to nepheline melilitite and tholeiitic basalts, from Mitchell (1986).

1.4.3.5. Radiogenic isotopes.

Radiogenic isotope chemistry show systematic Sr, Nd and Pb isotopic variations from Group I to Group II kimberlites. Both Groups I and Group II kimberlites have broadly similar incompatible element abundances and seem to be derived from sources with compositions close to bulk Earth with respect to Sr and Nd radiogenic isotopes (Fig.17). This is also similar to other asthenosphere-derived basaltoid magmas, such as oceanic island alkalic basalts and other types of alkalic intraplate volcanics.

Kimberlites are, however, enriched in incompatible elements relative to the other basaltoid rocks, as seen in the Nb enrichment factor of 10 relative to ocean island basalts. It is thought that kimberlites are formed by small degrees of partial melting of an asthenospheric REE-, Ti- and Ba-enriched carbonated ultramafic rock.

Group I kimberlites have low $^{87}Sr/^{86}Sr$ initial isotopic ratios of between 0.703 and 0.705. They are also depleted in Rb and have higher Nd and Pb isotopic compositions than Group II kimberlites (Fig.17) (Mitchell, 1986, 1989). Group I kimberlites have high initial $^{143}Nd/^{144}Nd$ values ranging from 0.51271 to 0.51287 (or ε_{Nd} values between -0.5 and +6), and Pb isotopic compositions which give negative (future) ages relative to known ages of intrusions (Fig.18) (Smith, 1983, Mitchell, 1989).

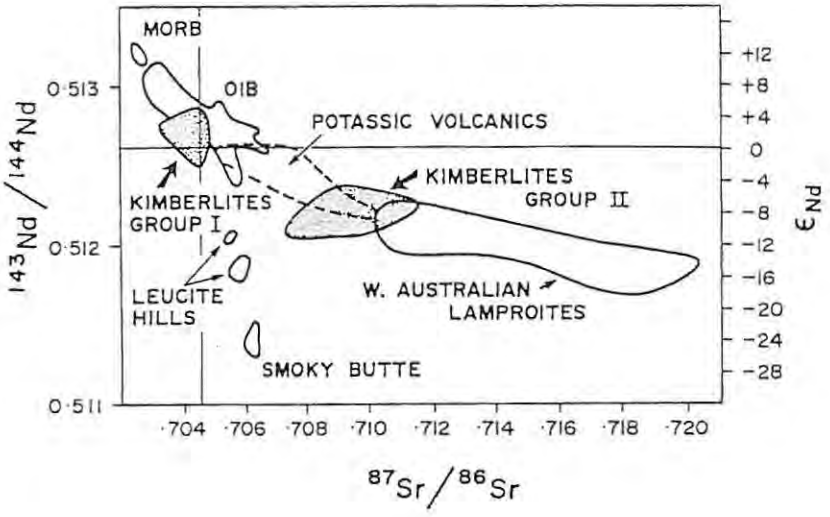

Fig. 17 ; Nd versus Sr isotope compositions of kimberlites and lamproites relative to those of the bulk earth reference composition, oceanic island basalts (OIB), mid-oceanic ridge basalts (MORB) and potassic volcanic rocks. Rocks with isotopic compositions close to those of bulk earth and within the upper left quadrant of the diagram are conventionally interpreted as being derived from asthenospheric sources. Rocks with isotopic compositions that plot in the lower right quadrant are believed to have been derived from ancient enriched lithospheric sources. Trends towards the bulk earth composition may reflect mixing with asthenospheric components, from Mitchell (1989).

Group I kimberlite isotopic signatures are interpreted to have been derived from mantle sources which were undifferentiated or slightly depleted with respect to bulk earth composition and are, therefore associated with relatively low Sm/Nd ratios (Mitchell, 1986 ; Scott-Smith, 1996).

Group II kimberlites have relatively high $^{87}Sr/^{86}Sr$ initial isotopic ratios of between 0.707 and 0.712 and initial $^{143}Nd/^{144}Nd$ values of between 0.51208 to 0.51228 (or negative ε_{Nd} values ranging from -7 to -12) (Fig.17) (Mitchell, 1986, 1989). They are enriched in Rb and have relatively depleted Nd and Pb isotopic compositions, with anomalously old relative ages compared to their known intrusive ages (Fig.18) (Smith, 1983, Mitchell, 1989).

Group II kimberlites are derived from an enriched source compared to the bulk earth Sm/Nd ratio, which is reflected in its relatively high Sm/Nd ratios (Mitchell, 1986 ; Scott-Smith, 1996).

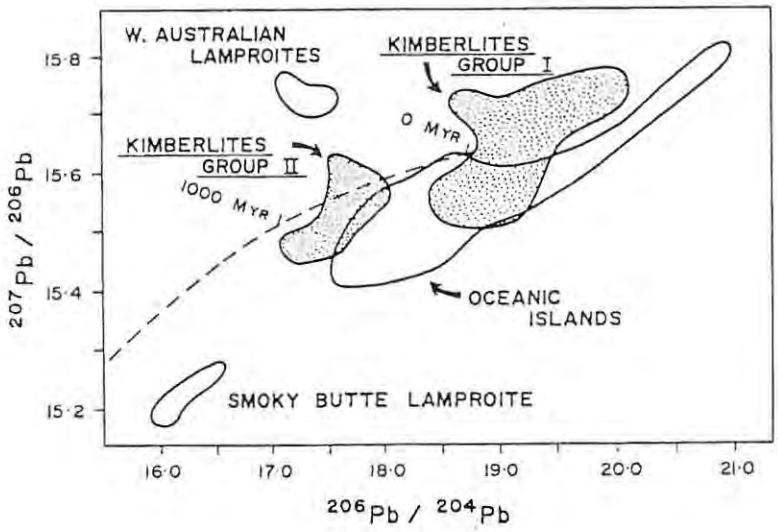

Fig. 18 ; Isotopic composition of Pb in kimberlites and lamproites (adapted from Smith, 1983). Dotted line is the Stacey-Kramers two stage growth curve for U-Pb systems, from Mitchell (1989).

1.4.3.6. Stable isotopes.

Stable isotope studies suggest that kimberlite magmas have interacted with groundwaters and that only carbon isotopic compositions reflect the composition of the primary magma. Sheppard & Dawson (1975) interpret the wide range in $\delta^{18}O$ (0 to 12 per mil) and δD (-85 to -147 per mil) of groundmass micas and serpentinites to be a consequence of mixing of magmatic fluids with hot meteoric fluids depleted in D and enriched in ^{18}O.

Kobelski *et al.* (1979) reported a wide range in $\delta^{13}C$ carbonate (-11.8 to +0.2 per mil) for Southern African kimberlites. Increased ^{13}C and ^{18}O values of groundmass carbonates in kimberlites which intrude dolomite indicate that assimilation of relatively heavy dolomite host rock inclusions contributes CO_2 to kimberlite. Wide ranges in the oxygen isotopic composition ($\delta^{18}O$ = 7 to 27 per mil) of kimberlite carbonate are believed to reflect loss of isotopically light water during emplacement or an influx of meteoric water at relatively low temperatures (Kobelski *et al.*, 1979).

For example the Finsch, Bellsbank and Swartruggens kimberlites intrude a thick sequence of Precambrian dolomite. The groundmass carbonates in these kimberlites have ^{13}C and ^{18}O values which trend from $\delta^{13}C$ = -6 per mil and $\delta^{18}O$ = 12 per mil, similar to those of other kimberlite carbonates, to values of $\delta^{13}C$ = -1 per mil and and $\delta^{18}O$ = 22 per mil, which approach those of sedimentary carbonates (Kirkley *et al.*, 1988).

1.4.3.7. A brief summary of Group I and Group II kimberlite characteristics.

The above-mentioned geochemical characteristics of Group I and Group II kimberlites are summarised in Table VI.

Table VI ; A comparison of Group I and Group II kimberlites.

	GROUP I KIMBERLITES	GROUP II KIMBERLITES
UPPER MANTLE SOURCE	Asthenospheric source.	Lithospheric source.
AGE	Range from 70 to 1600 Ma, although most intrusions fall between 70 and 114 Ma.	Range from 110 to 200 Ma.
MINERALOGY	Olivines show a wide range in composition for both megacrysts and phenocrysts. Rutile and ilmenite commonly present as inclusions in phenocrysts.	Restricted range in composition for both macrocrysts and phenocrysts. Microphenocrysts present in some. Rutile and ilmenite inclusions absent.
PETROGRAPHY	(a) Dominated by mixed calcite, serpentine, monticellite assemblage. Groundmass opaque oxides and perovskite are common. (b) Megacrystic suite characteristic - comprises Mg-ilmenite, Cr-poor titanian pyrope, Cr-poor subcalcic diopside, Ti-poor phlogopite and spinel.	(a) All are phlogopite varieties and some contain relatively abundant diopside. Groundmass opaque oxides and perovskite, if present, are fine-grained and rare. (b) No megacrystic suite.
MAJOR ELEMENT GEOCHEMISTRY	Enriched in CaO, H2O, CO2 and V2O5, depleted in K20 and SiO2.	Enriched in SiO2, Al2O3 and K20 and depleted in CaO H2O, CO2 and V2O5.
INCOMPATIBLE TRACE ELEMENT GEOCHEMISTRY	Depleted in LREE, Ba, Rb and P with low La/Yb ratios and enriched in Ti and Nb.	Enriched in LREE, Ba, Rb and P with high La/Yb ratios and depleted in Ti and Nb.
RADIOGENIC ISOTOPES	Mantle source rocks undifferentiated to slightly depleted relative to bulk Earth with respect to Sr and Nd, but not Pb. In other words low Pb/Sr and Sm/Nd, but high U/Pb. (a) Initial 87Sr/86Sr range from 0.703 to 0.705. (b) High initial 143Nd/144Nd values from 0.51271 to 0.51287. (c) Relatively radiogenic and variable Pb isotope compositions, similar to modern O.I.B., with 206Pb/204Pb values ranging from 18.95 to 20.05.	Mantle source rocks enriched relative to bulk Earth with respect to Sr and Nd, but not Pb, in other words high Pb/Sr and Sm/Nd, but low U/Pb. (a) Initial 87Sr/86Sr range from 0.707 to 0.712. (b) Low initial 143Nd/144Nd values ranging from 0.51208 to 0.5122 (c) Relatively unradiogenic Pb isotopic compositions, more primitive than M.O.R.B., with 206Pb/204Pb values ranging from 17.2 to 17.7.
DIAMONDS	Highly variable grades from > 200 ctpht to barren. Ratio of diamondiferous to barren on-craton kimberlite possibly 1/10.	Grades variable from > 400 ctpht to barren. Ratio of diamondiferous to barren on-craton kimberlites possibly 1/1.

1.5. Diamonds.

1.5.1. Diamond characteristics.

The word diamond is derived from the Latin "adamas" meaning unconquerable and is the hardest substance known, grading 10 on the Mohs scale. It has a very high index of refraction and exceptional colour dispersion. Uncut faces have a slightly greasy lustre, but cut faces show a brilliant (adamantine) lustre. The specific gravity ranges from 2.9 for industrial diamonds to 3.5 for gem-grade diamonds. Diamonds have high melting points, are insoluble in acids and oxidises at about 870^0 C (Cole, 1998).

Diamonds are composed of pure carbon and have isometric crystal structures, the most common being the octahedron. Carbon atoms are located at corners and face centers of the cube and also at points one-quarter or three quarters of the way along the diagonal. High temperatures and pressures are required to transform pure carbon to diamond instead of graphite (Cole, 1998).

Distinction is made between industrial and gem-quality diamonds in evalution of a deposit. Gem-quality diamonds are further classified by a standard called the 4 C's ; colour, carat weight, clarity and cut. The last factor only refers to polished diamonds. Diamonds have a wide range in colour, from faint yellow or brown to rare coloured stones of pink, blue, green and other colours depending on the impurities present within the crystal structure. A pure colourless stone is the most sought after.

The weight of a diamond is measured in carats, which is 0.2 grams. One carat can further be divided into "100" points. Clarity refers to the presence or absence of inclusions and/or micro-fractures, both of which are detrimental to the quality of the stone (Oldenziel, 1997).

1.5.2. Diamond formation and resorption.

Geothermobarometry of small inclusions of silicates, oxides and sulphides in diamonds indicate that diamonds formed at temperatures of 900 to 1400^0 C and pressures of between 40 and 60 kbar, which reflect depths of 150 to 250 km (Boyd *et al.*, 1985 ; Kirkley *et al.*, 1991). As the silica form of coesite, rather than the denser stishovite, is found as inclusions in diamond, and the inversion curve of coesite to stishovite has been calculated at a depth of approximately 305 km, this depth is regarded as the maximum for diamond formation.

Geobarometry involves the analysis of pressure-dependent minerals inclusions in diamonds to determine the pressure under which a mineral or rock formed.

The most important minerals used are ;

(1) aluminium substitution in orthopyroxene (enstatite),
(2) potassium substitution in clinopyroxene and,
(3) sodium substitution in garnet.

Elevated Al, K and Na are indicative of high pressures. As an example the ideal formula for a pyrope-almandine garnet is $(Mg, Fe)_3Al_2Si_3O_{12}$. The relative proportions of FeO and MgO and minor CaO differ as P-type garnets have a higher MgO and lower FeO than E-type garnets (Fipke *et al.*, 1995).

Mineral inclusions in diamonds and mineral assemblages in xenoliths show that diamond formation is associated with two rock types in the lithospheric upper mantle beneath cratons. The most abundant rock type is garnet peridotite (in which harzburgites predominate over lherzolites) and subordinately eclogites (Fig.5).

Diamonds with peridotitic inclusions are known as P-type diamonds and those with eclogitic inclusions as E-type diamonds. Helmstaedt & Gurney (1995) interpreted the predominance of P-type diamonds over E-type diamonds as being due to a chemically highly-depleted, peridotitic mantle incorporating lenses of eclogitised mafic rocks.

The inclusions of the peridotitic suite consist of purple-red Cr-rich pyrope garnet, Cr-diopside, forsterite olivine and enstatite. Although the inclusions are broadly similar to the constituents of the lherzolite and harzburgite upper mantle magma, they are distinctly richer in Cr. Some diamonds are thus derived from the disaggregation of such source rocks. The inclusions of the eclogitic suite consist principally of orange pyrope-almandine garnet, omphacitic pyroxene, kyanite and coesite, which is similar to the eclogite xenoliths found in many kimberlites (Mitchell, 1991 ; Kirkley *et al.*, 1991).

Both peridotitic and eclogitic diamonds occur in every known diamondiferous kimberlite, although peridotitic diamond inclusions are more abundant than eclogitic diamond inclusions. Peridotitic diamonds predominantly formed in chemically depleted peridotite near the base of the lithosphere, between 150 and 200 km, where they were metasomatised in a Ti-poor, LREE, K and Rb enriched event. Eclogitic diamonds are old, but show a range of ages all apparently younger than the oldest Archaean peridotitic diamonds (990 to 2700 Ma) (Fipke *et al.*, 1995).

As diamonds consist of pure carbon it does not contain any of the radiogenic elements used in geochronological techniques. Some of the minute inclusions, such as pyroxene and garnet, in diamonds are used as they contain elements involved in radioactive decay systems.

Richardson *et al.* (1984, 1990) and Richardson (1986) dated diamond inclusions from Kimberley, Finsch, Premier and Orapa and showed that the age of the diamonds are much older than the age of emplacement. The Sm-Nd geochronological method, combined with the Rb-Sr method, gave radiometric model ages for peridotitic diamonds in the range of 3000 to 3300 Ma (Richardson *et al.*, 1984), and for eclogitic diamonds in the range of 990 to 1670 Ma (Richardson *et al.*, 1990).

This indicates that a kimberlite intrusion can obtain diamonds from different geological source areas and that diamond formation and preservation can occur over long periods of time. For example the Finsch kimberlite pipe only intruded at approximately 90 to 100 Ma, compared with the associated P-type inclusions in diamonds giving ages of 3000 to 3300 Ma.

The source of carbon has been established by carbon isotope studies, specifically the ratio of carbon-13 to carbon-12, termed the "delta values". $\delta^{13}C$ values of both eclogitic and peridotitic diamonds mostly fall in the narrow range between -2 to -9 per mil, with a peak between -5 and -6 per mil, which is the area where almost all peridotitic diamonds plot. However, further studies have shown that eclogitic diamonds display a much wider range in $\delta^{13}C$ (from +3 to -35 per mil) than peridotitic diamonds (Miller, 1995).

The differences in the $\delta^{13}C$ values of eclogitic and peridotitic diamonds have been ascribed to different sources of carbon for diamond formation. Peridotitic diamonds were derived from residual carbon from the time of the Earth's creation, and eclogitic diamonds from carbon with a more complex mix of isotopes which may represent carbon thrust down into the Earth's mantle by Archaean tectonic processes (Miller, 1995).

With the formation of diamond only two primary surface textures are described as crystal growth, namely smooth octahedral or cubic crystal surfaces and triangular, stepped, occasionally imbricated octahedral crystals (Gurney, 1989). Smooth-faced octahedral or cubic diamonds crystallised slowly with atom by atom growth. Well-shaped octahedral diamonds grew by dislocation growth in a spiral manner with building blocks on the crystal face of the order of 5 Angstroms in height. Evidence for episodic growth of diamonds are shown by the common mineral inclusions found within diamonds. The diamonds from the Kalahari Craton are mostly fibrous with rough surfaces indicating rapid growth (Gurney, 1990). The other 39 identified surface textures have been interpreted as resorption features by Robinson (1978).

The amount of resorption affects the grade of a diamondiferous kimberlite because highly resorbed diamonds are characterised by rounded dodecahedra (tetrahexahedroid) which have lost as much as 50% of their original mass. Resorption of diamonds depends on the degree of graphitisation, combustion of CO_2 and dissolution in magma. Eggler (1989) states that dissolution in the magma is the most important resorption mechanism noted on all faces of primary octahedra to produce rounded dodecahedra in all kimberlites indicating up to 50% reduction of volume (Fig.19).

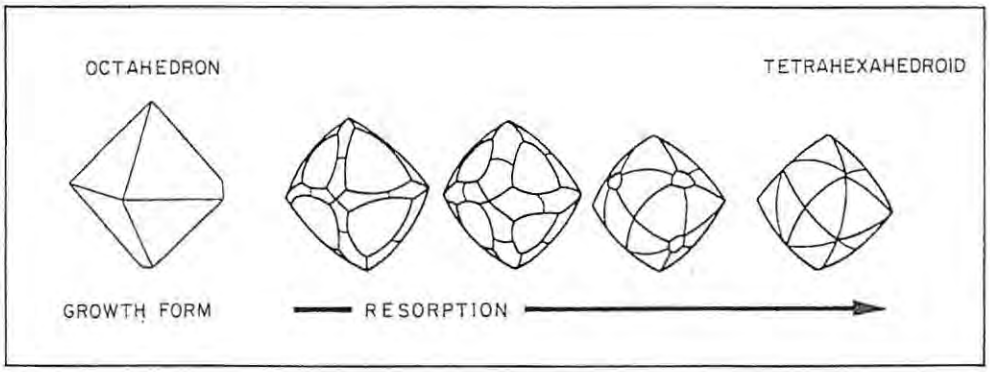

Fig. 19 ; Stages in the conversion (resorption) of a diamond octahedron to a tetrahexahedroid, from Eggler (1989).

2. Exploration techniques.

2.1. Introduction.

Area selection and follow-up prospecting requires a preliminary evaluation of the target area to delineate the most prospective areas within the region. The sequence of exploration techniques routinely used in kimberlite exploration programmes are a literature review on regional kimberlite distributions, tectonic setting and local structural controls, a landscape and surface processes reconnaissance study, indicator mineral sampling, remote sensing-, geophysical-, geochemical-, petrographic-, geobiological and geobotanical assessments and, ultimately drilling and evaluation of a deposit (Table VII).

Table VII ; An exploration programme sequence.

TARGET DEFINITION				
DESK STUDIES	Basic geological research ; (a) Conceptual studies of mineral deposits (b) Synopsis of regional geology	(a) Assessment of mineral resource potential (b) Identification of favourable geological environments		(a) Exploration programme planning (b) Market surveys
ANOMALY DEFINITION				
REGIONAL EXPLORATION	(a) Spectrometry (b) Magnetics (c) Electromagnetics (d) Radiometry	(a) Satellite imagery interpretation (b) Aerial photograph interpretation (c) Cartography		(a) Stream sediment sampling (b) Regional hydrogeochemistry (c) Heavy mineral sampling
PROSPECT DEFINITION				
PROSPECT GENERATION	(a) Detailed geological mapping (b) Fieldwork (c) Petrological analysis (d) Cartography	Detailed geochemistry ; (a) Stream sediment surveys (b) Soil sampling surveys (c) Pitting and trenching surveys (d) Lithogeochemistry	Geophysics ; (a) Spectrometry (b) Magnetics (c) Electromagnetics (d) Induced polarisation (e) Resistivity (f) Gravity	Scout drilling ; (a) Percussion drilling (b) Auger drilling (c) Scout diamond drilling (d) Borehole logging
PRE-FEASIBILTY STUDY				
PROSPECT EVALUATION	(a) Drilling pattern design (b) Detailed structural mapping (c) Detailed geological mapping	(a) Diamond drilling (b) Percussion drilling (c) Geostatistical analysis	(a) Reserve estimations (b) Assessment of infra-structural requirements	(a) Preliminary mineral processing testwork
FEASIBILITY STUDY/FINANCIAL MODELLING				
OREBODY EVALUATION	(a) Design of detailed sampling methods (b) Detailed geological and structural mapping	(a) On-going diamond drilling (b) Trial mining to allow detailed underground mapping, sampling and bulk sampling (c) Geostatistical studies		(a) Computerised orebody modelling (b) Mineral processing testwork on bulk samples (c) Ore reserve estimation
MINING				
MINE PLANNING	(a) Mine open pit design	(a) Geotechnical studies		(a) Plant flow sheet design

2.2. Southern African kimberlite distribution, grades and tonnages, tectonic setting, regional structural controls and intrusion ages.

The first step in any exploration programme is to assess and compile a historical review, present exploration activity and status of operating mines for the target area/s decided upon. Kirkley *et al.* (1991) state that there are more than 3000 known occurrences in Southern Africa alone, ranging from pipes to dykes and sills. The Southern African countries considered are Angola, Botswana, Lesotho, South Africa, Swaziland, Tanzania, and Zimbabwe. The information regarding the Southern African countries has mostly been based on, and adapted from, Cole (1998).

2.2.1. Angola.

2.2.1.1. Kimberlite distribution, grades and tonnages.

Of the 638 known Angolan kimberlite occurrences 300 are reported to be diamondiferous (Janse & Sheahan, 1995). The first kimberlite discovered in Angola was the Camafuca-Camazamba pipe in 1952. It occurs southwest of Lucapa in the Lunda Norte province of northeastern Angola. It has the largest known surface expression in the world at 1.6 km^2 (167.5 ha) and was worked on a small scale in the past. SouthernEra has been granted a 51% interest in the Camafuca-Camazambo kimberlite pipe (Mining Journal Supplement, 1997). A drilling program of 267 core-holes to depths of 120 m was completed and 1600 ct of diamonds, with an average estimated value of US$175/ct, was recovered. SouthernEra believes the pipe consists of at least four intrusive phases with grades varying from 0.78 ct/m^3 to 0.15 ct/m^3 (African Mining, 1998a).

Most of the known kimberlites occur in the Lunda Norte Province, but some are known as far south as the Namibian border. The only producing mine at present is the Catoca pipe north-northwest of Saurimo (African Mining, 1998). The Catoca kimberlite is a joint venture between Endiama of Angola (40%), Almazzy Rossi-Sakha of Russia (40%) and Oderbrecht of Brazil (20%). The consortium plans to produce an initial 235 000 carats/year from 600 000 tons. Grades are reported as about 46 cpht, with a 155 million tons resource, containing 70 million carats. De Beers have found more kimberlites near Catoca (Mining Journal Supplement, 1998).

De Beers, in a joint venture with Endiama, has prospecting rights for kimberlite exploration in parts of Lunda Norte and Lunda Sul provinces as well as in the Quela region of Malanje province and the Mavinga region of Cuando-Cubango province in the southeastern corner of Angola. DiamondWorks is planning to test the Camatchio and Camagico pipes, which are very large but low grade (Mining Journal Supplement, 1998).

Grades vary between 11 cpht (Camatchia) and 50 cpht (Catoca). Camutue 1, Caixepa, Camajico and Camatchia in northeast Angola are all considered to be economically viable (Janse, 1995) and there is a good potential for discovering more kimberlite deposits.

Total diamond production in Angola (1997) was 5.3 million carats worth US$ 806 million (Mining Journal Supplement, 1998). Almost all Angola's production comes from alluvial deposits. The large production from artisanal diggers and widespread smuggling makes the estimate unreliable. Endiama, the state-owned diamond mining company, owns the mining leases and diamonds in Angola by law, but the rebellion movement UNITA controls Angola's richest diamond-producing area, the Cuango Valley (Cole, 1998).

2.2.1.2. Tectonic setting, regional structural controls and intrusion ages.

Angolan kimberlites intruded an Early Proterozoic-Archaean craton, mostly at the intersection of major fault trends. In north-eastern Angola pipes occur at the intersection of north-northwest, east-northeast and, less commonly, east-southeast trending faults. In central Angola the fault trends are northeast, east and south-southeast (Reis, 1972). Host rocks vary from Archaean gneisses to Triassic sandstone and shale, Late Cretaceous sediments of the Calonda and Kwango Formations and extensive Kalahari Group sediments (Helmore, 1984).

Eighteen kimberlites have been dated as Early Cretaceous in age (Allsopp *et al.*, 1989). Kimberlite pipes are the most common, with many still possessing a crater facies indicating limited erosion. Diatreme facies as well as kimberlite dyke occurrences have been noted. Both peridotitic- and eclogitic type diamonds are present (Boyd & Danchin, 1980). Northeast Angola is overlain by extensive Kalahari Group sands (up to 100 m in thickness) which makes exploration difficult. De Beers uses ground magnetics and indicator mineral stream sediment sampling in northeast Angola (Mining Weekly, 1997a).

The alluvial deposits along the Luashima, Luembe, Chicapa, Cuango and Cuanza rivers in the north-central province of Luanda are within 100 km of twenty kimberlite pipes that intrude Proterozoic and Mesozoic sediments. The pipes are Late Jurassic in age and have intruded along a major northeast-southwest zone that fractures the Angola-Kasai shield during Mesozoic time (Cole, 1998).

2.2.2. Botswana.

2.2.2.1. Kimberlite distribution, grades and tonnages.

Janse (1995) reported 140 kimberlites, grouped into 11 clusters, of which 56 are diamondiferous. Orapa was the first pipe discovered in 1967 with follow-up work by De Beers leading to the location of 29 other pipes, including Lethlakane and Jwaneng, and some barren dykes (Baldock, 1977). Stream sediment sampling led to the discovery of Orapa after it was realised that tectonic upwarping during the late Tertiary had cut off the Moutloutse River from its diamondiferous source (Chadwick, 1983).

Orapa started production in 1971, with Lethlakane and Jwaneng soon after. The current production and grades of the three Botswanan mines are given in Table VIII. Eleven other pipes were also discovered in the Jwaneng area (Baldock, 1977). Lethlakane (11.6 ha) is a small mine producing around 5% of the total Debswana production (Oldenziel, 1997). Diamond production in Botswana is owned by De Beers in joint venture with the government-owned Debswana Diamond Company (Pty) Limited.

Orapa (110.6 ha) is the third largest economic pipe after Angola's Camafuca-Camazamba pipe (167 ha) and Tanzania's Mwadui pipe (146 ha). Jwaneng has a surface expression of 56 ha.

Falconbridge/Superior discovered 60 buried pipes in several fields during the late 1970's to early 1980's. Only one pipe, Gope 25, showed some economic potential (Baldock, 1977). A pre-feasibility study is presently being conducted by De Beers on Gope 25. A mining lease for a small complex of fissures and pipes, known as Martins Drift in eastern Botswana, has been granted to De Beers. Trial mining on five small kimberlites at Martin's Drift is in progress by Debswana. AfriOre, Falconbridge, BHP, Ashton Mining and De Beers are currently active in Botswana (Mining Journal Supplement, 1998).

Table VIII ; Economic comparison of the three most important Botswanan kimberlite mines, namely Orapa, Jwaneng and Lethlakane.

Kimberlite Mine	Mined tonnage (1997) (million tons)	Diamond production (1997) (carats)	Average grade (1997) (cpht)
Jwaneng	9	12 million	147
Orapa	8.5	6.7 million	70
Lethlakane	3.4	893 000	34

Sources :

Mining Weekly 1997b

Mining Journal Supplement (1998)

Orapa has a reserve of 80 tons of diamonds and Jwaneng 70 tons of diamonds. Total diamond production in Botswana (1997) was 20.1 million carats worth US$ 1 650 million (Mining Journal Supplement, 1998).

2.2.2.2. Tectonic setting, regional structural controls and intrusion ages.

Eastern Botswana occurs on the Kalahari craton and is overlain by Phanerozoic Karoo Supergroup platform rocks, in turn overlain by Tertiary and Quarternary Kalahari sands (Janse & Sheahan, 1995). More than two-thirds of Botswana is covered by Cenozoic sand, silt and minor calcrete, ferricrete and silcrete of the Kalahari Group, and range in thickness from a few metres at Orapa to 45 m at Jwaneng, 75 m at Gope and up to 140 m in Southern Botswana (Janse, 1995). Most of the kimberlites intrude the basalts, sandstones and mudrock of the Karoo Supergroup, although Jwaneng intrudes sandstone and mudrock of the Proterozoic Transvaal Supergroup and Archaean granite, whilst the Martin's Drift pipe intrudes Archaean gneiss of the Limpopo mobile belt (Cole, 1998).

Structural controls were inferred at Gope 25, which is located along a northwest trending fracture zone, and Jwaneng, which occurs at the intersection of northwest, north-northeast- and northeast-trending lineaments and fracture zones (Cole, 1998). The Orapa pipe occurs at the intersection of a northwest- and west-northwest fracture set (Baldock, 1977).

Orapa (90 Ma) and Lethlakane are Cretaceous in age and Jwaneng Early Triassic (Allsopp *et al.,* 1989). Eclogitic-type diamonds predominate over peridotitic-type diamonds at Orapa (nearly 90% eclogitic) and Jwaneng (Gurney, 1990). Most of the pipes have a crater and diatreme facies developed (Zweistra, *et al.*, 1998).

Good potential for further discoveries remain, although surficial Cenozoic Kalahari Group sediments of up to 200 m in thickness inhibits heavy mineral exploration effectiveness. The presence of Stormberg Group basalt north of latitude 24^0 S reduces the effectiveness of the magnetic method. The predominance of crater facies indicates that minor, if any, erosion has occurred prior to the blanket cover of Kalahari Group sediments. Only one diamondiferous kimberlite (Martin's Drift) actually outcrops, therefore stream sediment and soil sampling for indicator minerals in combination with low-level airborne and ground magnetic surveys are the main exploration techniques used (Cole, 1998).

2.2.3. Lesotho.

2.2.3.1. Kimberlite distribution, grades and tonnages.

The diamondiferous Kao 1 pipe was discovered in 1954, although other barren kimberlites were known by that time (Janse, 1996). The first kimberlites were found by locating abandoned workings that had exploited the ilmenite for pigments. Later stream sediment kimberlite indicator minerals sampling, airborne and ground magnetic surveys, photogeology, pitting and drilling was used as exploration tools (Cole, 1998).

In total about 180 kimberlites have been discovered, of which 8 in northern Lesotho, were diamondiferous (Nixon, 1973). No deposits are being mined in Lesotho at present. The bulk testing of the Liqhobong kimberlite in northern Lesotho has been completed by Messina Diamond Corporation and the assessment is in its final feasibility stage (Mining Journal Supplement, 1997, 1998).

2.2.3.2. Tectonic setting, regional structural controls and intrusion ages.

The Lesotho kimberlites occur on the eastern boundary of the Kaapvaal craton. Only the Hololo kimberlite intrudes sandstone of the Triassic Clarens Formation, whilst all the other kimberlite occurrences intrude basalt of the Jurassic Drakensberg Group (Cole, 1988).

Two of the eight diamondiferous kimberlites in the northern Lesotho are Cretaceous in age (Allsopp *et al.*, 1989). Peridotitic- and more rarely eclogitic nodules occur (Nixon, 1973). The diamondiferous kimberlites occur as pipes, with only Hololo consisting of two oval and linked dyke enlargements, situated on a west-northwest trending dyke (Dawson, 1962).

The majority of the barren dykes have a pronounced west-northwest orientation which is the regional joint direction in the Karoo Supergroup and several pipes are clustered where this trend is intersected by west-southwest fractures. Eluvial and colluvial basalt-derived gravels of up to 10 m in thickness cover the pipes. Diatreme facies predominate with only the Kao pipe having crater facies sediments (Rolfe, 1973). Resources vary from 30 000 to 8 million carats in the eight diamondiferous kimberlites (Cole, 1998).

2.2.4. South Africa.

2.2.4.1. Kimberlite distribution, grades and tonnages.

Jagersfontein, 1870, was the first kimberlite-hosted diamond occurrence found in South Africa. Shortly thereafter Dutoitspan and Bultfontein were discovered. Following the discovery of diamonds on the farm Vooruitzigt (1871) the Kimberley and De Beers mines were found in close proximity. Wesselton was found in 1890, only 3 km east of the Dutoitspan and Bultfontein pipes. About 15 additional pipes were found around Kimberley, but only the original four, plus the Wesselton pipe, became large producers (Janse & Sheahan, 1995).

In 1903 the large Premier pipe, 30 km east of Pretoria, was found by tracing alluvial diamonds which lay to the west of the pipe. The Jagersfontein and Koffiefontein pipes were discovered in the Orange Free State and kimberlite dykes at Barkly-West, Boshoff and Theunissen. Finsch was discovered in 1960 near Postmasburg and the Venetia pipe near Messina in 1980 (Cole, 1998). Klipspringer, 50 km southwest of Pietersburg, was found in 1995 (Lynn *et al.*, 1998). The Klipspringer deposit is made up of two kimberlite dykes, the Sugarbird and Leopard, and a number of blows, of which M-1 (situated on the farm Marsfontein) is the richest (Mining Journal Supplement, 1998).

Trans Hex runs a few dump treatment operations around Bellsbank, Sover and Roberts Victor mines in the Kimberley area and, operated the Dokolwayo mine in Swaziland. Rex Diamond Mining Corporation operates the Ardo Mine near Barkly West, a mine at Bellsbank, and an operation at Star near Theunissen. The Klipspringer project near Potgietersrus in the Northern Province is operated by SouthernEra, who have a 40% stake. De Beers own the other 60% shares (Cole, 1998).

There are 30 producing kimberlite mines with 18 exploiting dykes and 12 exploiting pipes (Mining Journal Supplement, 1997). The production and grades from the five most important kimberlite mines are shown in Table IX. Premier has an estimated 35 tons of diamond resource, Finsch 30 tons, Venetia 20 tons and Koffiefontein, Jagersfontein and the five Kimberley pipes between 1 and 10 tons of diamonds (Cole, 1998).

Table IX ; Economic comparison of the five most important South African kimberlite mines, namely Venetia, Finsch, Premier, Kimberley and Koffiefontein.

Kimberlite Mine	Mined tonnage (1997) (million tons)	Diamond production (1997) (carats)	Average grade (1995) (cpht)
Venetia	3.4	4.3 million	12.7
Finsch	3.7	2.2 million	75
Premier	3.2	1.4 million	50.6
Kimberley	3.8	612 000	100
Koffiefontein	2	136 000	7.5

Sources :
Mining Weekly 1997b
Mining Journal Supplement (1998)
Jennings (1995)

Grades in pipes vary from 0.5 cpht at Schuller Annex (near Premier) to 121 cpht at Venetia, and in dykes from 4.2 cpht at Salpeterpan (near Kimberley) to 500 cpht at Helam Mine (near Swartruggens) (Klump & Gurney, 1998). Some of the other well known pipe grades are Bultfontein 40 cpht, De Beers 90 cpht, Dutoitspan 20 cpht, Jagersfontein 7 cpht, Wesselton 27 cpht and Marsfontein 300 cpht.

The first bulk sample taken from the Klipspringer project consisted of 188 tons of primary kimberlite containing 264 diamonds with a total weight of 153 carats, running at a grade of 0.81 ct/t (Oldenziel, 1997). At present the Marsfontein reserve (Klipspringer project) is producing very good results - in the first 17 days of production a total of 179 950 carats were recovered from 22 960 tons, for a recovered grade of 652 cpht. This extreme enrichment is only found in the eluvial gravels on top of the weathered kimberlite pipe. Rough diamonds with a value of about $60 million had been mined in the first eight weeks of production, sufficient to pay of the development capital (Business Day, 1998).

Total diamond production in South Africa (1997) was 10.1 million carats worth US$ 983 million (Mining Journal Supplement, 1998).

2.2.4.2. Tectonic setting, regional structural controls and intrusion ages.

There are 935 known kimberlite occurrences in South Africa, of which 145 are diamondiferous. Of the diamondiferous occurrences 89 are pipe-like, 53 dyke-like and 3 low-grade sill-like kimberlites. No crater facies have been recognised and most of the pipes are characterised by diatreme- and hypabyssal facies.

Most of the well-known diamondiferous pipes have a surface area between 5 and 30 ha. The sizes of pipes in the Kimberley area are Kimberley (3.7 ha), De Beers (5.1 ha), Dutoitspan (10.6 ha), Bultfontein (9.7 ha) and Wesselton (8.7 ha). The sizes of the other important kimberlites in South Africa are Venetia (12.7 ha), Premier (32.2 ha), Jagersfontein (10 ha), Koffiefontein (10.3 ha) and Finsch (17.9 ha).

The presence of Archaean kimberlites has been deduced from diamonds recovered from the Witwatersrand Supergroup (2500 Ma). Known kimberlite intrusion ages range from 1180 Ma for Premier to 84 Ma at Bultfontein, but the majority have been dated as mid-Cretaceous in age ranging from 80 to 100 Ma (Allsopp *et al.*, 1989).

The Cambrian-aged (550 Ma) Venetia pipe is situated in the Limpopo Mobile Zone (LMZ) (Allsopp *et al.*, 1985). Because the LMZ had stabilised by the Late Archaean, it forms part of the Kalahari Craton.

Micaceous Group II kimberlites have ages ranging from 200 to 113 Ma, whereas younger kimberlites are of Group I affinity (Smith & Barton, 1995). The Group I source was tapped only sporadically prior to 113 Ma and the Group II source was completely eliminated as a kimberlite source after 113 Ma (Smith & Barton, 1995). The intrusion of kimberlites can also occur in the same area at different ages. An example is the Precambrian dykes in the Wesselton area and the Cretaceous Wesselton kimberlite (Janse, 1985).

There is a general peridotite : eclogite source abundance ratio of 3 : 1 for diamonds in South Africa, although some individual localities, such as the Kimberley Mine have peridotitic diamonds that comprise up to 90% of the total population. All diamondiferous kimberlites have sampled diamond peridotite and eclogite, although peridotite predominates in Group I kimberlites (Gurney, 1990).

Northwest- and southeast trending fractures are the main structural controls for kimberlite emplacement in South Africa (Friese, 1998). Kimberlite dykes occupy both sets of fracture zones and some kimberlite pipe clusters occur where these Phanerozoic fracture zones intersect major Archaean crustal fault systems within the craton (Friese, 1998). The fragmentation of Gondwana during the Cretaceous triggered the main period of kimberlite intrusion with the main structural controls being deep fractures, faults or shear zones (Friese, 1998).

2.2.5. Swaziland.

2.2.5.1. Kimberlite distribution, grades, tonnages and tectonic setting.

The Dokolwayo kimberlite pipe (2.8 ha), intruded into Archaean granite-gneiss (Daniels & Gurney, 1989). The upper portion of the pipe consists of diatreme facies implying severe erosion and removal of the crater facies since Late Triassic times (Turner & Minter, 1985). The kimberlite is a Group II type and has sampled both diamond peridotite and diamond eclogite (Daniels & Gurney, 1989). The deposit is small, with < 1 ton of diamonds grading 40 cpht. Production ceased in 1996 having produced 0.65 million carats between 1983 and 1995 (Janse, 1995).

2.2.6. Tanzania.

2.2.6.1. Kimberlite distribution, grades and tonnages.

Seven kimberlite deposits have been economically exploited in the past, namely Mabuki, Mwamanga, Usongo (Nzega), Kizumbi, Uduhe, Kahama and Mwadui Mines. The Mabuki pipe was the first kimberlite discovery in 1910 and thereafter several diamondiferous kimberlites were discovered between Lake Victoria and Tabora (Gobba, 1989). In 1926, Mwadui (146 ha), which is the second largest kimberlite in Southern Africa, was discovered 25 km northeast of Shinyanga. The Mwadui pipe is operated by Williamson Diamonds Limited, a joint venture between De Beers and the Tanzanian government. Mwadui is a large pipe with a crater of up to 1500 m in diameter and up to 300 m deep (Janse & Sheahan, 1995). Additional pipes were subsequently discovered around the Mwadui pipe.

The kimberlite deposits are generally small with less than 1 million carats, with Mwadui being the exception at 10 tons of diamonds, having produced 4 tons of diamonds up to 1992 (Dirlam *et al.*, 1992). Grades are very low in the primary kimberlites ranging from 0.6 to 6 cpht, but grades are considerably higher in the overlying eluvial and colluvial gravels grading 10 to 12 cpht (African Mining, 1996). Only the Mwadui pipe is being mined at present with 20 million carats produced from 1925 to 1995. The Williamson diamond mine produced 116 750 carats during 1997. Total diamond production in Tanzania (1997) was 127 000 carats worth US$ 19 million (Mining Journal Supplement, 1998).

2.2.6.2. Tectonic setting, regional structural controls and intrusion ages.

Over 400 kimberlites have been discovered in Tanzania of which 54 are diamondiferous (Janse & Sheahan, 1995). All the diamondiferous kimberlites occur on-craton and have intruded Archaean granite, gneiss, phyllite, schist, amphibolite, quartzite and banded ironstone, as well as Late Proterozoic dolerite dykes. Most of the kimberlites occur in three clusters, in a belt approximately 150 km wide (Edwards & Howkins, 1966). Surface diameters of pipes in Tanzania vary from a few metres to 146 ha (Mwadui pipe). Diatreme facies rocks are predominant, with the Mwadui pipe being an exception as it comprises a 300 m thick crater facies (Edwards & Howkins, 1966). Dykes and sills are common but rarely exceed a few metres in thickness (Gobba, 1989).

Age dating for Mwadui has given ages of 45 Ma and 52 Ma, respectively, Nzega 53 Ma (Gobba, 1989), and a kimberlite near Bubiki northwest of Shinyanga 1097 Ma (Kashabano, 1989). Peridotic and eclogitic-type diamonds are present (Nixon & Condliffe, 1989).

Kimberlites in the Mwadui area intruded along deep-crustal lineaments and occur at the intersections of major lineaments, shears and fractures. The Mwadui pipe is situated within a northwest trending shear zone, a northeast to southwest trending dolerite dyke swarm and a prominent north-northeast to south-southwest aeromagnetic lineament. Other lineaments in the area also follows this orientation, including Nzega, Kilimatinde and Rungwa wrench faults. The lines of weaknesses that occur at the granite-greenstone contacts also seem to localise kimberlite emplacement (Gobba, 1989).

South of Lake Victoria more than 120 kimberlite structures intrude the ancient granite shield. Many are associated with lines of weakness such as fault zones or the contact between basement granite and pendants of metasediments which generally lie in a very broad zone trending north-northwest for 300 km from southern Lake Victoria (Dawson, 1970).

Since 1945 exploration programmes have relied mostly on airborne magnetic- and electromagnetic surveys, as well as stream sediment sampling and soil sampling of kimberlite indicator minerals, as the primary exploration techniques (Dirlam *et al.*, 1992). Geophysical techniques are used to detect kimberlite bodies obscured by the thick cover of laterite and other superficial sediments characteristic of Tanzania. Heavy mineral sampling has found limited success in areas of low relief and recent alluvial cover, such as the Manonga-Wembere depressions, covered by thick lacustrine deposits and the Itigi-Manyoni area, characterised by thick terrestrial deposits. The latter area contains a large number of kimberlite indicator grains in post-Cretaceous sediments (Gobba, 1989).

2.2.7. Zimbabwe.

2.2.7.1. Kimberlite distribution, grades and tonnages.

The first diamondiferous kimberlite, Colossus, was first discovered in 1907, 106 km southwest of Gweru (Stocklemayer, 1981). Other kimberlites were discovered soon thereafter between Bulawayo and Gweru. Janse (1995) lists 30 kimberlites, seven of which were diamondiferous, that were found up to mid-1995. In 1996 airborne and ground magnetic surveys, together with indicator-mineral sampling, led to the discovery of a kimberlite 80 km north of Beitbridge (Mining Weekly, 1996).

Grades vary from 0.55 cpht at Shingwize, 61 km southwest of Chiredzi, to 42.8 cpht at River Ranch (Stocklemayer, 1981 ; Mining Weekly, 1997c). Deposit sizes are small with River Ranch being the largest with a diamond resource of 4.5 million carats (Janse, 1995). There are no producing kimberlite mines in Zimbabwe at present, although River Ranch produced 0.864 million carats or 98% of the cumulative production in Zimbabwe, to the end of 1996 (Janse, 1996 ; Mining Weekly, 1997d). River Ranch produced 464 000 carats, worth US$ 17 million, until it closed down in 1998 (Mining Journal Supplement, 1998). In addition to River Ranch, 3 other diamondiferous kimberlites have been exploited on a small scale between Bulawayo and Gweru, the highest production being 143.6 carats from the Colossus pipe (Stocklemayer, 1981).

Total diamond production in Zimbabwe (1997) was 464 000 carats worth US$ 8 million (Mining Journal Supplement, 1998).

2.2.7.2. Tectonic setting, regional structural controls and intrusion ages.

Diamondiferous kimberlites are widely spaced, being located northeast of Hwange, between Bulawayo and Gweru, southeast of Chiredzi and in the region of Beitbridge. Six of the seven diamondiferous kimberlites are pipes and the other, Wessels, is a sill (Cole, 1998). The kimberlites mostly intruded granite and gneiss of the Archaean Kalahari craton, which includes the Limpopo Mobile Belt.

The Colossus pipe, 50 km northeast of Bulawayo, intruded during the Cambrian (Allsopp *et al.*, 1985) and the River Ranch pipe, 12 km northwest of Beitbridge, during the Silurian (Allsopp *et al.*, 1995). The Sebungwe kimberlite, 82 km northeast of Hwange intrudes Karoo Supergroup sediments and is post-Triassic in age (Stocklemayer, 1981).

There seems to be a link between the timing of kimberlite emplacement and Pan-African orogenesis of the River Ranch and Venetia pipes (Allsopp *et al.*, 1995), whilst the post-Triassic Sebungwe pipe could be associated with the development of the northeast trending Mid-Zambezi rift valley (Stocklemayer, 1981).

Most of the pipes are small, with the largest Towla, 80 km north of Beitbridge, having a surface area of 17 ha (Mining Weekly, 1996). The Wessels sill, 55 km northeast of Bulawayo, averages 1 m in thickness, dips 16 degrees west-southwest and has a strike-length of at least 365 m (Hawthorne, 1968).

Stocklemayer (1981) and Allsopp *et al.* (1985) describe the occurrence of both diatreme and hypabyssal facies kimberlite. Inclusions of both eclogite- and peridotite-type diamonds have been reported (Hawthorne, 1968)

About 25 kimberlites were known in Zimbabwe up to 1994, but recent prospecting activities have increased this number. The Reunion company alone has reported 35 kimberlite bodies, unfortunately all are barren (Holloway, 1997). Several Canadian- and Australian-based junior companies, Rio Tinto and De Beers are actively prospecting in the country (Janse & Sheahan, 1995).

Since most of Zimbabwe is underlain by the Kalahari Craton, there is potential for discovering more kimberlite bodies, particularly in the northwestern part of the country where a cover of Cenozoic Kalahari Group sediments is present. Most of Zimbabwe, however, is comprised of Archaean basement rocks and extensive erosion has led to the preservation of only diatreme or hypabyssal facies.

2.3. Landscape analysis and surface processes.

The geomorphological evolution of the landscape subsequent to kimberlite emplacement determines the degree of preservation. Uplifted areas are subject to erosion and removal of the upper levels of the kimberlite, whilst subsidence leads to the burial of the kimberlite by younger sediments. Regional soil or stream sediment sampling, detailed geological mapping and geophysical surveys can only be planned after a landscape analysis has been completed.

Most known kimberlite occurrences have experienced varying degrees of erosion. The worldwide average rate of erosion of 1 m per 30 000 years suggests that a kimberlite pipe will erode down to the root zone in 69 Ma (Kirkley *et al.*, 1991). Hawthorne (1975) estimated that erosion removed about 1400 m of the Karoo Supergroup in South Africa as well as the intrusive kimberlite occurrences within them.

The present day land surface intersects many of the pipes about 500 m above the base of the diatreme facies. Extrapolating pipe walls upwards from the base of the diatreme at an angle of 82^0 indicated that the major pipes in the Kimberley district probably had craters of the order of 1 km in diameter.

The erosion levels of Southern African Cretaceous pipes illustrates denudation rates of between 3 and 12 m per million years, ignoring pipes that may have been protected from erosion by younger cover formations. The erosion levels of some well known kimberlite mines are shown in Fig.20.

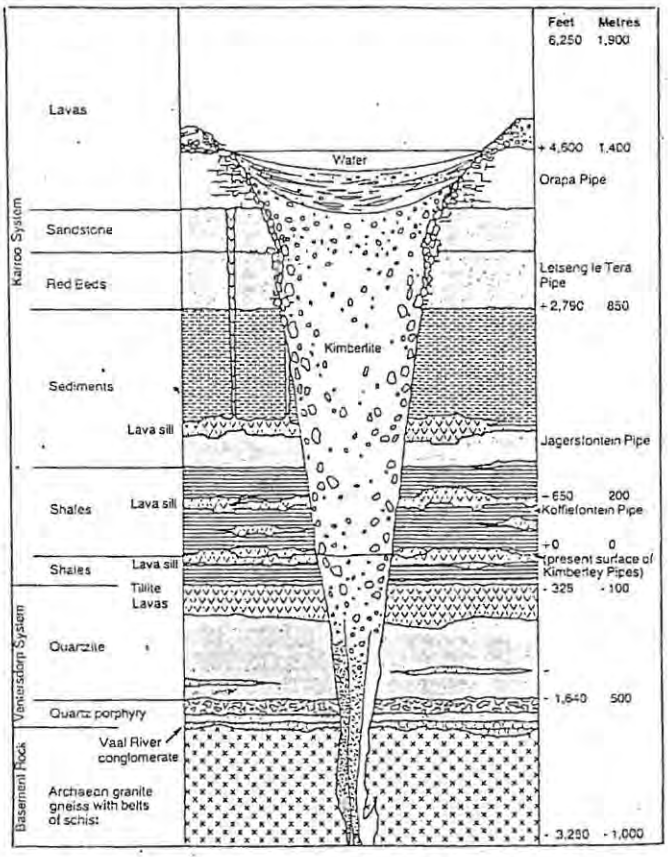

Fig. 20 ; Composite section through a kimberlite pipe with examples of the erosion levels of some well known pipes. The surface of the Kimberley pipes is taken as the datum, from Cox (1978).

The existence of preserved diatremes of Proterozoic age implies that widespread transgressive deposition of sediments over cratons and their margins has interrupted denudation (Nixon, 1995). Where pipes have intruded platform rocks a large part of the diatreme zone, and in rare cases, the crater zone may be preserved. South African examples are the barren kimberlites at Kuruman, which intruded at 1600 Ma (Shee *et al.*, 1989), and the diamondiferous Premier kimberlites, which intruded at 1200 Ma (Allsopp & Kramers, 1977), that were buried beneath intra-cratonic sediments and basaltic lavas of the Karoo Supergroup.

In contrast, deposition of platform sequence rocks or surficial overburden during, or subsequent to, kimberlite intrusion may preserve and conceal diamondiferous kimberlites. As an example Kalahari Group sediments, mostly sands, are developed extensively over Botswana and range in thickness from a few metres at Orapa to an average of 45 m at Jwaneng, 75 m at Gope and up to 140 m in Southern Botswana (Janse, 1995).

Surface processes govern the amount of indicator minerals present in the dispersion halo or alluvial drainage and depends on ;

(1) the content of the kimberlite host rock,
(2) the transport distance involved which leads to the physical/mechanical destruction of indicator minerals down-stream and,
(3) the chemical destruction of indicator minerals in the weathering profile (especially in lateritic environments).

The influence of the weathering environment on garnet grains was studied at the ferricretised Goedgevonden kimberlite, in the North West Province (South Africa). The study showed that a marked decrease occurred in grainsize and quantity of garnets recovered with depth. This was attributed to progressive chemical leaching and physical fracturing of garnets during lateritic weathering. The larger grainsize and quantity of garnets on surface was ascribed to residual concentration due to deflation processes. Ilmenites and chrome diopsides did not show chemical dissolution to the same extent (Henckel, 1992).

Therefore, the surface processes active in a given target area will influence the selection of the sampling methodology used for indicator mineral sampling.

2.4. Indicator mineral sampling.

The abundance of indicator minerals, relative to diamonds, and their resistance to chemical and physical weathering have made them suitable exploration indicators for kimberlite occurrences. Erosion of kimberlites releases and disperses these minerals by soil creep or sheet wash into topographic lows and drainage systems. They tend to concentrate, together with diamonds, in the fluvial environment because of their high specific gravity. The important indicator minerals, in decreasing order of resistance to weathering are ; zircon, chromite, picro-ilmenite, pyrope- garnet, chrome diopside, rarely olivine and phlogopite.

The morphological features on garnet, ilmenite or chromite indicator surfaces can further be used for identifying secondary physical abrasion or chemical weathering characteristics. This is useful in estimating the dispersion distance from the primary source and the influence of chemical weathering on the indicators. The primary surface- and chemical decomposition (resorption processes) features, as well as the mechanical abrasion (fluvial or surface processes) features of diamonds and indicator minerals should be noted, as it provides insight into the nature of kimberlite source and subsequent erosional history of these minerals (Appendix I and II).

The distribution of the recovered indicator minerals are plotted to delineate areas for follow-up geochemical and indicator mineral sampling, geophysical and structural interpretation, geological mapping and ultimately drilling.

A heavy mineral concentrate is produced from the sampled material and the indicator minerals extracted or "picked" by the use of a binocular microscope. The development of the electron microprobe has facilitated rapid analysis of the chemistry of individual mineral grains. The study of diamond inclusions and of the chemistry of minerals in known diamondiferous and barren kimberlites has led to the major advantage that indicator minerals can now be used to discriminate between the probability of finding diamondiferous versus barren kimberlites (Gurney & Zweistra, 1995).

Use of mineral chemistry, especially pyrope garnets, chrome spinels and ilmenites, followed by microdiamond analysis was succesfully pioneered by Falconbridge in Botswana for determining which of many pipes found under deep sand cover should be sampled (Jennings, 1995). Notable diamond mines discovered by indicator mineral sampling include Mwadui (Tanzania), Finsch (South Africa), Orapa/Lethlakane (Botswana), Jwaneng (Botswana), Venetia (South Africa) and the recently discovered Klipspringer and Marsfontein occurences in South Africa.

2.4.1. Sampling programmes.

2.4.1.1. Sampling type.

When exposed at surface kimberlites rapidly weather to clay and/or residual mineral and rock components. The weathering and dispersal rate of kimberlite indicator minerals into the regolith, and the survival in the secondary environment, depends on the weathering and erosional processes active and the lithological- and geomorphic nature of the terrain. Landscape analysis and the surface processes active in the target area require investigation in order to define the most appropriate type of sampling method, size fraction and sampling interval.

During sampling cognisance has to be taken of possible contamination from cultural features such as roads, fences, powerlines, railway lines, old diggings or excavations, rural-, farming- and built-up areas or geomorphological features such as pans and deflation surfaces. Additional comments are also useful for future follow-up sampling and especially during geophysical surveys as it may explain anomalous data.

The recording and plotting of sampling positions should be accurately represented on basemaps. Accurate navigation to, and collection of, samples at the planned positions are necessary and can be facilitated by using 1 : 50 000 topographic sheets, aerial photographs, measuring tapes or hand-held GPS.

Drainage sampling.

Stream sediment sampling is the most effective in areas of high relief, with well developed and complex drainage systems, both of which are favourable to the physical dispersion of indicator minerals and diamonds. Aerial photographs and topographic maps are useful in planning the most effective sampling positions. Even areas of low relief with rudimentary drainage networks are conducive to stream sediment sampling. The advantage of stream sediment sampling is that the whole drainage basin can be assessed rapidly.

The selection of regional stream sediment sampling density depends on the overall regional trap site quality, regional geology, topography and geomorphology, maturity of rivers and drainage density (Fig.21).

Sedimentary or acidic igneous rocks, mountainous terrain and a good network of fairly immature rivers affords a greater sampling spread because of good trap site availibility.

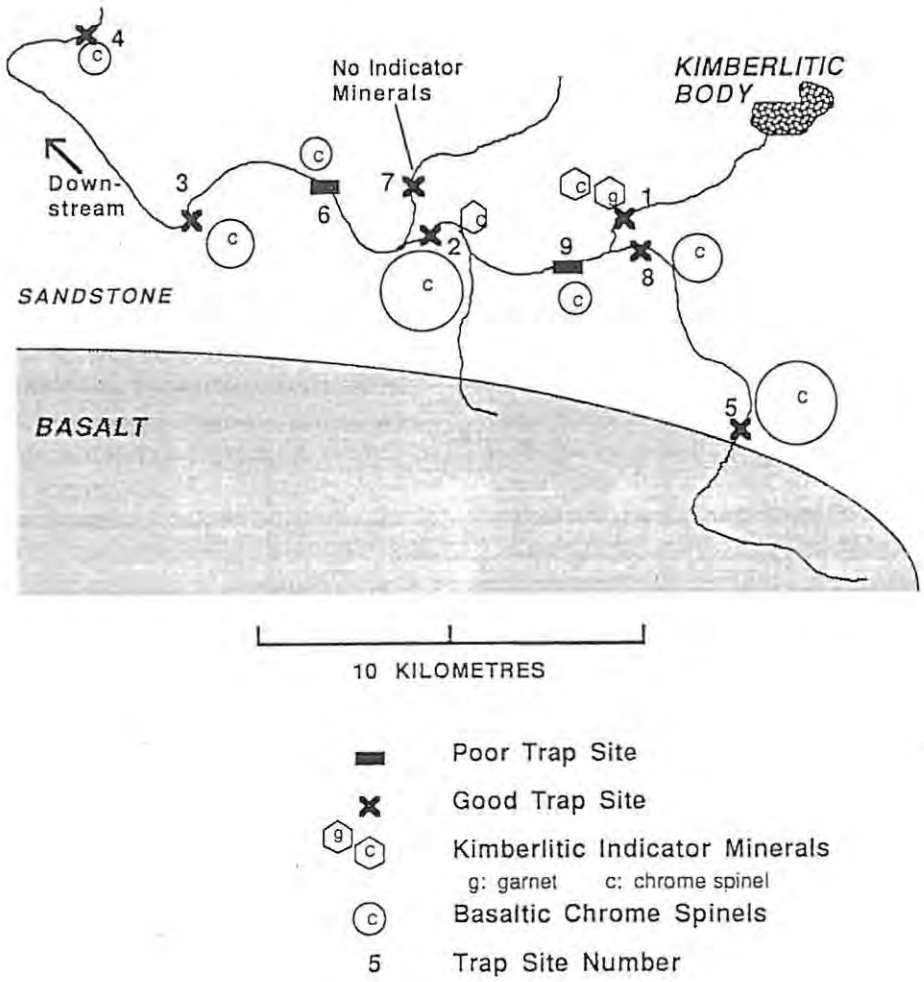

Fig. 21 ; Drainage sampling, from Muggeridge (1995).

Indicator minerals have high specific gravities and accumulate in trap sites where gravels have been deposited in the riverbed. The most likely trap sites are amongst large boulders and bedrock projections or in depressions or bedrock cavities such as potholes and crevices. Gregory & White (1989) describe the best trap sites, in general decreasing order of importance as, large fossil or active pot-holes or gravel-filled depressions in the stream bed, plunge pools near the base of waterfalls, the lee of rock bars and basal gravel accumulations.

Muggeridge (1995) describes the factors that control heavy mineral concentration within fluvial systems as ;

(1) particle sorting at grain, bed, bar and system scales and bed roughness characteristics,
(2) natural jigging and sagging processes, operating at the deeper levels of the flow regime,
(3) lateral, rather than downstream, flow separation effects around a midstream obstacle,
(4) constrictions in the flow regime,
(5) packing effects and coarse clastic alluvial frameworks (gravel that is clast-supported, poorly sorted and tightly packed is suitable for heavy mineral concentration),
(6) grain size and shape ; spherical grains are mobilised at lower water flow speeds relative to prismatic grains with respect to traction movement, but at higher flow rates the latter are more easily transported and,
(7) bed sediment porosity.

Fig.22 is a useful rating of river sample sites as proposed by Muggeridge (1995).

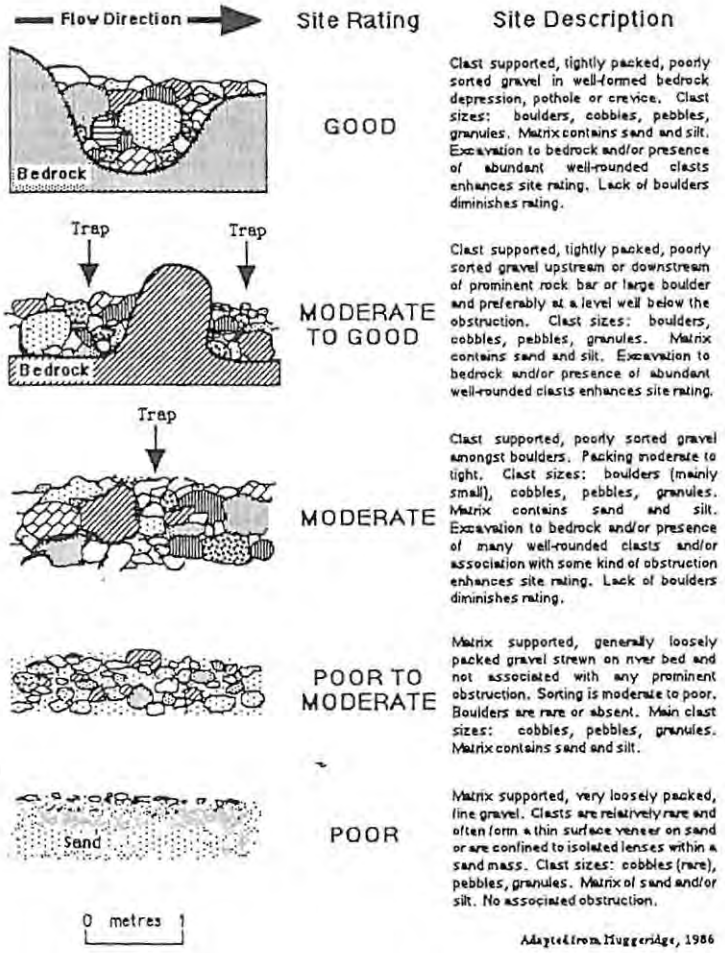

Fig. 22 ; River sample site classification, from Muggeridge (1995).

An upstream train of anomalous indicator minerals should theoretically lead to a kimberlitic source. Ilmenite and spinel, and subordinately garnet, are the most resistant minerals in the warm, seasonal rainfall climate of Southern Africa. Reconnaissance stream sediment samples are usually between 8 and 20 kg in weight, collected at 3 to 15 km intervals along streams or 1 sample per 50 km^2.

Follow-up sampling depends on the dispersion and abundance of indicator minerals from the regional work - a small number of recovered indicator minerals will require a denser sampling spacing. The screening or selection of sample size depends on the nature of the sampled material with fine sand requiring smaller screen sizes, although a minimum grain size of 0.3mm is a practical cut-off for laboratory treatment (Muggeridge, 1995).

Soil sampling.

Dispersed material, including indicator minerals, typically range from 2 mm to < 0.5 mm in size. Low relief areas with poor drainage are more susceptible to regional grid soil sampling. A rudimentary idea of the expected depth of overburden is important as soil cover of 10 m or more of transported material effectively masks the kimberlite. Additional geophysical methods and deflation- as well as termite mound sampling methods are successfully employed in Southern Africa. In locations where bioturbation is active, for example the Kalahari region, deflation zone sampling is often effective whilst in rocky areas like Kimberley, trap site sampling becomes important (Jennings, 1995).

Regional sample grid spacings may vary from 1 km by 1 km to 200 m by 200 m. Follow-up detailed sampling is usually carried out on 100 m by 100 m grids or smaller. The dry climate, weakly developed drainage systems and residual or transported overburden associated with the Southern African landscape has led to the development of grid sampling of the top centimeter of soil, or deflation surface. It is common practice to use only the material at the surface, in other words the top 1 cm or so of soil, based on the concept that lighter material would have been removed by wind action, leaving a relative concentration of heavier minerals on the deflated surface. Concentrations of soil at the base of grassy clumps and boulders or rocks is also sampled preferentially.

Dispersion haloes for coarse grain sizes could be up to six times the pipe diameter (Atkinson, 1989). In residual overburden a circular anomaly may indicate a kimberlite pipe and a linear anomaly a dyke swarm or palaeodrainage system. Biological factors, such as termite activity, is beneficial in areas with transported overburden. An initial grid-patterned soil sampling programme at 1.5 km spacing, typically collecting 15 kg dry samples, will then be followed up depending on the recovery of indicator minerals.

A grid soil sampling programme is used as a local sampling method covering the whole area systematically or in follow-up sampling of magnetic- or stream sediment sampling targets. Alternatively, a point sample can be collected at the center of a target anomaly, generated for example by geophysical or indicator mineral sampling methods, with samples taken from 50 to 100 m north, south, east and west of the sample position (Fig.23). For follow-up grid sampling a "loam" soil sample is preferable to a deflation sample. A sample is taken 20 cm below surface, in the B-horizon (zone of accumulation or illuviation), with the idea that it represents the concentration of the heavy indicator minerals within the underlying weathered regolith.

In the Mwadui area of Tanzania heavy mineral grid and point sample surveys were used over airborne magnetic anomalies to confirm the presence of kimberlite bodies. Soil samples, ranging from 10 to 15 kg in mass, were taken at 50 m intervals over the anomalies. The coarse fraction (+ 0.5 mm) was hand gravitated in the field. The indicator mineral suite consisted of red-brown pyrope (discrete nodule suite), purple-red chromium pyrope (depleted lherzolite suite), ilmenite, chromium diopside (depleted lherzolite suite) and a few coarse chromite, enstatite and olivine grains (Gobba, 1989).

Grid sampling is the most effective in the following environments;

(1) flat-lying poorly drained terrain where stream sediment sampling is less effective,
(2) where prospective target zones have been localised through stream sediment sampling, geophysical or other methods and,
(3) where anomalous features are of sufficient interest to warrant a detailed analysis.

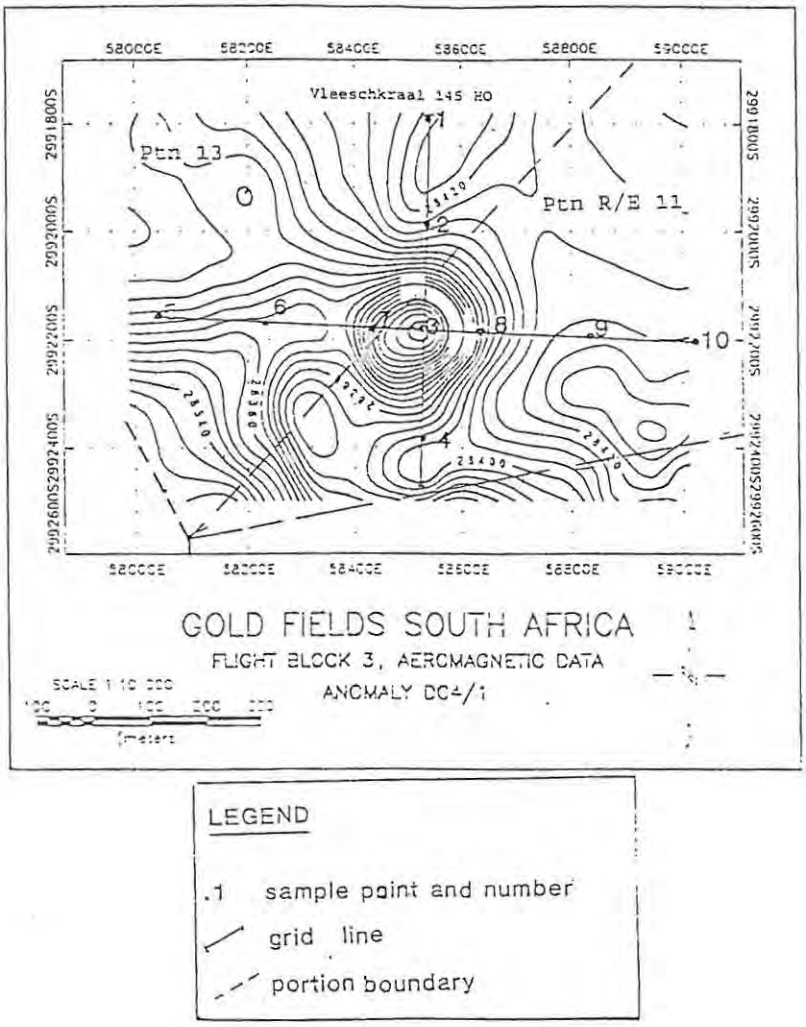

Fig. 23 ; An example of a point sample taken over an acromagnetic target.

In Southern Africa regional soil sampling grids with point spacings of 1 km and more have been used with success. As mentioned before, in order to recover the maximum potential of ilmenite, pyrope and chrome diopside indicators a minimum cut-off size of 0.3 to 0.4 mm is required. Fig.24 is an example of the detection limit - a 500 m spacing would be unreliable for small to medium size bodies (up to 10 ha), but would be unlikely to miss larger bodies of about 20 ha (Muggeridge, 1995).

The follow-up sampling from anomalous grid soil sampling usually entails grid sampling at closer spacing, ground geophysics and/or geochemistry. If a kimberlite source is confirmed drilling, pitting or excavation will be done followed by bulk sampling (Muggeridge, 1995).

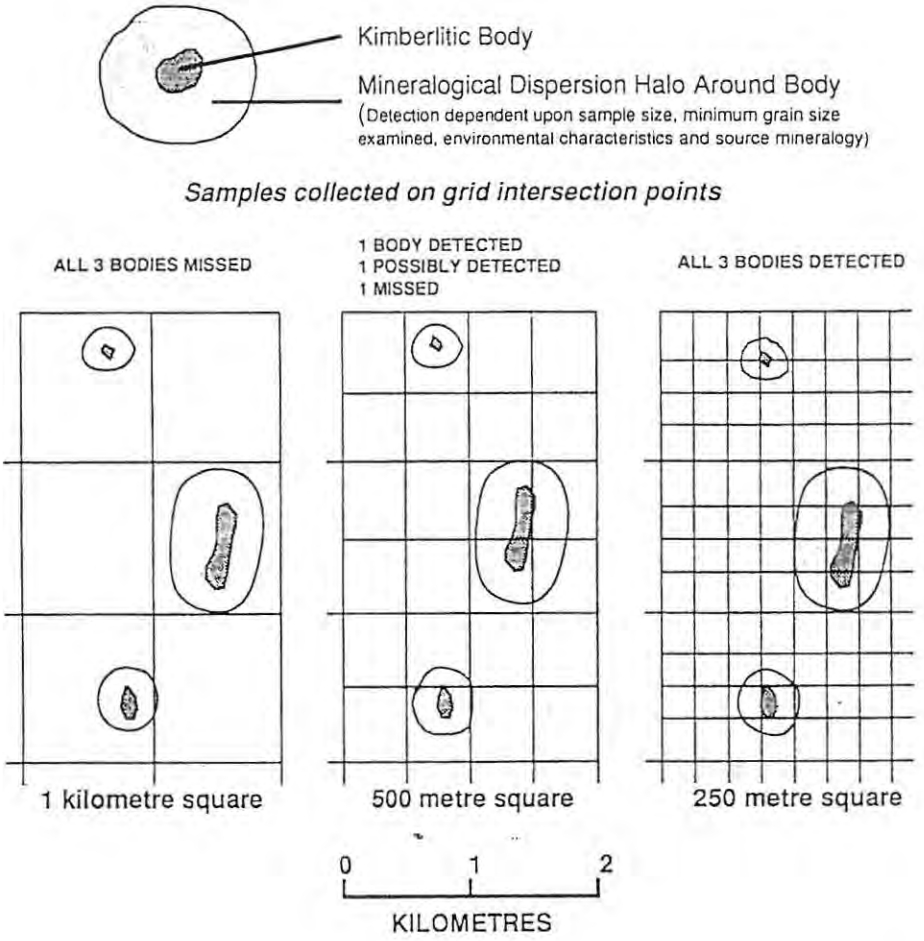

Fig. 24 ; Soil sampling grids, from Muggeridge (1995).

2.4.1.2. Sample collection.

Standard equipment necessary in sampling programmes include spades, pick axes, buckets, +300 μm to -2000 μm sieves, plastic sample bags, paper and aluminium tags (for numbering purposes) and staplers or nylon thread for securing samples. Some companies are known to prefer the +425 μm sieve size range as the lower limit.

For a heavy mineral point sample a 3 to 4 kg sample, in the +300 μm to -2000 μm mesh size range, should be recovered from the top 1 to 2 cm of soil (deflation surface) within a radius of 50 m from the centre of the sample position. Continuous scoop samples are collected along traverse lines, such as dirt roads, fences and relatively flat areas. The deflation surface along a dirt road is sampled continually over 100 m with the central position over the 100 m sampled noted as the sampling position.

The most common sampling problems encountered are ;

(1) poor sample site selection,
(2) contamination due to dirty equipment carried over from previous sample sites,
(3) incorrect sample site plotting on maps or aerial photographs (GPS systems are widely used at present) and,
(4) sample handling as well as recovery.

Routine checks on correct labelling of sample bags and tags, retrieving all samples from the field, as well as careful packing and transporting of samples is necessary (Muggeridge, 1995).

2.4.1.3. Sample preparation and processing.

Field processing of coarse-grained (> 1 mm) soil or stream sediment sampling may be done by crude gravity separation using panning or wet-screen jigging methods. Jigging by small mechanical jigs are effective for recovering indicator minerals down to 0.8 mm grain size. Jigging of a sample in water seperates different grain densities through suspension and gravity effects. Diamond, ilmenite and magnetite tend to concentrate at the centre of the sample. Contamination should be avoided at all costs, therefore quality control is important. Screens, pans and brushes should be cleaned thoroughly before processing of each sample to avoid carry-over contamination (Muggeridge, 1995).

Where the sampled fraction is finer-grained laboratory processes such as Wilfley tables (only used in Australia), heavy liquid-, electromagnetic- and high tension separation, alkali fusion or acid digestion is used (Atkinson, 1989). Laboratory extraction of microdiamonds and indicator minerals reduces the bulk sample size which can be up to 40 kg, to a small concentrate of usually less than 300 g. The concentrate can then be observed under the binocular microscope and indicator minerals can be extracted.

Towie & Seet (1995) describe a typical laboratory procedure as the ;

(1) initial weighing for sample quality comparisons,
(2) sieving of the -100 micron fraction (20 g) for possible geochemical spectrographic analysis,
(4) milling whenever the sample is not free flowing but contains a fair amount of clay,
(5) wet screening at 2 mm to remove both oversize and undersize material,
(6) drying the final concentrate, which usually falls within the -2 to +0.3 mm size range,
(7) dry sieving to liberate the fine sand grains and,
(8) heavy liquid (usually a liquid from an organic compound) and/or magnetic separation .

The indicator mineral concentrate fraction is extracted by visual observation and hand picking under a binocular microscope. The concentrate grains of a sample of -0.5 to 0.4 mm concentrate weighing 100 g will entail the observation of more than 600 000 grains (Towie & Seet, 1995).

2.4.1.4. Sample analysis and results.

The heavy mineral indicators are recovered under binocular microscope and plotted on a basemap for interpretation of the distribution pattern (Fig.25).

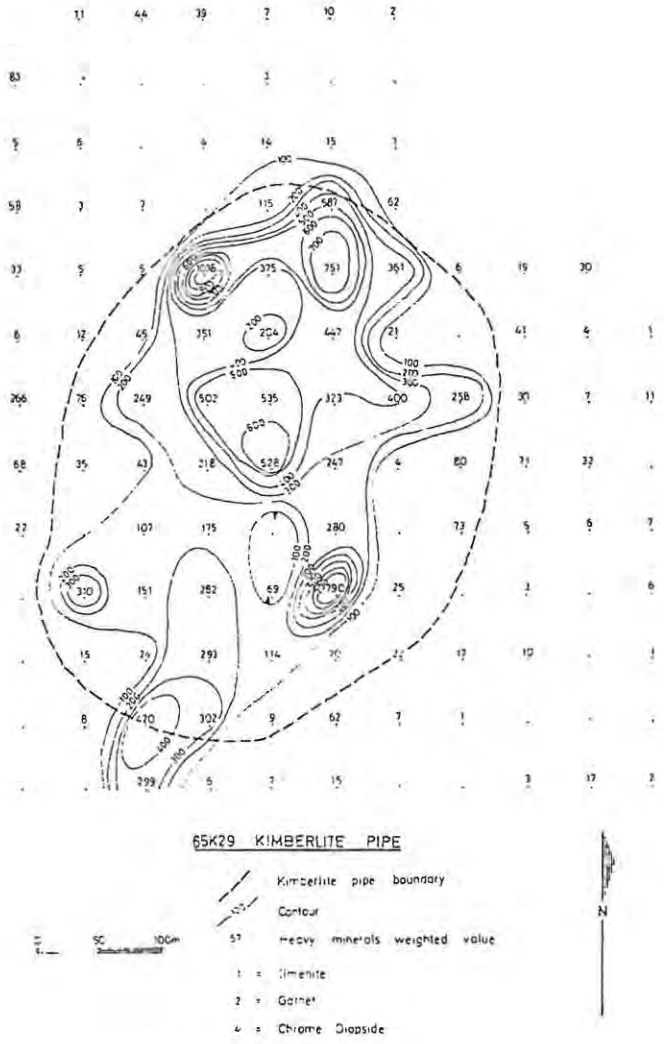

Fig. 25 ; A trail of kimberlitic indicator minerals over a kimberlite pipe in Tanzania. The northern part of the pipe shows a higher concentration of minerals over kimberlitic tuffs which come near to surface, from Gobba (1989).

The indicators are also analysed for their elemental chemistry. Nickel variability can be plotted on a baseplan to give an indication of the underlying geology, for example Ni contents will decrease from greenstone-hosted meta-sediments to dolerite dykes and sills to andesites. Quartzites, shales, conglomerates and granites would show no nickel.

According to Fipke *et al.* (1995) and Gurney (1998) heavy mineral indicators of particular interest and, in general decreasing order of importance are ;

(1) High Cr, low Ca, harzburgitic garnets,
   (a) of which the Ni content of the harzburgitic garnet gives an idea of the temperature of formation (thermometer) and,
   (b) high Na megacrystal garnets, which are not kimberlitic, indicates high pressure.
(2) High Cr, low Ti chromite (chromites are highly refractory and can survive acidic and metasomatism which will destroy the garnet and ilmenite).
(3) Ilmenites with >16% MgO and > 6% Cr_2O_3 and,
(4) Clinopyroxene (chrome-diopsides) which does not usually travel more than 5 km from their source can be used as a thermobarometer.

Observation and description of indicator minerals under the binocular microscope is important. General information regarding sample number and position, surface processes active in the area, size, colour, shape, crystal state and crystal form should be noted, as well as detail information on primary surface features, chemical decomposition features and mechanical or fluvial surface features (Appendix I and II).

2.4.2. Mineralogy.

Because diamonds are unrelated to their host rock and were sampled, along with many other rock varieties, during emplacement it is difficult to differentiate between non- diamondiferous and diamondiferous kimberlites. The prediction of kimberlites that have favourable conditions for the presence and preservation of diamonds were pioneered by Gurney (1985), Gurney & Switzer (1973), Sobolev (1977) and Griffin *et al.* (1989).

Diamonds are gradually liberated into the kimberlite by disaggregation of the diamondiferous eclogite and peridotite *en route* to the surface from depths of at least 150 km. Diamondiferous xenoliths have been noted in surface outcrop, with diamond eclogite much more common than diamond peridotite. Macrocryst diamonds are found as xenocrysts in kimberlite. Both peridotitic and eclogitic mineral inclusions in diamonds have been noted at every primary diamond source, although peridotitic diamond inclusions predominate in most localities.

Indicator minerals permit an assessment of the diamond potential of their source based on the composition of the indicator minerals. The more common indicator minerals are pyrope garnet, picro-ilmenite, chrome diopside (clinopyroxene), chrome spinel, phlogopite (mica), forsteritic olivine, enstatite/bronzite (orthopyroxene, zircon, potassic richterite/magnesio-katophorite (amphibole), priderite and diamond. Table X is a summary of indicator minerals as given by Muggeridge (1995). Since orthopyroxene is reactive with kimberlite magma and olivine and pyroxene do not survive well in the main secondary environments, garnet and chromite are the most useful diamond indicators (Fipke *et al.*, 1995).

Table X ; Characteristics of important pathfinder (indicator) minerals from kimberlitic rocks, from Muggeridge (1995).

MINERAL	CRYSTAL SYSTEM	KIMBERLITIC MACROPHASE	MAXIMUM GRAIN SIZE RANGE (mm) normal - rare	COLOUR	SPECIFIC GRAVITY	HARDNESS (MOH'S SCALE)	VISIBLE DIAGNOSTIC FEATURES	MAIN SOURCE ROCK
Pyrope garnet	Isometric	Megacryst macrocryst phenocryst?	1-15	Purple, red, crimson, mauve, orange, yellow	3.51	7.5	Anhedral, rounded shape ; kelyphite rim (reaction corona), characteristic colours	Peridotite, kimberlite, lamproite, lamprophyre, carbonatite, certain mafic volcanics
Picro-ilmenite	Trigonal	Megacryst macrocryst	2-10	Black	4.5-5	5-6	Anhedral shape (rounded or blocky) ; characteristic surface pitting, leucoxene coating	Kimberlite, lamproite, carbonatite
Chrome diopside (clinopyroxene)	Monoclinic	Megacryst macrocryst	2-15	Emerald-green	3.3-3.6	5-6	Anhedral, blocky (usual : in kimberlites) ; prismatic form (usual : in lamproites) ; cream-white surface alteration, characteristic colour	Kimberlite, lamproite, carbonatite
Diopside (clinopyroxene)	Monoclinic	Megacryst macrocryst phenocryst	2-15	Bright-green	3.3-3.6	5-6	Anhedral, rounded (in kimberlites), cream-white surface alteration, characteristic colour	Metamorphic rocks, picrites, lamprophyre, kimberlite, lamproite, alkaline mafic volcanics
Chrome spinel	Isometric	Macrocryst phenocryst	0.2-0.8	Black	4.3-4.57	5.5	Grain surface morphology : e.g. satin-like sheen and fine layering, matte pitted surface, edge bevelling, smooth glossy surface	Lamproite, kimberlite, various ultramafic and mafic rocks
Phlogopite (mica)	Monoclinic	Megacryst macrocryst phenocryst	1-10	Bronze, reddish-brown, green	2.76-2.85	2.5-3	Characteristic colour, rounded crystal edges	Ultramafic rocks, metamorphosed limestones, lamproite, kimberlite, lamprophyre
Forsteritic olivine	Orthorombic	Megacryst macrocryst phenocryst	2-15	Yellow-green	3.2-3.33	6-7	Characteristic colour, irregular crystal apices, vermiform etching	Peridotite, carbonatite, kimberlite, lamproite
Enstatite/bronzite (orthopyroxene)	Orthorombic	Megacryst macrocryst	2-17	Olive-green, brown	3.1-3.3	5.5	Characteristic colour, prismatic form, characteristic cleavage and striae	Peridotite, kimberlite
Zircon	Tetragonal	Megacryst macrocryst	1-4	Colourless, grey, yellow, honey-brown, pink, reddish-brown	4.68-4.7	7.5	Anhedral, blocky shape, characteristic colour, characteristic surface pitting and "frosting" fluoresc	Plutonic igneous rocks, kimberlite, high grade metamorphics, carbonatite
Potassic richterite (amphibole)	Monoclinic	Phenocryst	0.05-0.4	Brownish-red	3.66	6	Characteristic colour, adamantine lustre, basal cleavage or acicular form	Lamproite, carbonatite, kimberlite
Diamond	Isometric	Xenocryst	1-3 (Cullinan = 6 cm)	Colourless, pale colours (especially yellows and browns)	3.52	10	Adamantine lustre, characteristic crystal forms, resorption features, step layering	Kimberlite, lamproite (certain lamprophyres, certain high grade metamorphics)

2.4.2.1. Garnets.

Garnets range in colour from orange (mostly Cr-poor eclogitic garnet) to lilac, purple, burgundy and red (mainly peridotitic Cr-rich pyropes). Rarer green (knorringite- uvarovite-pyropes) varieties have also been noted. Garnets in kimberlites are members of the solid solutions between pyrope ($Mg_3Al_2Si_3O_{12}$), almandine ($Fe_3Al_2Si_3O_{12}$), grossular ($Ca_3Al_2Si_3O_{12}$) and uvarovite ($Ca_3Cr_2Si_3O_{12}$).

It has been suggested that the relative importance of peridotitic xenoliths with respect to diamonds are garnet harzburgite > chromite harzburgite > garnet lherzolite (Gurney, 1984). Mitchell (1989) describes the megacrystal garnets as typically single crystals of low Cr titanian pyrope (0 to 15% TiO_2) of variable Cr_2O_3 (0 to 3%) content and Mg/(Mg + Fe) ratios ranging from 0.86 to 0.68.

Many of these garnets have well-developed and visually distinct reaction rims or coronas (Scott-Smith, 1996). The diamond-bearing hartzburgitic rocks that produce sub-calcic (G10) garnet macrocrysts (> 2 mm), are present in all kimberlites and are derived from the disaggregation of mantle rock xenoliths sampled by the kimberlite, hence the reaction rims (Dawson, 1972 ; Boyd & Gurney, 1986). This process can be ascribed to either decarbonation reactions or to the presence of an interstitial volatile melt enriched in K, LREE and CO_2 (Harte *et al.*, 1980).

Eclogite xenoliths in kimberlites consist of two varieties. Group I eclogites are texturally and chemically homogeneous and contain measurable enrichments of sodium in garnet and potassium in clinopyroxene, whilst Group II eclogites do not show these enrichments (Sobolev, 1977 ; Gurney, 1985, 1989).

Diamonds are only found in association with Group I eclogites, with the most diagnostic diamond potential indication being anomalous trace enrichments of sodium in garnets (usually in the range 0.06 to 0.7 wt % Na_2O), commonly accompanied by moderate to high levels of TiO_2. The cut-off concentration for diamond indicator eclogitic garnets was taken where 85% of the values were > 0.07 wt % Na_2O (Gurney, 1985). This cut-off was considered to indicate equilibration at pressures high enough to be compatible with the presence of diamond (Gurney, 1984).

Peridotitic (chrome-rich) garnets have been used to differentiate between most diamondiferous and non-diamondiferous localities by comparing CaO against Cr_2O_3 ratios. An arbitrary line has been drawn parallel to the lherzolite trend, but on the CaO-depleted side of it, and an inclined line at Cr_2O_3 = 4 wt %, in such a way that 85% of the diamond- inclusion garnets are seperated from the lherzolite field. This has been described as the "85% line", G9/G10 line or lherzolite line (Fig.26).

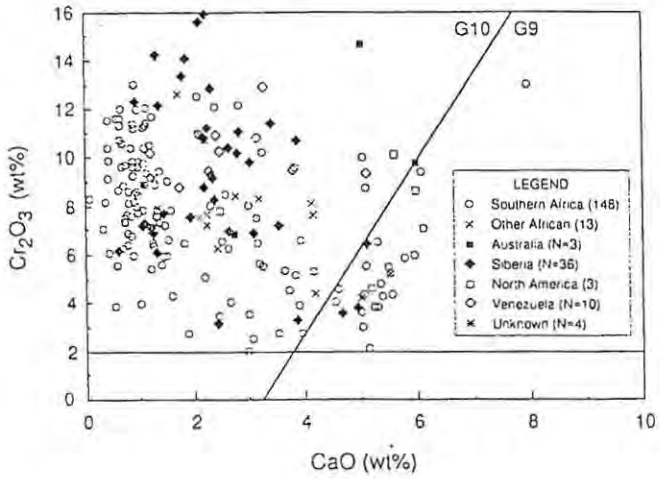

Fig. 26 ; Cr_2O_3 vs CaO plots for peridotitic garnet inclusions in diamonds from worldwide localities. Eighty-five percent of the garnets plot on the CaO-poor side of the inclined line which was defined by Gurney (1984). These subcalcic compositions are referred to as G10 garnets. The horizontal line drawn at 2 wt % Cr_2O_3 is used as an arbitrary division between eclogitic garnets below the line and peridotitic garnets above it, from Fipke *et al.* (1995).

The line was originally drawn to eliminate all garnets from known garnet lherzolites, from the G10 calcium-depleted side of the line. The sub-calcic garnets were termed G10 and the calcic garnets G9. All known diamondiferous kimberlites have garnets that plot within the low calcium field defined by this line. The calcium saturation level in a garnet derived from a garnet lherzolite varies, with the lowest calcium values being found in the garnets from lherzolites with the highest equilibration pressures (Gurney, 1984, 1985).

Although most garnets that plot within the sub-calcic G10 field are derived from harzburgites, some equilibrated with chrome diopside at very high (> 50 kbar) pressures and are lherzolitic garnets which are also diamond indicators (Gurney & Zweistra, 1995). According to Fipke *et al.* (1995) garnet lherzolite is not a major component of a diamond inclusion suite at any locality yet described. This is fortunate, since garnet lherzolite is the most common mantle xenolith found in kimberlite, and major element compositions cannot readily differentiate between a diamond-bearing and a barren garnet lherzolite. Therefore, garnets of lherzolitic composition have to be discriminated against in any exploration programme (Fipke *et al.*, 1995).

At lower pressures, lherzolite garnets plot well into the G9 field. In such circumstances, some harzburgitic garnets plot in the sub-calcic G9 field. However, it has been empirically noted that peridotitic garnet suites from diamond-bearing kimberlites always have garnets that plot in the sub-calcic field. In poorly mineralised bodies, such garnets will plot close to the line and be rare, whilst more abundant, more sub-calcic garnets are found in better mineralised bodies. The 85% line could therefore be called the diamond in line. The horizontal line drawn at 2 wt % Cr_2O_3 is to discriminate between peridotitic (Cr-rich) and Cr-poor garnets which are probably eclogitic or megacrystic (Fipke *et al.*, 1995).

An important aspect of any peridotitic garnet population is that localities with higher diamond contents tend to have garnet compositions that scatter across and well into the subcalcic field. Thus, low calcium, high chromium garnets are associated with higher diamond contents (Gurney & Zweistra, 1995).

With respect to peridotitic diamonds the garnet plots for Finsch, Premier, Koffiefontein, Orapa and Colosssus are shown in Fig.27. All these localities agree with the diamondiferous potential shown by the CaO vs Cr_2O_3 graph, although no indication of diamond quality can be inferred with this method (Gurney & Zweistra, 1995).

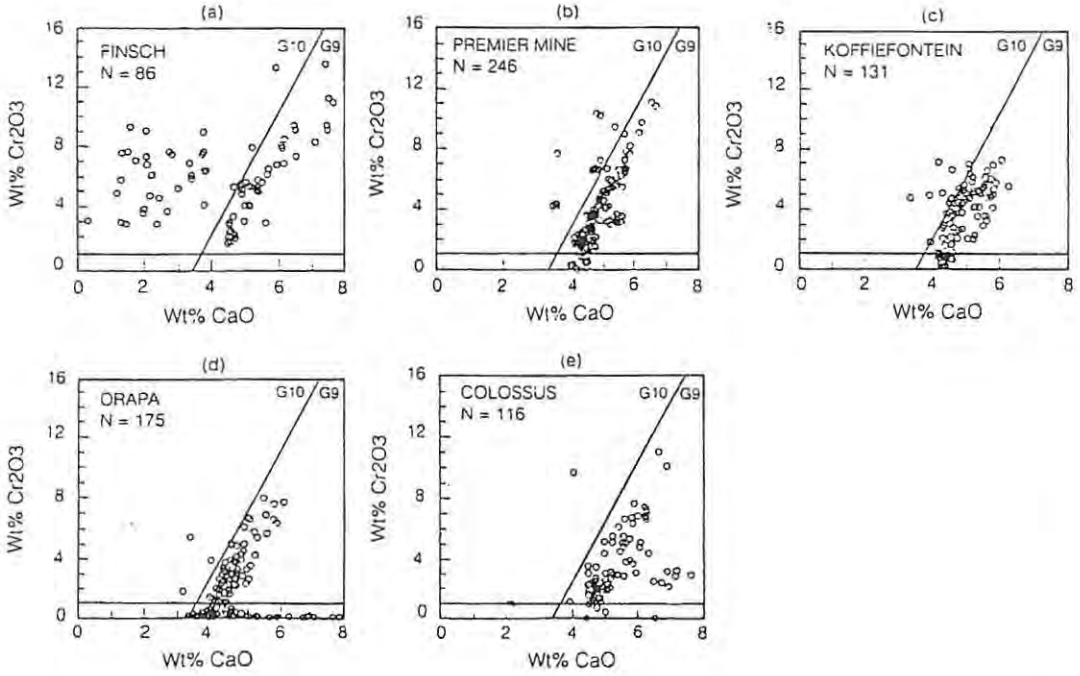

Fig. 27 ; CaO vs. Cr_2O_3 plots for five diamond-bearing localities. (a) Finsch : high grade, predominantly peridotitic diamonds, (b) Premier : medium grade, peridotitic/eclogitic diamond ratio of approximately 40/60, (c) Koffiefontein : low grade, mainly peridotitic diamonds, (d) Orapa : high grade, mainly eclogitic diamonds and, (e) Colossus : very low grade, peridotitic/eclogitic diamond ratio unknown. It is important to note that this plot is only useful for P-type diamonds, from Gurney & Zweistra (1995).

Overall peridotitic inclusions in diamonds outnumber eclogitic inclusions in diamonds 3 : 1. At individual locations these ratios differ substantially. At the Finsch Mine, in the Kimberley area at all pipes and at River Ranch in the Limpopo Mobile Belt peridotitic inclusions, and by inference peridotitic diamonds are in a ratio of > 3 : 1. However, at Premier, Lethlakane and Orapa eclogitic inclusions are much more abundant, approaching 90% at Orapa (Gurney, 1989).

The Ni-thermometer.

The diamond potential of diatremes can also be assessed from the composition of chrome-pyrope garnets in mantle-derived xenoliths. Under upper mantle conditions the partitioning of Ni between garnet and olivine is strongly temperature dependent (Griffin *et al.*, 1991 ; Griffin & Ryan, 1995). From this relationship the "Ni-thermometer" was calibrated, enabling the estimation of equilibrium temperatures from the Ni-content of single Cr-pyrope garnet grains.

The variation in the Ni distribution coefficient D^{Ni} defined as (ppm in garnet)/(ppm in olivine) is almost entirely due to variation in the Ni content of the garnet - the Ni content of garnet-peridotite olivine is essentially constant at 2900 $\pm$ 360 ppm of garnets with $T_{Ni} < 950^0$ C. This allows the construction of a thermometer, based on the assumption that each garnet has equilibrated with olivine of uniform Ni content (Fig.28). This thermometer gives the temperature of equilibration of a single grain of Cr-pyrope garnet to a typical accuracy of approximately 50^0 C. The thermometer is insensitive to major-element composition of the garnet and pressure (Griffin & Ryan, 1995).

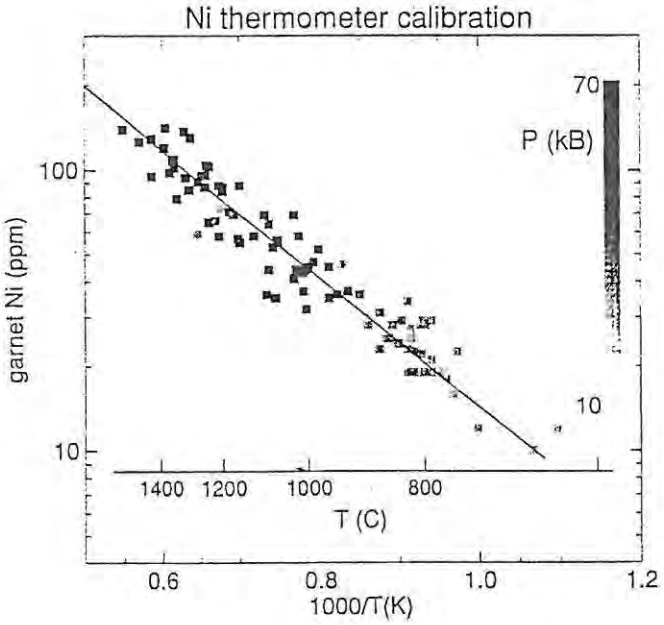

Fig. 28 ; Ni content of garnets from peridotite xenoliths, plotted against olivine-garnet temperature. The regression line is the Ni thermometer and no P dependence is observed, from Griffin & Ryan (1995).

Assuming a steady state geotherm of 40 mW/m^2 and based on xenolith as well as diamond inclusion data, the garnets should yield temperatures in the range 950 to 1250^0 C. When the Ni-thermometer is applied to garnet concentrates from kimberlites, Griffin *et al.* (1991), showed that in areas where a "cratonic" geotherm is applicable, diamond-rich kimberlites contain high proportions of garnets with Ni-temperatures (T_{Ni}) within the "diamond window" (950 to 1250^0 C). On the other hand diamond-poor diatremes have a very low proportions of garnets with Ni-temperatures within the "diamond window". An example of the prediction of high diamond content accompanied by a high proportion of garnets with Ni temperatures in the "diamond window" is given using South African Group I and II kimberlites (Fig.29)

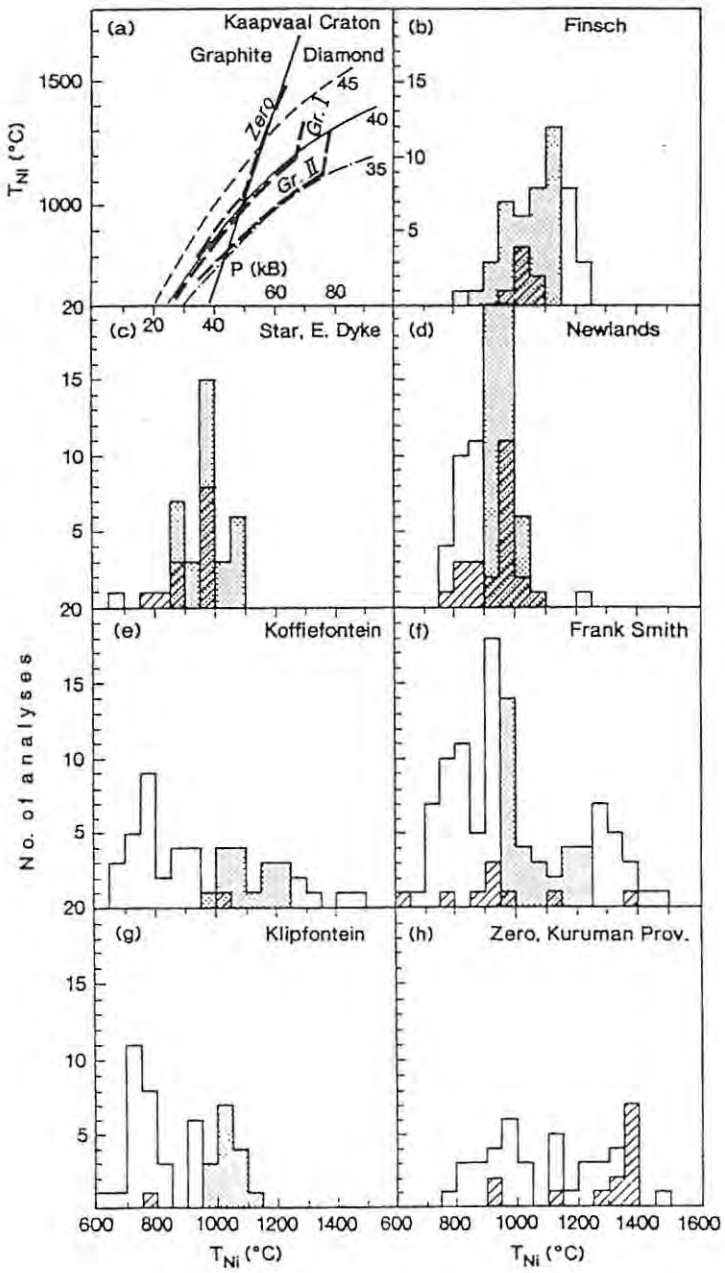

Fig. 29 ; Garnet geotherms and T_{Ni} histograms for garnet concentrates from South African kimberlites (Group I and Group II). Shaded areas on histograms represents the "diamond window" derived as in Fig. 3, whilst cross-hatching shows sub-calcic "G10" garnets, from Griffin & Ryan (1995).

2.4.2.2. Ilmenite.

Ilmenites are solid solutions members between $FeTiO_3$, $MgTiO_3$ and Fe_2O_3. They generally have high MgO- (4 to 19%) and Cr_2O_3 contents (0.1 to 11%), together with very high $MgTiO_3$ (50 to 90 mol.%) and low Fe_2O_3 (<10 mol.%). Mafic igneous rocks have comparatively low Mg- and Cr- ilmenites. Groundmass ilmenite occurs as euhedral prisms, intergrowths with spinel and perovskite as well as inclusions in olivine (Mitchell, 1989).

Ilmenite is only useful in exploration for some Group I kimberlites, being very rare in Group II rocks (Atkinson, 1989). Although ilmenite is a very rare inclusion in Group I diamonds, it is very abundant in some kimberlites as a macrocryst derived from the megacryst suite of minerals. Megacrysts are thought to be cumulates which formed close to the time of emplacement of host magma and are much younger than eclogitic or peridotitic diamonds. Any relationship between them are indirect since megacryst ilmenites are generally thought to be xenocrysts with respect to their kimberlite host.

Two aspects led to the suggestion that the chemistry of ilmenite reflected the redox conditions (oxygen fugacity in terms of Fe^{3+}) in the mantle and the diamond resorption potential during the time of emplacement (Haggerty & Tompkins, 1983). Firstly it was noted that diamonds found in peridotite and eclogite xenoliths were generally better preserved than diamonds recovered from the host magma. Secondly it was noted that diamondiferous kimberlites had a larger proportion of ilmenite high in MgO and low in Fe_2O_3 than barren kimberlites.

As diamond resorption can remove up to 50% of the diamond content from a kimberlite, a diamond preservation index is important for any forecast of diamond potential (Gurney & Zweistra, 1995). Diamond preservation depends on the level of oxygen fugacity at elevated temperatures outside the diamond stability field. Conditions within the magma *en route* upwards must at some stage be outside the diamond stability field which may convert diamond to graphite, or more frequently to CO_2. Ilmenite suites with low Fe^{3+}/Fe^{2+} ratios are associated with better diamond preservation than those of higher ratios. In ilmenites from kimberlites, highly oxidising conditions are associated with low MgO and Cr_2O_3 (Gurney & Moore, 1991 ; Fipke *et al.*, 1995).

An example of the above-mentioned low MgO and Cr_2O_3 indicating oxidising conditions is the Premier kimberlite which shows resorption of most diamonds (Fig.30).

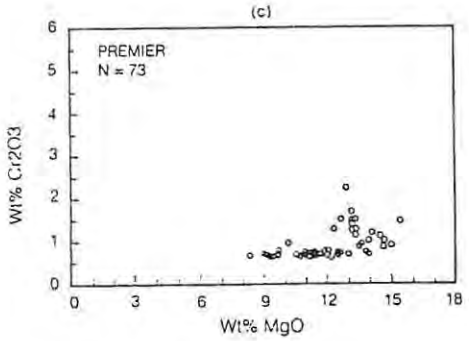

Fig. 30 ; Cr_2O_3 vs MgO plot for the diamondiferous Premier kimberlite showing resorption of most diamonds, from Gurney & Zweistra (1995).

Fig.31 shows a plot of Fe_2O_3 and MgO for four localites. A hyperbolic trend is defined where Fe_2O_3 and diamond resorption increase with decreasing MgO. Tshibua (Zaire) has a high grade with diamonds exhibiting late stage growth, suggesting a reduced mantle at the time of kimberlite emplacement. Tshibua has only very reduced ilmenites (low Fe_2O_3).

Premier Mine is a medium grade producer with considerable resorption. Palmietfontein has about 1 ct of extremely resorbed diamonds per 100 tons of kimberlite and Iron Mountain diatremes are barren or nearly so. This suggests that a qualitative correlation exists between the most oxidised ilmenite compositions at a particular locality and diamond resorption. Ilmenite compositions can only be used qualitatively and where diamonds are present (Gurney & Zweistra, 1995).

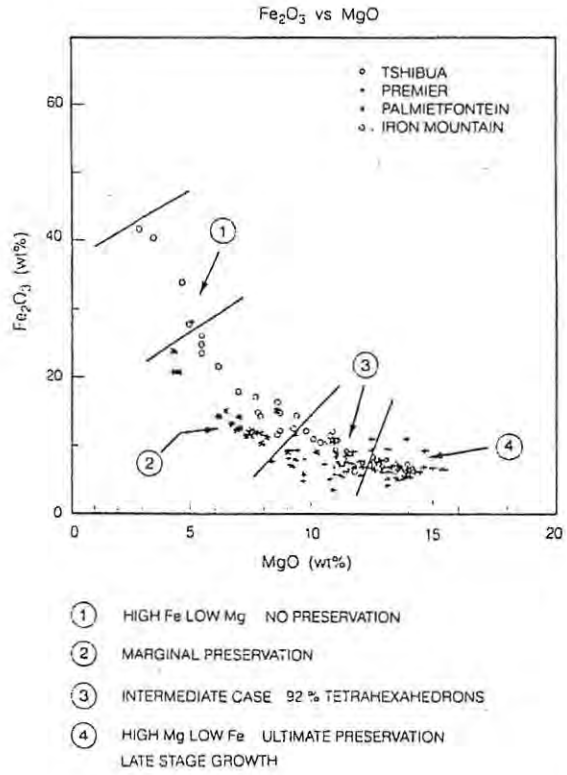

Fig. 31 ; Plot of MgO against Fe_2O_3, the latter calculated from electron microprobe major element analysed. The four locations Tshibua, Premier, Palmietfontein and Iron Mountain is discussed in the text, from Gurney & Zweistra (1995).

2.4.2.3. Clinopyroxene (chrome diopside).

Many of the megacryst peridotite-derived clinopyroxene is chrome diopside which has a characteristic emerald-green colour (Scott-Smith, 1996). Kimberlitic pyroxenes where divided into those with variable chromium and low iron content of ultramafic affinity and those of higher sodium and $Al^{6+} > Al^{4+}$ of eclogitic affinity (Sobolev, 1977).

Megacrystic pyroxenes in Southern Africa typically have low Cr_2O_3 (<1%), TiO_2 (<1%), Al_2O_3 (<3%) and Na_2O (<2%) contents, that differ distinctly from eclogitic or lherzolitic pyroxenes. Megacrysts of pyroxene range in composition from subcalcic diopside to diopside with Ca/(Ca + Mg) ratios increasing in pyroxenes from monomineralic megacrysts, lamellar intergrowths with ilmenite and small granular inclusions in ilmenite megacrysts (Mitchell, 1986, 1989).

The most Mg-rich ilmenites in a kimberlite are associated with pyroxenes which have the highest Ca/(Ca + Mg) ratios. The trends in the Ca/(Ca + Mg) ratios suggest that initial crystallisation of pyroxene megacrysts was followed by pyroxene-ilmenite intergrowths with magma differentiation (Mitchell, 1989).

2.4.2.4. Olivine.

Olivine is not usually used as an indicator due to the fact that it typically alters to serpentine or rapidly weathers to clay. Olivine was preserved in the cold climate of Yakutia (Russia) where it was used as a tracer element. Magnesian ilmenite, chrome spinel and needle-like rutile are present as inclusions in some olivines, with anomalous values of chromium in these inclusions noted by Meyer & Boyd (1972).

Olivine occurs as rounded macrocrysts and euhedral to subhedral microphenocrysts that give kimberlite the characteristic inequigranular texture. Groundmass olivine inclusions of enstatite, Cr-pyrope, Cr-spinel, Cr-diopside, Mg-ilmenite, chromite, rutile and Cu-Ni sulphides are common. Macrocrysts typically range from Fo_{76} to Fo_{94} with the groundmass olivines about Fo_{88}. Groundmass olivine are usually small (<0.5 mm) euhedral-to-subhedral single crystals. Serpentinisation occurs preferentially along fractures and grain boundaries with pseudomorphs of olivine replaced by calcite in places (Mitchell, 1986, 1988).

2.4.2.5. Spinel.

Spinel, a component of mantle xenoliths and of the kimberlitic groundmass, shows a wide variety in its morphology and chemical composition. Spinel occurs predominantly as macrocrysts (0.1 to 0.5 mm in size) and as primary groundmass minerals (0.001 to 0.1 mm in size). Small euhedral to subhedral spinels can comprise up to 30% of the groundmass. Macrocrystal spinels (chromites) are Ti-poor (<1% TiO_2) magnesian aluminous chromites and aluminous magnesian chromites with a wide range in Cr/(Cr + Al) ratios (0.3 to 0.95) and Fe/(Fe + Mg) ratios (0.3 to 0.6) (Mitchell, 1989).

Chrome spinels are marked by their high chromium content, generally > 61 wt % Cr_2O_3 (Meyer & Tsai, 1976), amongst the highest Cr_2O_3 contents ever observed (Daniels, 1991 ; Gurney & Zweistra, 1995). They are also characterised by moderate to high levels of magnesium (12 to 16 wt % MgO) and very low contents of titanium, usually less than 0.3 wt % TiO_2.

Fig.32 (worldwide examples) and Fig.33 (South African examples) show that chromite compositions high in MgO and Cr_2O_3 levels are regarded as indicative of the diamond potential of the kimberlite (Atkinson, 1989 ; Gurney & Zweistra, 1995 ; Fipke *et al.*, 1995).

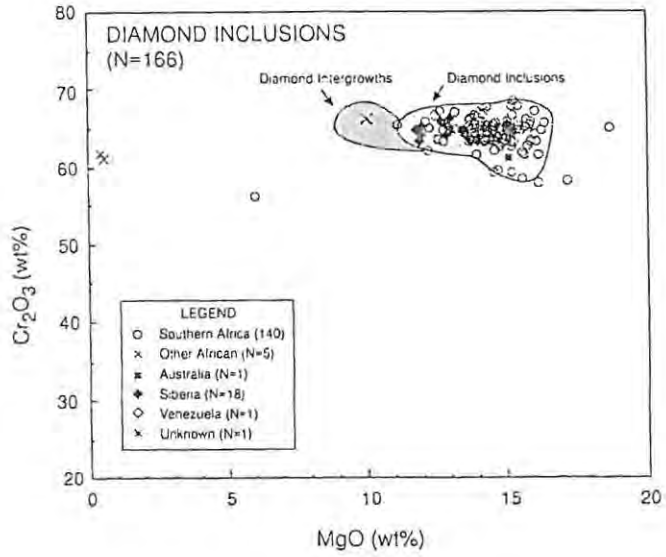

Fig. 32 ; Cr_2O_3 vs MgO plots for chromite inclusions in diamonds from worldwide localities. Note the highly restricted, chrome-rich character of the inclusions. The preferred compositional field indicated includes > 98% of the data points, from Fipke *et al.* (1995).

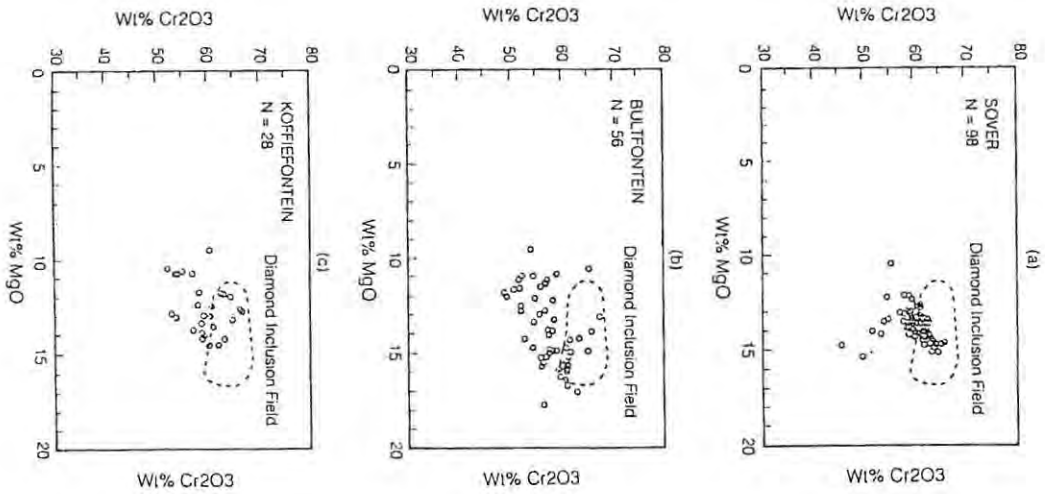

Fig. 33 ; Cr_2O_3 vs MgO plots for chromite from three diamond-bearing kimberlites. (a) Sover : medium to high grade with significant peridotitic and eclogitic diamond components Group II kimberlite. Chromites are very abundant, many falling into the phenocryst rather than xenocryst category, (b) Bultfontein : medium grade Group I kimberlite and, (c) Koffiefontein : low grade Group I kimberlite of mostly peridotitic diamonds, from Gurney & Zweistra (1995).

Mantle-derived chromites show a wide variation in both major and minor element concentrations and several sub-populations of chromite may be present in the xenocryst suite recovered from any one diatreme (Griffin & Ryan, 1992).

Fipke *et al.* (1995) state that these subpopulations may represent ;

(1) macrocrysts derived from a wide range of source rocks (such as dunites, harzburgites, lherzolites and pyroxenites) which have been sampled from diverse regions of the upper mantle both within the diamond stability field and from shallower levels,
(2) magmatic (phenocryst) chromites or,
(3) xenocrysts which have reacted with the host volcanic rock.

The important compositional types of chromites in exploration are the diamond inclusion and intergrowth type (DI chromites) and high content Cr-Ti chromites. The former group plot within the field of high MgO and high Cr_2O_3 compositions characteristic of chromites included or intergrown with diamond. DI chromites generally contain < 0.6 wt % TiO_2, whilst Cr-Ti chromites contain > 0.8 wt. % TiO_2 and plot within the high Cr-Ti field characteristic of kimberlites. The detection of high Cr-Ti chromites in regional stream sediment sampling programmes is useful for identifying the presence of a kimberlite source (Fipke *et. al*, 1995).

2.4.2.6. Zircon.

Although zircons ($ZrSiO_4$) are a rare accessory phase in kimberlites, they are commonly found in the heavy mineral concentrates together with diamonds (Mitchell, 1986). Zircon in kimberlites and related rocks occur as rounded, frosted grains often with a thin whitish coat of baddelyite. The very low uranium and thorium contents of kimberlitic zircons, generally less than 100 ppm, differentiates them from granitic zircons (Mitchell, 1986 ; Atkinson, 1989).

2.4.2.7. Phlogopite.

Red-brown magnesium-rich mica (phlogopite) is a common mineral in nodules, megacrysts and groundmass of kimberlite. Phlogopites are divided into the megacrystal/macrocrystal micas and microphenocrystal-groundmass micas. The megacrystal/macrocrystal micas are commonly rounded, broken, distorted or kink-banded showing undulose extinction. Replacement by calcite, chlorite and serpentine along cleavage planes is common. Micas in micaceous kimberlites form closely packed mosaics of tabular-to-square cross-section microphenocrysts (Mitchell, 1986).

Groundmass micas typically contain abundant inclusions of spinel and perovskite. In some kimberlites there is a trend of decreasing TiO_2 and Cr_2O_3 with increasing FeO, as macrocryst mica is followed by groundmass mica, crystallisation. Individual grains are uniform, but there are substantial inter-grain variations. Most are aluminous phlogopite that has a wide range of TiO_2 (0.5 to 5.5 wt %) and Cr_2O_3 (0.1 to 2 wt %) (Mitchell, 1986, 1989).

2.5. Remote sensing techniques.

Remote sensing includes satellite imagery, aerial photography, geophysical exploration and instrumental chemical analysis, all of which are presented in the following three sections. Remote sensing techniques use the energy from some part of the electromagnetic spectrum shown in Fig.34.

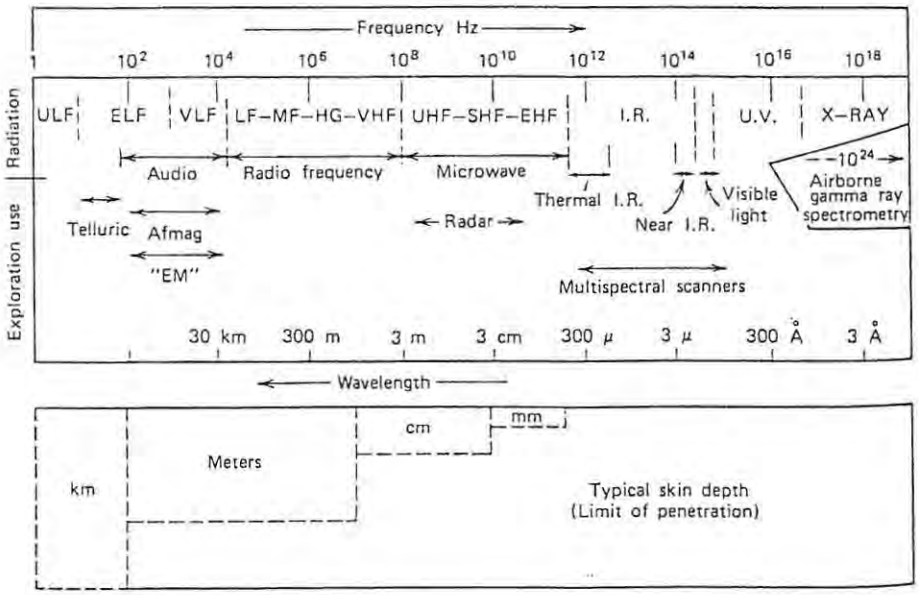

Fig. 34 ; Reconnaissance exploration techniques in the electromagnetic spectrum, from Peters (1978).

2.5.1. Satellite imagery.

As reconnaissance work begins with a synoptic view Landsat Multi Spectral Scanner (MSS) and Thematic Mapper (TM) satellite data, is the most useful techniques for regional structural-, geomorphological-, vegetational- and lithological mapping. The data can then be used in combination with regional gravity-, seismic-, magnetic- and geochemical datasets.

The Landsat TM and MSS imagery is generated from the visible and near visible light reflective qualities of the earth's surface and is especially useful for regional scale analysis. The relatively coarse resolution (mostly from 80 by 80 m to 30 by 30 m picture elements, or pixels), only provides for large scale structural-, lithological- and surficial spectral data to be interpreted (Harris, 1998). Individual kimberlites, which are typicaly less than 150 m in diameter, can not readily be detected by remote sensing data (Atkinson, 1989).

Landsat MSS data is restricted to the visible and very near infrared (VNIR) portion of the electromagnetic spectrum, ranging from 0.4 to 1.1 μm. Remote sensing interpretation relies on absorption features related to iron, hydroxyl and water which is characteristic of many kimberlite sample spectra, mostly due to the presence of serpentine minerals, or subordinately caused by hydroxyl and water associated with micas (Fig.35).

Shuttle Multispectral Infrared Radiometer (SMIRR) imagery has been used for the identification of calcite, kaolinite and montmorillonite weathering which is characteristic of kimberlite weathering. SMIRR imagery uses narrow band radiometry in the 2 to 2.5 μm wavelengths (Goetz *et al.*, 1982).

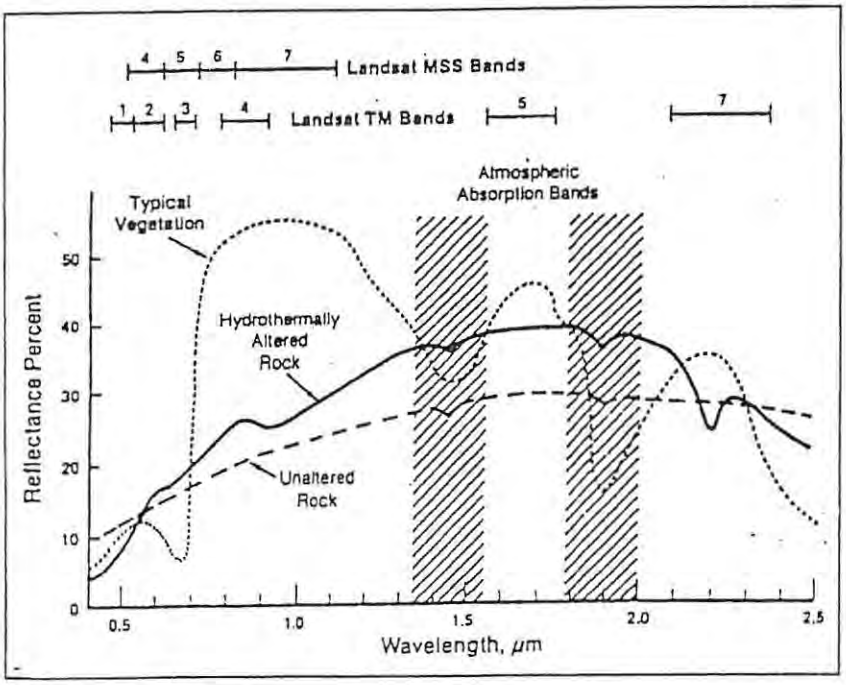

Fig. 35 ; Spectral bands for TM and MSS systems. Reflectance curves for vegetation, unaltered rocks and hydrothermally altered rocks, from Harris (1998).

The Landsat TM system extends spectral coverage into the NIR band (band 5 at 1.55 to 1.75 μm and band 7 at 2.08 to 2.35 μm). Together with airborne MSS, which gathers narrow band data within these longer wavelengths, they provide a new technique for identifying soils rich in vermiculite and smectite group clays, which have strong absorption in the 2.2 μm region. New techniques are being developed that would be able to produce higher spatial resolution. This would enable image processing down to individual outcrop scale with its associated distribution of mineral suites, like serpentine, smectites and carbonates (Kingston, 1989).

Geomorphological mapping can be performed at present by detailed digital topography maps as a by-product of GPS aircraft navigation combined with laser or radar altimetry. Digital topography maps derived from GPS navigation can only be accurate at pixel sizes comparable to the flight line spacing, but higher resolution data may be obtained from radar imagery (Macnae, 1995).

Low level airborne multispectral scanning can also provide higher resolution data than satellite imagery. This method can then be used to measure the reflectance of clay minerals in the soil which are indicative of kimberlite weathering products. Unfortunately, the presence of surficial cover masks the above-mentioned spectral reflectance features (Kingston, 1989).

2.5.2. Aerial photography.

Regional structural and fracture patterns, lithological boundaries and geomorphology can be delineated by aerial photograph interpretation. The higher resolution available from aerial photographs have led to the recognition of vegetation differences over kimberlite pipe and/or dyke soil relative to host rock soil. These features may be expressed as tonal differences or as circular depressions (pans) or mounds due to increased bioturbation in the softer, weathered kimberlite (Cole, 1998).

Aerial photographs are helpful for drainage analysis, planning optimal stream sediment sampling sites and as a supplement to other target generation methods, for example regional structural- and geomorphological analysis, groundmapping and vegetation anomalies (Fipke *et al.*, 1995). The stereographic aerial photograph method is useful in analysis of three-dimensional features on the Earth's surface. This method can assist in mapping lithological contacts and major structures in rugged terrains or areas of extensive outcrop.

Access routes and geological-, geophysical- and geochemical groundwork can often be planned more effectively with aerial photographs in conjunction with topographic maps in remote areas with poor infrastructure and rugged topography.

2.6. Geophysical techniques.

Helicopter or fixed-wing aircraft (airborne) geophysical surveys are rapid and relatively low cost reconnaissance tools. Geophysics has especially been useful in large areas where no previous work has been carried out or where follow-up work has to be done over kimberlite targets generated by other methods, such as kimberlite indicator mineral sampling. Modern geophysical surveys gather digital data which enables rapid processing and imaging abilities and can readily be integrated with geological-, structural-, geochemical- and other datasets.

The most commonly used geophysical techniques are magnetics, electromagnetics and gravity. Geophysics is only effective where sufficient contrast in magnetic susceptibility, conductivity, specific gravity, etc. between the kimberlite and its host rock exist.

2.6.1. Magnetic method.

Aeromagnetic data is the most commonly used method as it is relatively low cost, highly sensitive, rapid and reliable. Rock magnetism is a function of magnetic susceptibility, in other words the ease with which the constituent minerals may be magnetised. The highly susceptible magnetic mineral content in kimberlites can range from 5 to 10% of iron oxides, most of it in the form of magnetite and ilmenite. Magnetite is also formed as a secondary mineral during the serpentinisation of kimberlite (Gobba, 1989).

The three physical properties controlling kimberlite responses are remanent (fixed) magnetisation, induced (variable with applied external field) magnetisation and viscous (slowly varying in an applied field) magnetisation. Induced magnetism is exactly parallel to the applied field, but may enhance or oppose it - in the case of ferro-or ferri-magnetism it enhances the applied field. The magnetic properties of kimberlites are thus not only caused by variations in magnetic susceptibility, but also the direction and amplitude of remanence (Corner, 1998).

Magnetic susceptibilities are more distinct where kimberlite intrusions occur within a background of low-susceptibility (non-magnetic) host rocks, such as platform-sediments or basement granite-gneisses.

As magnetite is the most common accessory found in the crust and has the highest magnetic susceptibility it is used on a regional scale for the recognition of both linear structures, circular features or localised magnetic lows. In some areas regional and local structural controls are less apparent due to the buried or poorly outcropping basement. In such cases the basement features such as lithological contacts, faults, folds and any anomalous concentrations of magnetic ore may be identified through geophysics.

For the direct detection of kimberlites a flight line has to pass over or close to the pipe for an appreciable contrast with the surrounding rocks. A flight-height of 50 to 100 m and a flight-line spacing of 250 m is the most cost-effective for airborne magnetometer kimberlite exploration. Generally known kimberlites have a bull's eye appearance on contoured magnetic and/or EM data and pipes tend to be clustered within a few kilometers with coincident visible features on aerial photographs. The selection of these circular anomalies can be done by visual inspection of the aeromagnetic map or by using automated Euler deconvolution. Euler deconvolution shows the fitted location and depth to an assumed magnetic source and can accurately define the spatial location of the source of any linear features in a magnetic data set (Keating, 1995).

Gerryts (1967) reviewed trial airborne magnetometer surveys conducted by De Beer's over a number of known pipes at a low flight altitude of 150 m. Some of the known pipes were not detected as they were only marginally anomalous relative to their background, some where missed completely because of their small sizes, and those that returned anomalous values did not exceed 60 gammas over the background. The results obtained from the Koffiefontein area in South Africa during the De Beer's survey is shown in Fig.36.

Ground magnetometer surveys also gave variable results with some pipes giving anomalies exceeding 500 gammas and others showing no detectable anomalies at all (Gerryts, 1967). Gerryts (1970) observed that airborne magnetic anomalies were in the zero to 500 nT range for several economic South African kimberlite pipes. Since diatremes are localised a confined anomaly is expected of an amplitude between zero and 1000 nT, but commonly in the tens or low hundreds of nT (Macnae, 1995).

In Tanzania airborne magnetics returned disappointing results over several pipes, including the Mwadui pipe. The presence of nearby magnetic basic dykes may have complicated the magnetic field in some areas (Gerryts, 1967). The magnetic susceptibilities of kimberlites in the Mwadui area are in the range of 68×10^{-6} to 6338×10^{-6} cgs units, in contrast to the 10×10^{-6} to 65×10^{-6} cgs units of the Archaean granite country rocks (Gobba, 1989). As the kimberlites were invariably weathered the magnetic minerals were converted to non-magnetic iron oxides, which, together with the superimposed Tertiary-to Recent sediments blanketed the magnetic response. The Mwadui kimberlite is also an example of where the hypabyssal facies at depth is strongly magnetic, but the weathered crater facies only weakly magnetic, giving a small surface response (Gobba, 1989).

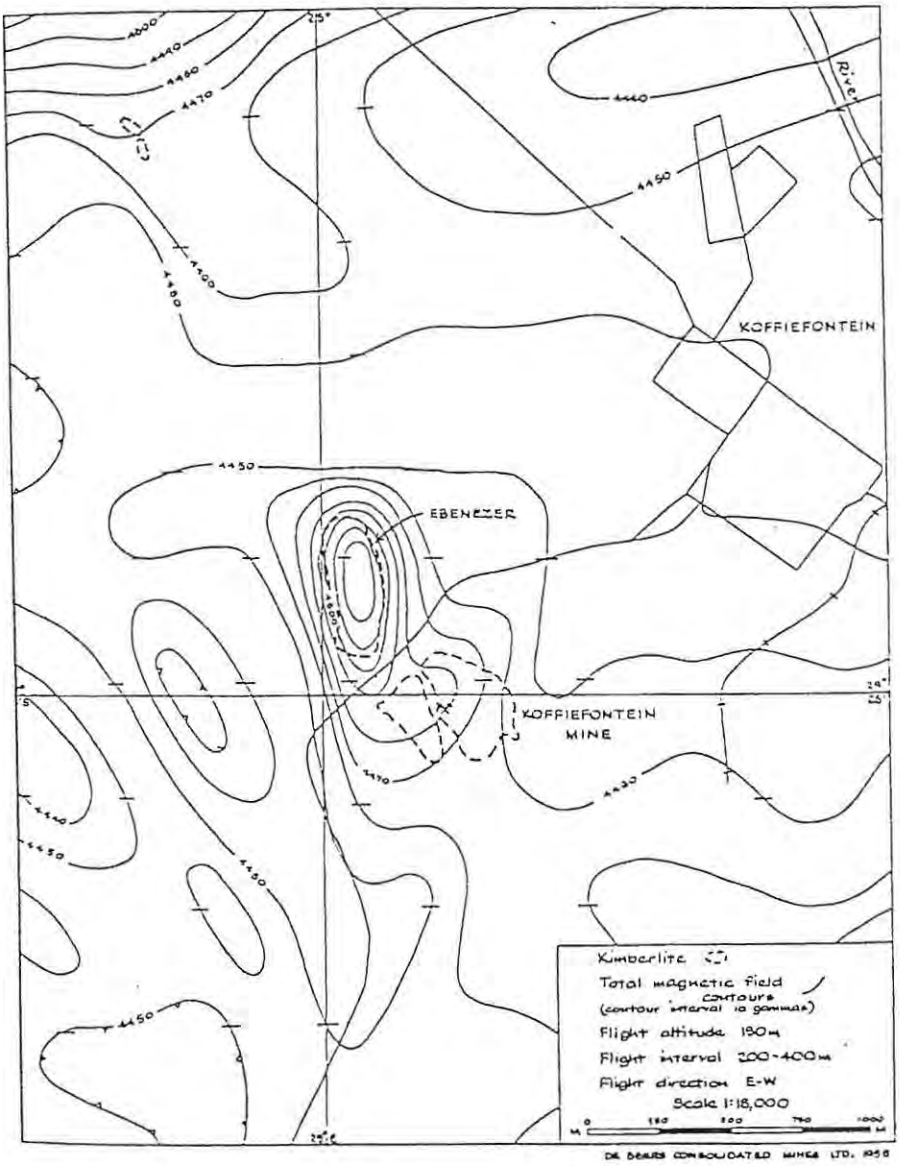

Fig. 36 ; Aeromagnetic map of the Koffiefontein area, South Africa, from Gerryts (1967).

The highly variable nature of kimberlite susceptibilities are thought to be a function of differential weathering of the pipe or the remanent magnetism of the pipe determined by the prevailing magnetic field at the time of intrusion (Fipke *et al.*, 1995). Atkinson (1989) suggests that it reflects the nature of the body itself, in other words its mineralogy, successive intrusive phases, weathering, size and geometry. Ground magnetics is frequently used for follow-up work and as a mapping tool for outlining kimberlite pipes.

Other common sources for confined magnetic anomalies cited by Macnae (1995) are ;

(1) amphibolites,
(2) sulphides (which may show strike and dip with an associated gravity high),
(3) confined mafic or ultramafic bodies (with a associate gravity high),
(4) alkaline diatremes,
(5) magnetite skarns (that usually show up as very large magnetic anomalies),
(6) magnetite concentrations in granite,
(7) surficial maghemite or magnetite pockets in regolith (which show up as shallow, depth limited magnetic sources) and,
(8) cultural features.

2.6.2. Gravity method.

Density is the physical property that determines gravitational response, in particular the density of the target with its surroundings. Differences in rock density produce small changes in the gravity field of the Earth which can be measured.

On a regional scale regions with thick, cool lithosphere exhibit relatively positive Bouguer gravity anomalies with respect to regions with hotter, thinner lithosphere. A problem with accurate gravity readings is the extreme sensitivity required for geometric and topographic corrections, therefore airborne gravity measurements is only used for regional work. Gravity is of very limited use in areas of rugged topography. With GPS navigation systems the cost for auxiliary data collection to correct gravity measurements are reduced substantially and gravity surveys may become more widely used. Anomalous masses of as little as a few thousand tons may be detected by careful surface gravity measurements for bodies that lie just below the surface (Macnae, 1995).

The gravity method is predominantly used as a follow-up technique once the pipe has been located. A negative gravity response is characteristic over kimberlite pipes due to rapid serpentinisation and weathering or the presence of thick crater facies sediments. The lack of response from the denser, fresh kimberlite is ascribed to the greater depth of burial and shrinking carrot-shaped geometry in depth (Atkinson, 1989). In South African mines the specific gravity (SG) of kimberlite below the zone of weathering has been measured between 2.64 and 2.98 g/cm^3, with an average of 2.75 g/cm^3 (Gerryts, 1967).

As the density of weathered or crater facies kimberlite is somewhat lower than the density of common sediment and volcanic hosts, gravity readings on the ground are effective in delineating kimberlites. Unweathered diatreme facies may be of higher density than these common hosts (Paterson *et al.*, 1977).

More than two hundred kimberlite occurrences are known in Tanzania (Edwards & Howkins, 1966). Many of these kimberlites are represented at the surface by small structural basins of sediments which occupy craters connected with the underlying pipes. These sedimentary basins are usually smaller than 30 m in diameter. In 1958 and 1960 a gravimetric survey was conducted over Mwadui and several other kimberlite occurrences in Tanzania by the Geophysical Division of the Overseas Geological Survey of Great Britian.

Spectacular gravity lows were recorded over crater facies kimberlites such as Mwadui (Fig.37). After the regional gradient was removed from the Mwadui area the anomaly appears as a circular negative zone centered over the pipe. The maximum anomaly at the center is about -6 milligal. This striking anomaly is due to the strong contrast in density between the sedimentary beds in the crater facies and the surrounding granite/schist country rock (Gerryts, 1970).

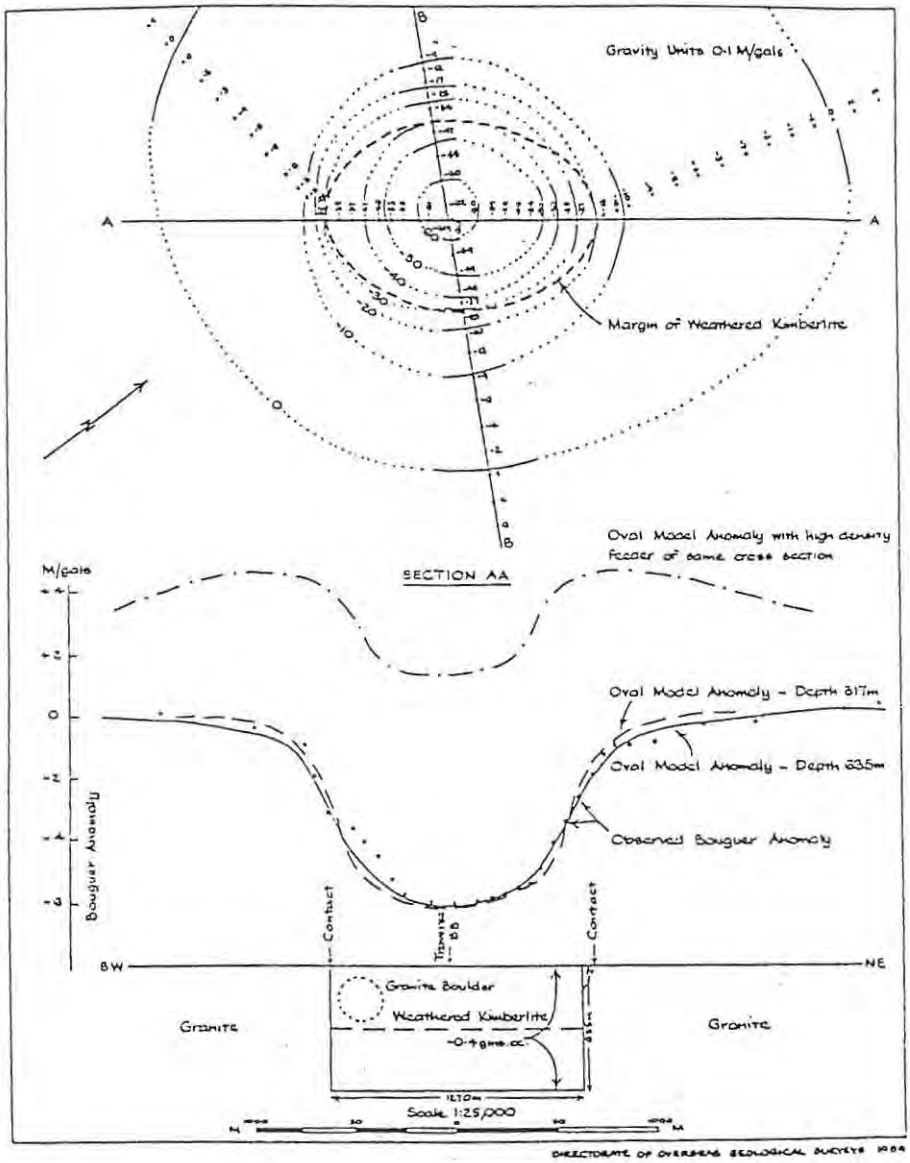

Fig. 37 ; Gravity survey, Mwadui Mine, Tanzania, from Gerryts (1970).

Other kimberlite pipes also produced a well-defined closed negative anomaly, with the weathered upper parts of the pipes having a roughly circular margin with steeply plunging walls. The maximum anomalies are roughly proportional to the diameter of the pipe, about 1 mg/ 200 yards of diameter. If an indication of the proximity of kimberlite has been obtained by sampling a gravity survey can establish the existence or non-existence of a pipe and delineate its margins in one or two days Mason-Smith (1960).

2.6.3. Electrical methods.

2.6.3.1. Electromagnetic (EM) methods.

Electromagnetics provides a means of mapping the electrical conductivity of the uppermost rocks in the Earth's crust. The method involves the production of an alternating current from a transmitting coil (active system) or from larger, more remote systems such as atmospheric electricity or radio stations (passive system) which subsequently generates an electromagnetic field in the Earth's crust. Where the field impinges on an anomalously conductive body eddy currents are induced which generate a secondary electromagnetic field that is measured by a detector coil (Corner, 1998).

Depth penetration is a function of delay time or frequency and an EM measurement at one location can be used to deduce, within severe limitations, the conductivity structure as a function of depth. A large number of choices can be made for the transmitter, receiver and plotting methods and all the variables need to be understood when interpreting data (Macnae, 1995).

Electrical measurements only came into their own when airborne resistivity measurements became viable for primary kimberlite exploration in the mid 1970's. Before that electrical methods were mostly used in groundwork for delineating pipe geometry and the determination to depth of known kimberlite. Airborne electromagnetics (AEM) is commonly used in addition to magnetic surveys.

The target of AEM is the conductive material in the top of the pipe, either the crater facies or the porous or weathered diatreme facies kimberlite. Fixed wing AEM systems have large transmitter strengths and can energise and be sensitive to conductors within a large volume of ground, at a radius of 200 to 300 m from the plane. Helicopter-borne transmitters energise a more local volume, between 50 to 100 m radius. Ground EM has involved time domain instrumentation in recent years.

Kimberlites are characterised by low resistivity readings because of the various assemblages of clay minerals from weathered kimberlite. The rapid near-surface weathering of ultramafic kimberlitic material and high porosity of tuffaceous and brecciated parts of the original diatreme facies acts as a conduit for groundwater flow. The clays developed in the weathering process can produce very conductive cover at the top of pipes, especially where crater facies rock is present. The conductive part of the pipe will thus form at the top and will be fairly shallow, with the effectiveness of EM surveys also depending on the conductivity contrast between the weathered kimberlite and the surrounding country rock (Macnae, 1995).

Gobba (1989) shows the effectiveness of a pulse EM survey over crater and weathered diatreme facies of a pipe in Tanzania (Fig.38).

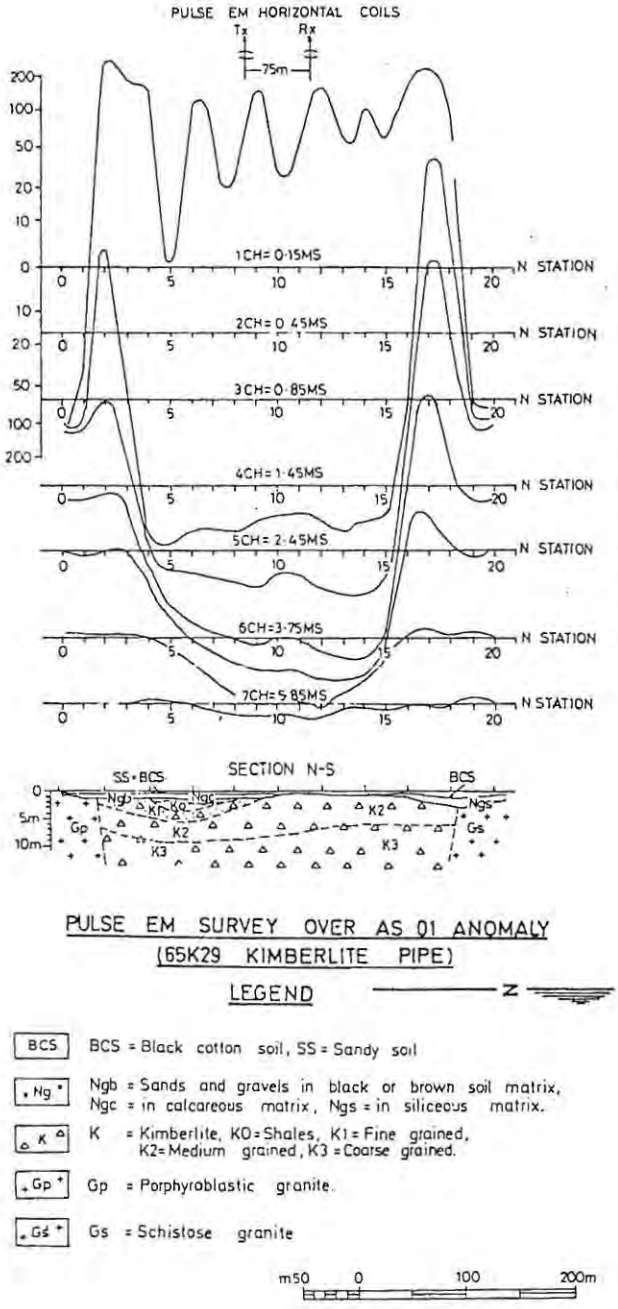

Fig. 38 ; Pulse EM trace over 65K29 kimberlite pipe. The positions for the margins of the pipe appear to be more sharply defined by the pulse EM method, from Gobba (1989).

The conductive contrast between a kimberlite and surrounding rock also depends on the conductivity and thickness of the host rock, regolith thickness, overburden and watertable depth. Saline groundwater and conductive sediments (e.g. graphitic shales) return anomalous values. Fresh kimberlite typically have resistivities above 200 Ω m.

Anomalies over kimberlites typically show high amplitudes and relatively slow decay rates, reflecting the high conductivity of the source. Modelling results from HLEM field data led McNae (1979) to conclude that the responses found were compatible with those expected over flat lying conductors represented by the weathered zone.

Conversely, in areas of clay-altered host rock, graphitic zones and water-rich regions due to extensive faults and fractures, EM methods are likely to be ineffective. EM has also been found to be ineffective in areas with widespread laterised sedimentary cover (Fipke *et al.*, 1995). For example Gobba (1989) notes the highly variable electromagnetic response of the Tertiary sediments and Recent alluvium obscuring the basement rocks of northeastern Tanzania. The variation is interpreted as being due to the heterogeneous, sometimes wet and highly conductive nature of the superficial deposits.

According to Macnae (1995) other common sources for confined conductive anomalies are ;

(1) weathered amphibolites,
(2) sulphides,
(3) weathered local mafic and ultramafic bodies,
(4) weathered alkaline diatremes,
(5) some magnetite skarns,
(6) overburden or sediment patches,
(7) sediments contained in depressions and,
(8) cultural features.

2.6.3.2. Resistivity and induced polarisation (IP) methods.

Induced polarisation (IP or overvoltage) measures the resistivity, or difficulty in sending an electrical current through a substance. The two modes of electrical conduction that occur in mineralised rocks are ionic (in pore fluids) and electronic (in "metallic" minerals). The weathered nature of kimberlites enable ionic electrical conduction. IP surveys are carried out by using the time-domain method, that measures the decay phenomenon produced by the overvoltage, or the frequency-domain method, using the resistivity contrasts between the kimberlite body and surrounding host rocks (Corner, 1998).

Resistivity surveys require at least four points of contact with the ground and the physical movement of significant lengths of wire connections. Depth of penetration is controlled by altering transmitter-receiver geometry. The electromagnetic method has been used to locate kimberlites by measuring the thickness and conductivity of the deeply weathered, usually highly conductive, material overlying the fresh kimberlite and country rock. Resistivity probing is usually carried out to establish the overburden thickness and the best electrode spacing to use (Macnae, 1995).

Resistivity surveys are much slower and more expensive than EM. In some cases it has been used for the routine mapping of the lateral extent of pipes. Resistivity techniques have the advantage that variations in the properties of both resistive and conductive materials as well as the structure of the ground can be investigated. Kimberlite pipes are characterised by low resistivity signatures.

Induced polarisation is a refinement of the resistivity method that can measure dispersive effects caused by minerals such as clays or sulphides (Macnae, 1995). As an example the end-products of the weathering process in Tanzanian kimberlites (e.g. Mwadui), which are light cream coloured crater facies sediments occurring at the surface underlain by reddish pink to brown sediments that give way to green-blue tuffaceous diatreme facies kimberlite, have been tested by IP and resistivity methods. Although these weathered zones are commonly non-magnetic, their clay-rich nature gives them a low electrical resistivity (typically between 10 and 30 ohm-metres), which can give a strong electrical response (Fig.39). The crater facies volcaniclastics are moisture sinks and may create a strong conductivity in contrast to the country rocks, which may give rise to significant induced polarisation and resistivity anomalies (Gobba, 1989).

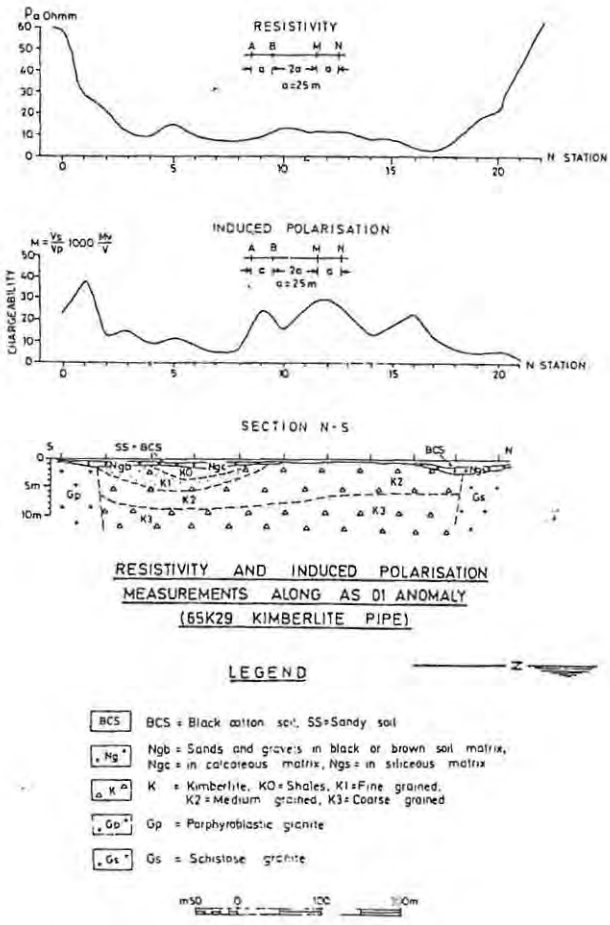

Fig. 39 ; Resistivity and induced polarisation measurements over 65K29 kimberlite pipe. The marked resistivity contrast allows the extent of the pipe to be delineated. The induced polarisation values are lower in the crater facies fine sediments and show higher values in the coarser kimberlitic tuffs, from Gobba (1989).

Da Costa (1989) presented the results of a resistivity survey over the Palmietfontein pipe in South Africa. Fig.40 presents contours of apparent resistivity over the Palmietfontein pipe and a more resistive satellite body. Resistivity soundings also showed the difference between conductive weathering in the pipe to a depth of 58 m compared to 18 m in the surrounding norite.

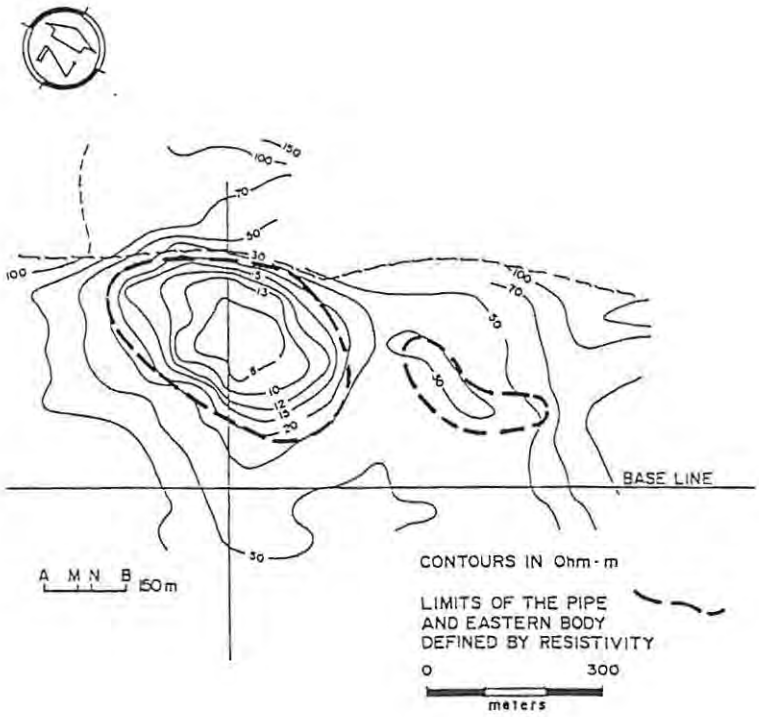

Fig. 40 ; Resistivity contours from a Schlumberger array ground electrical survey over the Palmietfontein kimberlite pipe. The gradual decrease in contoured resistivity values towards the centre of the pipe is more a function of the AB dipole spacing of 150 m than any true increase in conductivity, from Da Costa (1989).

During the dry season in Southern Africa the contact resistance of electrodes can be high and give rise to erratic results with an ordinary alternating current instrument. This difficulty is overcome by confining dry season work to the valleys which retain sufficient surface moisture to ensure good electrode contacts. The second problem is caused by deep weathering in some valleys or parts of valleys. These areas often give rise to anomalies similar to those found over kimberlites. In the case of large pipes resistivity surveys with different electrode spacings would probably be able to distinguish pipes from weathered bedrock (Gerryts, 1967).

2.6.4. Radiometric method.

Radiometric surveys use gamma-ray spectrometry and total-radiation radiometrics methods to measure the radiometric signal from the Earth's surface. The detecting unit emits a flash of light (a scintillation) when struck by a gamma-ray. The intensity of the scintillation is directly proportional to the energy of the gamma-ray, which in turn, is a measurable function of the uranium, thorium or potassium source (Peters, 1978).

The usefulness of radiometrics is dependent on the amount of exposure, degree of residual cover, size and radioactivity of the target. The radioactive signal from radiometrics is rapidly reduced and masked by a few centimeters of transported overburden, although residual soil may still provide a signal (Atkinson, 1989).

Kimberlites do not have a marked radioactive response, although anomalous concentrations of potassium (up to 10% in leucite) can be significant. Thorium and uranium are of lesser importance (Macnae, 1995). Paterson *et al.* (1977) presented the results of ground radiometric surveys over some kimberlites in Lesotho and although the data exhibited some anomalies they were not sufficiently diagnostic to justify routine application in exploration.

2.6.5. Seismic methods.

The main physical properties sensed by seismic systems are seismic velocity (refraction surveys) and velocity and/or density contrasts (reflection surveys).

Seismic refraction is mostly used to establish the poorly consolidated layers near the ground surface, such as the depth of weathering of kimberlite pipes, and for determining the depth and configuration of bedrock in alluvium-covered areas. Reflection seismics is used for deeper level work and may be useful in locating major unconformities or structures. Seismic data is gathered by producing a shockwave and measuring the resultant travel times (or arrival times) in milliseconds between the arrivals of different forms of waves along a linear array of geophones. The refraction- and reflection paths are produced by the differences in density at the contacts between two mediums.

Reflection seismics has also been used in defining the lithosphere- asthenosphere- mantle interfaces. Xenolith studies were used to establish the density, chemical composition and P-T values (through geothermobarometry), for a given region. These values were then used to calculate the seismic velocity of a given rock type and constrained the geophysical models for the stratigraphy and structure of the upper mantle as well as the nature and depth of the Moho (O'Reilly, 1985).

The petrology of mantle root-derived xenoliths has indicated that the lithosphere under Archaean cratons are cooler and more refractory than that of the adjacent upper mantle. This is supported by seismological (and geothermal) data suggesting that plates in older continental regions are of greater than average thickness and are underlain by an extensive layer of anomalous mantle material. Jordan (1988) refers to these lithospheric roots as tectosphere and propose that they remained attached to the continents during plate motions. The seismic properties of mantle roots are thus consistent with the model of relatively cool and chemically depleted, highly refractive lithospheric roots proposed on the basis of petrological studies.

On the basis of seismic tomography Grand (1987) found that the shield and stable platform of North America coincide with a region of relatively fast shear waves and that deep, high-velocity mantle roots are situated beneath the Archaean Superior and Slave provinces of the Canadian shield. As the roots are gravitationally stable and thus must be composed of less dense material, the higher shear wave velocities within the roots require cooler temperatures relative to adjacent hotter asthenosphere (Helmstaedt & Gurney, 1995).

Due to the generally high porosity and low density within a kimberlite, velocity lows are to be expected within the kimberlite and large contrasts are expected at the contacts between a kimberlite and its surroundings (Macnae, 1995). Refraction seismics was used succesfully by Da Costa (1989) to accurately map the edge of the Palmietfontein kimberlite in South Africa.

2.6.6. Heat flow models.

Heat flow models of mantle roots are consistent with cratonic areas characterised by thick, cool lithosphere which adequately explains the differences in surface heat flow between the Archaean cratons and surrounding younger terrains.

For example Ballard & Pollack (1987) state that a cratonic root of relatively cool, non-convecting and poorly-conducting, depleted material, extending to depths of 200 to 400km, can divert enough heat away from the Kaapvaal-Limpopo-Zimbabwe craton to account for 50 to 100% of the observed contrast in surface heat flow between the craton and surrounding mobile belts. The craton areas are characterised by heat flows of about 40 mW/m^2 compared to the 65 mW/m^2 heat flows measured in the younger surrounding mobile belts. Diamondiferous kimberlites only occur in areas with heat flows below 40 mW/m^2.

2.6.7. Down-hole geophysics.

All of the above-mentioned techniques can also be used to establish the internal physical properties of a kimberlite pipe from borehole intersections.

2.7. Geochemical techniques.

The source material of kimberlites originate from different parts of the upper mantle, therefore the different content of compatible versus incompatible elements in the source rock results in a highly variable chemistry for kimberlites. Many pipes show successive intrusions over time, as shown by variations in indicator mineral and mantle xenolith populations. During kimberlite emplacement variable differentiation-, fractionation-, alteration- and magma-mixing processes may be active in each kimberlite. Furthermore, near surface devolitisation and interaction with country-rocks and meteoric water will further influence and complicate kimberlite geochemistry (Skinner, 1998).

Whole-rock geochemistry is routinely used where weathering and oxidation of the kimberlite makes petrographic and mineralogical analysis difficult. This weathering and oxidation is characterised by the so-called "yellow ground" in temperate to tropical climates and can range from 20 to 100 m in depth (Atkinson, 1989).

Kimberlites are olivine-rich, undersaturated ultramafic rocks (SiO_2 between 25 to 35 wt % and MgO between 25 and 30 wt %), with unusally low Al_2O_3- (generally < 5 wt %), as well as Na_2O contents (< 0.5 wt %), expressed as low Na_2O/K_2O ratios of < 0.5 wt %. They are enriched in ultramafic elements, such as Mg, Co, Ni, Cr and Cu, similar to other ultramafic rocks, reflecting their high modal abundances of olivine and spinel. Kimberlites are also enriched in CO_2, TiO_2, K_2O and P_2O_5 and contain an extremely high volatile component, commonly > 10 wt % (mainly from CO_2 and H_2O incorporated in primary and deuteric carbonate and serpentine) (Mitchell, 1989 ; Skinner, 1998).

There is a clear difference in CO_2 content between hypabyssal facies rocks (3 to 17 wt %) and the degassed diatreme facies rocks (< 4 wt %) of kimberlites. Kimberlites are also strongly enriched in incompatible trace elements such as Rb, Sr, Zr, Nb, Ba, Cs, Th, U, Pb, P and the light rare elements (LREE) (Scott-Smith, 1996 ; Mitchell, 1989 ; Skinner, 1998).

Wedepohl & Muramatsu (1979) compared the average element concentrations of 11 South African kimberlites with an average ultramafic rock. The investigators found the following elevations for kimberlites (Table XI) ;

Table XI ; Average element concentrations of kimberlite vs ultramafic rocks, adapted from Wedepohl & Muramatsu (1979).

Element enhancement	Range	Elements
Moderate	5 to 10 x	Ca, Fe, Co, B, Mo, Pt, Y, Se, Bi and HREE
High	10 to 100 x	K, Rb, Pb, Ce, Nd, Sm, Nb, Ta, Zr, Ti, Ba, Sr, Tl and F
Extreme	> 100 x	U, Th, La and Cs

Geochemical point samples over kimberlites are collected in an area of 50 m radius around the sampling position. Usually a 2 to 3 kg soil sample is collected from the top 1 to 5 cm of both the A- and B-horizon of the soil profile. A geochemical sample can also be extracted from normal grid- or stream sediment samples, but are less effective due to the very localised nature of element distribution. Geochemistry has also been used in identifying weathered outcrop and drill cuttings.

The preparation of geochemical samples prior to analysis entails sieving to 15 to 20 g of less than 65 μm fraction. The samples are powdered and the powdered pellets analysed by X-ray fluorescence (XRF), inductively-coupled plasma spectrometry (ICP) or atomic absorption spectrometry (AAS) laboratory techniques. The XRF technique has relatively high concentration detection levels but is capable of multi-element determination. It is mostly used for whole rock chemical analysis. The AAS and ICP techniques are widely used at present because they are inexpensive, relatively cheap and can determine about 40 elements at low levels of detection. The selection of an appropriate analytical technique depends on the number of elements to be determined and their apparent concentration levels, the required detection limit (sensitivity) and the requirements for precision and accuracy (Peters, 1978).

The suite of elements usually analysed for are Mg, Ni, V, Co, Cr, Ti, Nb, La, Sc, Ce, Ta, Zr, Hf, P, Ba, Sr, Th, P, U and LREE. In practice the most useful elements are Y, Ni and Nb. Altered ultramafic alkaline rocks can be distinguished from common mafic and ultramafic rocks by comparing the abundance and inter-element ratios of the above-mentioned elements (Mitchell, 1995).

Geochemistry is not particularly useful in exploration programmes. For instance, Fipke *et al.* (1995) report that stream sediment sample dispersion trains of anomalous values rarely extend for more than a few hundred metres. Even for a large exposed or near surface body the geochemical dispersion halo for Ni, Cr, Mg and Nb in soils IS limited to a few tens of metres from the source, generally up to 50 m, and a body buried by more than 3 m of transported material is often undetectable (Muggeridge, 1995). With geochemical interpretation caution should be taken in areas where cultural activities may lead to contamination, for example fertiliser (especially enhanced potassium and phosphorus concentrations) has proved to be problematic in farming areas.

In some cases geochemical analyses may be useful. Nixon (1980) reported anomalous Cr and Ni values around kimberlites in Lesotho. Geochemical anomalies also revealed elevated Nb values in the -80 mesh fractions of stream sediment samples of Lesotho.

In the Mwadui area geochemical samples were collected over kimberlite pipes and from drill samples (Gobba, 1989). The samples were analysed for Zr, Rb, Y, P_2O_5, Nb_2O_5, K, Ca, Te, F, SiO_2, Al_2O_3, Mg, Cr, Cu, Zn, Pb, Co, Mo, S, As, Se, Sb and Bi. It was found that only Nb, together with Ba, Ni and P, were useful indicators for kimberlites in the granitic and metamorphic rock backgrounds as shown in Fig.41 and 42.

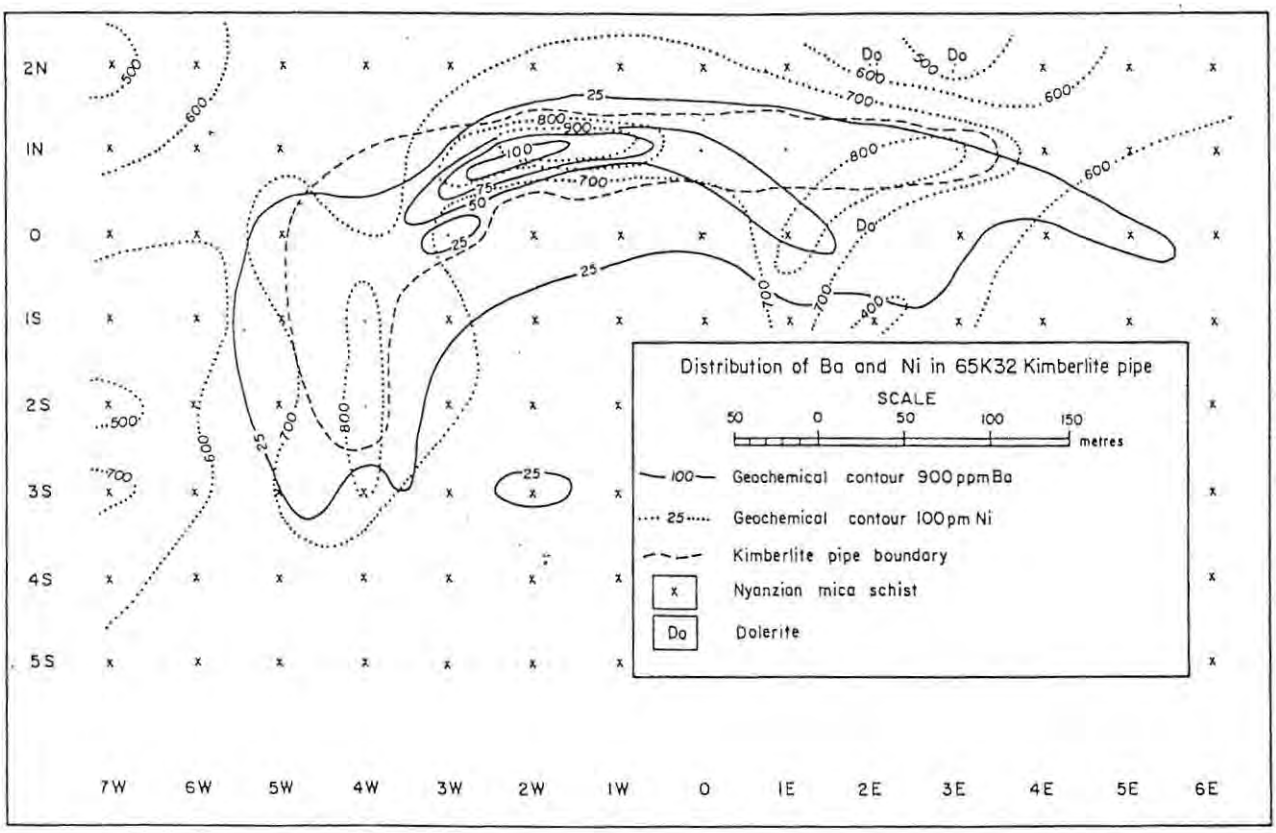

Fig. 41 ; Geochemical dispersions for Ba and Ni in soils over a kimberlite pipe in Tanzania. The metal contents show higher values at the centre of a dyke-like pipe. The presence of a dolerite dyke in the eastern part appear to be traced by Ni values, from Gobba (1989).

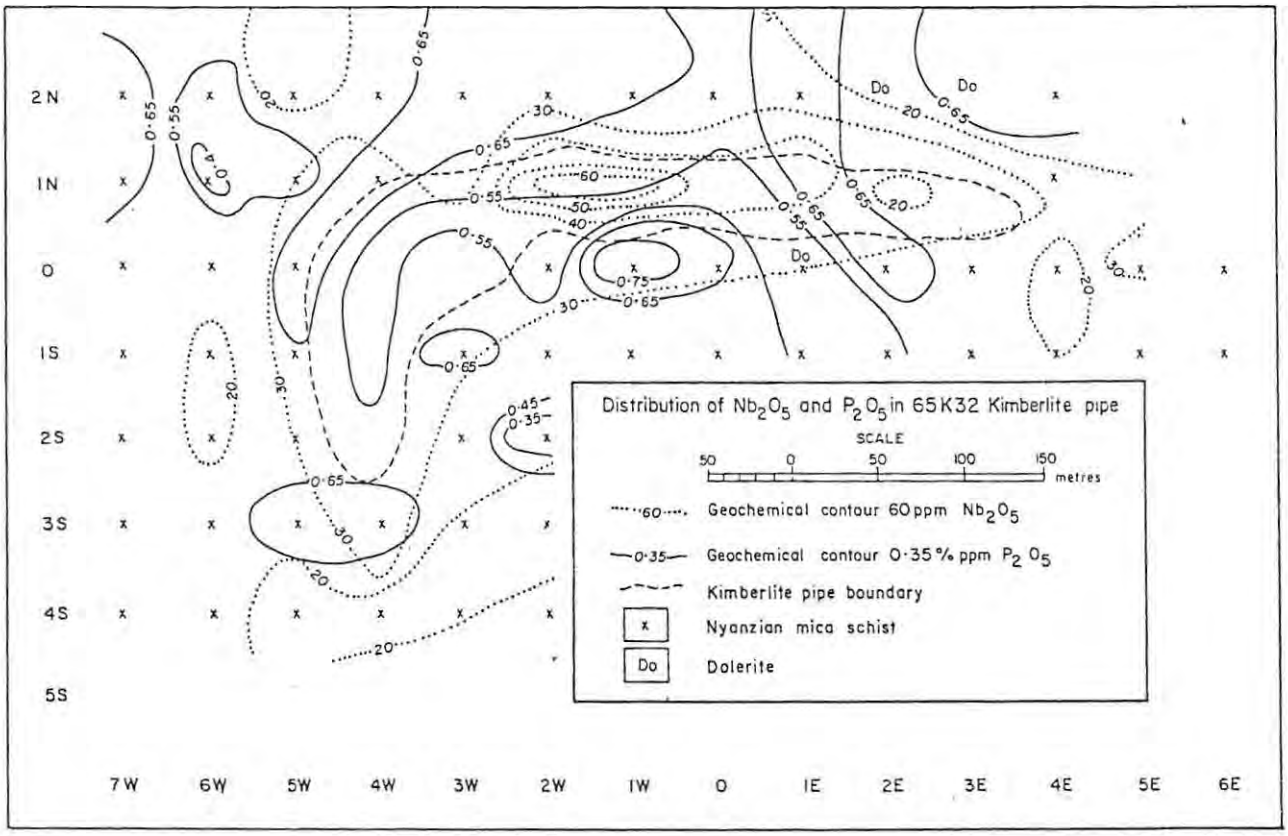

Fig. 42 ; Geochemical dispersions for Nb_2O_5 and P_2O_5 over a kimberlite pipe in Tanzania. Nb_2O_5 is a better indicator than P_2O_5 in Nyanzian mica schist country rocks, from Gobba (1989).

According to Pybus *et al.* (1998) the properties of the magnesium-bearing minerals serpentine and talc, which are commonly associated with weathered kimberlite, have also been used to locate kimberlites by a portable infrared mineral analyser spectrometer. The kimberlites, however, have to be exposed at surface.

2.8. Petrographic- and electron beam techniques.

The macroscopic examination of exploration samples may permit the identification of potentially diamondiferous rock. Standard transmitted light thin section petrography permits identification of many macrocrystal, phenocrystal and groundmass minerals, although only generalisations regarding the composition of the minerals can be made. Many kimberlites are characterised by very dark, optically unresolvable, complex groundmass which obscures the majority of accessory phases under transmitted light. However, transmitted light observation is important in assessing the textural character of the rock. Where identification of primary minerals is possible, as in fresh kimberlite samples, bulk rock geochemistry is not necessary as it is a direct reflection of the modal mineralogy (Mitchell, 1995).

Unfortunately reflected light petrography does not provide significantly more information than transmitted light studies as many of the critical diagnostic minerals are not opaque. Standard thickness (30 microns) thin sections do not permit adequate resolution of the groundmass and thinner sections (15 to 20 microns) or double-sided polished thin sections can be used (Mitchell, 1995).

Groundmass minerals of kimberlites are routinely examined by electron microbeam methods. The two techniques used for describing and identifying fine-grained or complex rocks are back-scattered electron imagery and energy dispersive X-ray spectrometry. Both techniques use carbon-coated polished-section samples and are analysed under electron microprobes or scanning electron microscopes (Mitchell, 1995).

Back-scattered electron images are formed when incident electrons are elastically scattered from minerals. The degree of back-scattering increases with the average atomic number of the sample. Consequently, discrimination of common silicate minerals (mica, olivine, feldspar, etc.) from oxides (spinels, ilmenite, rutile, perovskite) and sulphides is readily permitted. In addition, the high resolution of the images fascilitates observation of the smallest details of the groundmass (Mitchell, 1995). Examples of some back scattered images ares shown in Fig.41.

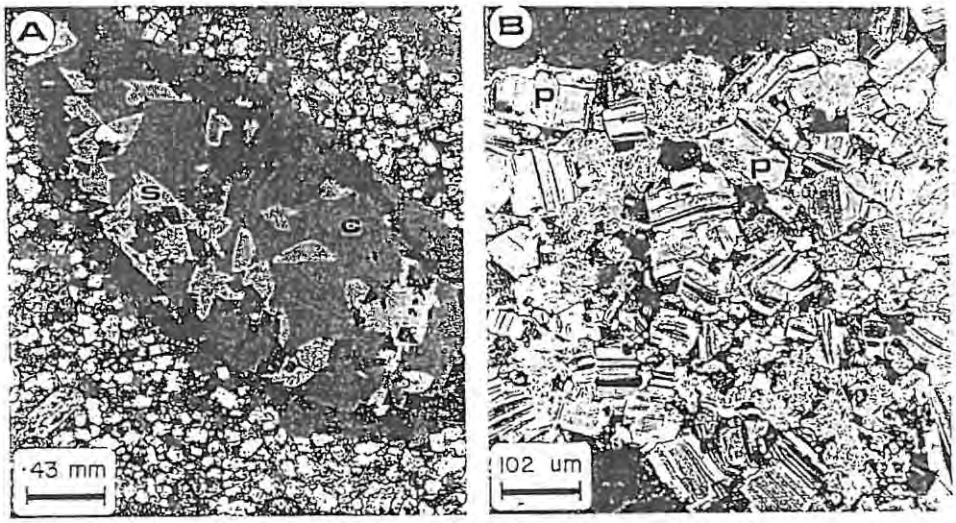

Fig. 43 ; Back scattered electron images. (A) Ovoid carbonate segregation in the Benfontein kimberlite (South Africa), consisting of euhedral dolomite (dark grey) and siderite (s) set in a calcite (c) and dolomite matrix. The euhedral phase is ancylite (white). The segregation is set in a groundmass consisting of subhedral spinel (light grey) and calcite, (B) Orangeite from Swartruggens (South Africa) consisting of microphenocrysts of phlogopite (p) which are zoned to margins of tetraferriphlogopite (white) set in a groundmass of calcite (light grey and porous) and serpentine (black). From Mitchell (1995).

Energy dispersive X-ray spectrometric analysis of minerals is used in conjunction with back-scattered electron images. Minerals are initially identified qualitatively from their characteristic X-ray spectra. Individual minerals may subsequently be quantitatively analysed by standard techniques. X-ray spectra of the minerals are used to estimate their gross composition. It is thus possible to determine whether ilmenite, Nb-ilmenite, Mn-ilmenite or Mg-ilmenite is present simply by observation of their X-ray spectra (Mitchell, 1995).

Altered samples have compositions that represent mixtures of secondary phases (serpentine, chlorite, calcite) and residual phases. These samples are best identified by a combination of optical-, electron beam- and geochemical methods. Optical methods are mostly used to examine primary mineral- and relict textures that characterised the original rock, especially the habit of olivine pseudomorphed by serpentine and lath-shaped, deuterically-altered melilite pseudomorphs. Oxide minerals, such as rutile, ilmenite and K-Ba-titanites, may also reflect their original character when all the primary silicate minerals are destroyed and can be identified by electron beam methods. Bulk compositions reflect mixing lines between fresh samples and completely altered rocks (Mitchell, 1995).

The first stage of Mitchell's (1995) mineralogical-genetic classification procedure is based upon recognition of the typomorphic major minerals listed in Table XII. The second stage is undertaken when a particular sample has been identified as having high diamond potential.

Table X II; Initial assessment of magma type and diamond potential, from Mitchell (1995).

TYPOMORPHIC MINERAL	MAGMA TYPE	DIAMOND POTENTIAL
Sanidine	Lamproite (evolved) Minette Orangeite (evolved) Leucitite	low nil low nil
Plagioclase	Common magma types	nil
Melilite	Melilitoids (alnoite) Kamafugites (katungite)	nil nil
Kalsilite	Kalsilite pyroxenites Kamafugites	nil nil
Lueucite	Lamproite (evolved) Leucitites	nil nil
Ti-garnet	Melilitoids	nil
Nepheline	Nephelinites Leucitites Mafic phonolites	nil nil nil
Olivine and none of the above	Kimberlite	high
Olivine, phlogopite and none of the above	Orangeite Kimberlite Olivine lamproite Melilitoids (aillikite, ultramafic lamprophyres)	high high high

Diatreme and crater facies diamondiferous rocks are petrographically classified according to the textural-genetic scheme outlined by Clement & Skinner (1985) and Mitchell (1991) (refer to Fig.14). These schemes reflect volcanic processes that are not unique to kimberlites. A textural- genetic scheme should only be done after the identity of the rock has been determined (Mitchell, 1995).

2.9. Geobotanical- and geobiological techniques.

Geobotanical studies of the soil and vegetation above kimberlitic bodies indicate that there is some vegetational and soil expression above many kimberlites, which can often be seen as colour contrasts on aerial photographs. Vegetation is often greener and more profuse over kimberlites, and stay green longer in the dry season because of the better moisture retention capacity of associated montmorillonitic clays. Secondly trace element enrichment over kimberlitic soils, including elements like niobium, phosphorus, nickel and potassium, are also conducive to plant growth (Atkinson, 1989). The Bobbejaan and Star dyke systems, the Finsch kimberlite, and the dykes and pipes located near Victoria West have been cited as examples of vegetation anomalies noted on aerial photographs (Fipke *et al.,* 1995).

Geobiological influences in kimberlite exploration has been reported in Botswana where considerable reliance has been placed on indicator mineral sampling of termite mounds. Bioturbation by ants and termites in dry parts of Southern Africa have brought kimberlitic minerals to the surface from kimberlites covered by overburden of 60 m or more, for example Jwaneng. Some of the indicator minerals were brought up to surface by termites, who in their search for water, occasionally bring up kimberlite indicator minerals from the aquifers lying on bedrock depressions. These depressions may be caused by kimberlite pipes, far below surface. Excavations by burrowing animals may also exhume indicators (Muggeridge, 1995 ; Miller, 1995).

Geobotanical- and geobiological methods are only used as a supplement to other methods in kimberlite exploration.

2.10. Evaluation techniques.

2.10.1. Introduction.

The ore reserve estimation of all deposits are based on a geological model, which will determine the sampling grid pattern. Table XIII is a summary of the characteristics of worldwide kimberlite pipe occurrences, as determined by Bliss (1992). A geostatistical model is constructed based on the grid sampling values, from which the best estimate of average grade and the confidence limits thereof, can be formulated.

Ore reserve estimation of a deposit requires the estimation of both the volume of ore reserves (tonnage) as well as the *in situ* value of the deposit. The *in situ* value of kimberlite deposits have to be calculated from the grade, size and quality of the diamonds. Grade is usually reported as carats/hundred tons (cpht) or carats/m^{-3}. Value is usually converted to US $/carat and the value of the deposit expressed as US $/ton.

Table XIII ; Rule of thumb characteristics from worldwide kimberlite deposits, adapted from Bliss (1992).

Median tonnage (t)	26 000 000
Median diamond grade (cpht)	0.25
Median diamond size (ct)	0.07
Median percentage industrial quality diamonds	67
Median outcrop area (ha)	12

Evaluation of kimberlite pipes and dykes involve increasingly large representative bulk samples, put through a small pilot plant. The reason for the large scale sampling necessary for kimberlite evaluation is that even high grade ore from a typical kimberlite may have diamond grades of approximately 100 cpht, which equates to only 0.2 g/t or 0.2 parts per million (Miller, 1995).

Furthermore, diamond grades of economically viable pipes range upward from 3 cpht to more than 200 cpht. The reason for this wide range in economic grades is due to the considerable spread in average value of diamonds in a deposit, which may vary from US$ 9 per carat to more than US$ 150 per carat (Jennings, 1995).

Bulk sampling gives a sample of diamonds of sufficient size to be valued and assists in determining the metallurgical characteristics of the host material and permits final plant design. Evaluation usually develops over three stages (Table XIV).

Table XIV ; The three stages in kimberlite ore reserve estimation and evaluation.

Stage I	Stage II	Stage III
Drill sampling and logging of individual kimberlite phases and facies (1) Visual examination of ; (a) abundance of kimberlitic indicator minerals, (b) colour of pyrope garnets, (c) presence/absence of eclogitic and/or peridotitic nodules (d) kimberlitic facies and description of drill core or chippings (2) Major and trace element chemistry of borehole samples (3) Collection of a minimum of 50 kg drill core or surface sampling for ; (a) microdiamond tests (b) recovery of heavy mineral concentrates for geochemical and mineralogical analysis.	Mini-bulk sampling for a rough estimate of the grade and tonnage (1) Collection of between 20 and 100 tons of kimberlite (2) Processing in a small pilot plant for simulation of actual mining recoveries	Bulk sampling of at least 1000 tons or 300 carats for estimation of grade and value per carat (1) At least 10 000 tons or 5000 carats are required for a complete feasibility study

Sources :

Atkinson (1989)
Levinson et al. (1992)
Rombouts (1995)

2.10.2. Kimberlite sampling methods.

Ore reserve and grade estimation requires conventional drilling, pitting and trenching methods, from which representative samples are used to characterise the entire orebody. The geological parameters that potentially define different diamond populations within the kimberlite needs to be delineated. This is done by orientation pit-, trench- or large diameter borehole sampling. Successive intrusions within the same kimberlite, facies changes, structural complexities and country rock xenoliths may all influence the variation of diamond populations in the same pipe. After orientation sampling has been done a systematic, square sampling grid, taken normal to the ore zone whenever it displays a preferred orientation or trend (such as with kimberlite dykes), provides a good statistical coverage and can be used in geological cross sections with a minimum of projection.

The objective in optimising a sampling pattern is to provide the exact number of samples needed to represent the distribution and characteristics of the diamond population, as well as the dimensions of the orebody (kimberlite), at an appropriate level of precision. Zones of influence are often related to adjacent samples on a geometric basis, but the two adjacent samples must be correlatable at some acceptable confidence level (Peters, 1978).

The optimal grid sampling density and unit sample volume is calculated from the statistical parameters of the diamond stone sizes and density distributions. The bulk samples from the regular grid sampling is processed in a small pilot plant that simulates the actual mining recoveries to be expected in the future mine plant (Rombouts, 1995).

The influence of ore-forming processes on diamond distribution is varied. For example crater facies kimberlite consists of near-horizontal, interbedded epiclastic sediments and volcanic tuffs. The samples have to be split up with depth and treated seperately, to determine grade variations from layer to layer. Coarse-grained tuff layers reflect higher energies during deposition from the air during the time of the volcanic explosion, whilst coarse-grained epiclastic sediments reflect the winnowing of the loose tuffs in the crater lake, with the larger and denser particles settling in the bottom garvels. Because of the reworked nature of coarse-grained layers they are expected to have larger stones and higher grades.

In kimberlite diatreme facies grades are likely to be more variable in the horizontal plane than with depth. Differences in grade can be correlated with different vents, or with a concentric pattern of facies differentiation. The surface processes active over kimberlites after intrusion leads to eluvial and colluvial gravel development over kimberlites. It is a well known fact that high diamond grades are found in the top part of most kimberlite occurrences (Rombouts, 1995).

Bulk sampling of kimberlites covered by surficial deposits are costly. As an example the Jwaneng pipe (Botswana) was covered by 60 m of Kalahari sands. Large core drilling (200 to 380 mm drill bits) were used to sample the kimberlite for micro-diamonds (< 0.5 mm in size) and macro-diamonds. Sampling was carried out along a 50 m grid to a depth of 200 m. The large diameter core were then split into 6 m sections. Unit samples were only 0.68 m^3, sufficient to recover several stones per sample, as the Jwaneng deposit is very rich (1.3 to 1.6 carats/ton). The drilling results were confirmed with six pits of 3 by 3 m to a depth of 165 m (Chadwick, 1983).

Orapa, in Botswana, consists of a 760 by 530 m oval basin filled with crater facies sediments up to a depth of 90 to 285 m. The crater facies is underlain by diatreme facies kimberlite. Ore reserve evaluation was done by drilling to assess the continuity of the orebody at depth and by pitting along a 76 m grid to assess the diamond content. Pits were sunk to a depth of 12, 24 or 36 m and samples were split into 1.5 m sections. The samples were treated in a heavy media pilot plant to determine grade variations between the different layers of kimberlitic sediments. To obtain a sufficient number of diamonds for value estimation, additional pits were sunk on a 38 m grid to depth of 30.5 m (Allen, 1981)

2.10.3. Sample processing.

To effectively assess the grade of economic kimberlite deposits samples have to be of the order of several tons, as a poor diamond recovery rate will result in a very skewed grade distribution with a high percentage of barren samples. As diamonds are rare their recovery from hard rock needs to take care of liberating them without breaking them. Samples are washed and diamonds recovered in a pilot plant, which usually consists of a crushing plant, if the ore is hard, a desliming trommel, vibrating screens and a gravity concentrating system (Rombouts, 1995).

The ore is broken down into particles of less than 10 mm size, usually in a jaw crusher or hammermill. Particles between 4 and 10 mm is sent to the concentrating plant and the rejects crushed in a second stage by a semi-autogenous mill to a maximum particle size of 0.4mm. The 0.4 mm is treated together with the 0.4 mm fraction of the first stage crushing in the concentrating plant. If the ore is soft a trommel and scrubber disintegrates the ore to avoid clayballing. Screens seperate the fraction to be concentrated, usually from 0.5 mm to 16 mm, but this fraction size may vary (Rombouts, 1995).

Most concentrating systems are based on gravity. Rotary pans, jigs and heavy media cyclones all seperate the lighter material from the important heavy minerals, including diamonds (which have a specific density of 3.5 g/cm^3). The final recovery is done either by hand picking, a grease belt table (as diamonds are hydrophobic and stick to the grease) or X-ray sorter. As the concentrate passes through an X-ray beam the diamond flouresces, which is detected by a photocell, and the particle is blown aside by a jet of compressed air (Rombouts, 1995).

2.10.4. Diamond grade distributions.

A geostatistical ore reserve estimation consists of two phases. The first phase quantifies the trends and variability of the mineralisation within the orebody, which is based on the geological model and the results from diamond drilling, by means of experimental variograms in a number of directions through the orebody. The second phase uses the variogram model and the grade sampling results to estimate block grades by geometrical- or distance-weighting methods. The most commonly used procedure used at present is the distance-weighting method known as kriging.

2.10.4.1. Experimental variogram model.

The variogram function deals with regionalised variables that have specific distance and directional characteristics. A semivariogram is a graph (Fig.44) that shows the relationship between differences in pairs of sample values at increasing distances between sample sites in a particular direction (Peters, 1978).

The relationship is shown by the formula for the geostatistical variance, the gamma function. For samples taken at uniform intervals, the gamma function would be ;

$$\gamma(h) = 1/2n \, \Sigma[\, g(x) - g(x+h)\,] \text{ where}$$

(1) $g(x)$ is the value at the sample point x,
(2) $g(x+h)$ is the value at a point $(x+h)$ meters away,
(3) h is a distance vector and,
(4) n is the number of data pairs counted.

The gamma values change as the lag (interval) between pairs of samples increases. In Fig.44 a spherical (the most commonly used model) is fitted to an experimental variogram plotted from sample data. At a lag called the range (a) of the variogram, the influence of the closer samples is lost and the growth curve reaches a plateau of independent (random) behaviour. The sill of the variogram ($C_1 + C_0$) is at the plateau and is the overall total variance of the complete ore zone. The maximum acceptable spacing between samples in a particular direction would be the distance or zone of influence shown by the range of the variogram (David, 1977 ; Peters, 1978).

Samples taken at greater spacing (near or beyond their distances of influence) would be likely to miss the significant correlation. Samples taken at a much closer spacing would show the correlation but would be unnecessarily close. C_0 is known as the nugget effect and C_1 is the size of the sill (David, 1977 ; Peters, 1978).

Where the range shown in one of a group of differently orientated variograms is smallest in one lateral direction or in the vertical dimension, sample sites would have to be spaced closer together in that direction, for example drilling closely spaced holes across the suspected trend of the orebody. In deposits with a strong random component (dominated by the nugget effect rather than the regionalised element), and in deposits with multiple geological controls, geostatistical techniques may be difficult or impossible to use. For example, the fewer the average number of stones recovered per sample, the more important the effect of chance in recovering a stone in a sample. The variance will, therefore, contain a Poisson (or "nugget") effect, which is random and without spatial structure (David, 1977 ; Peters, 1978).

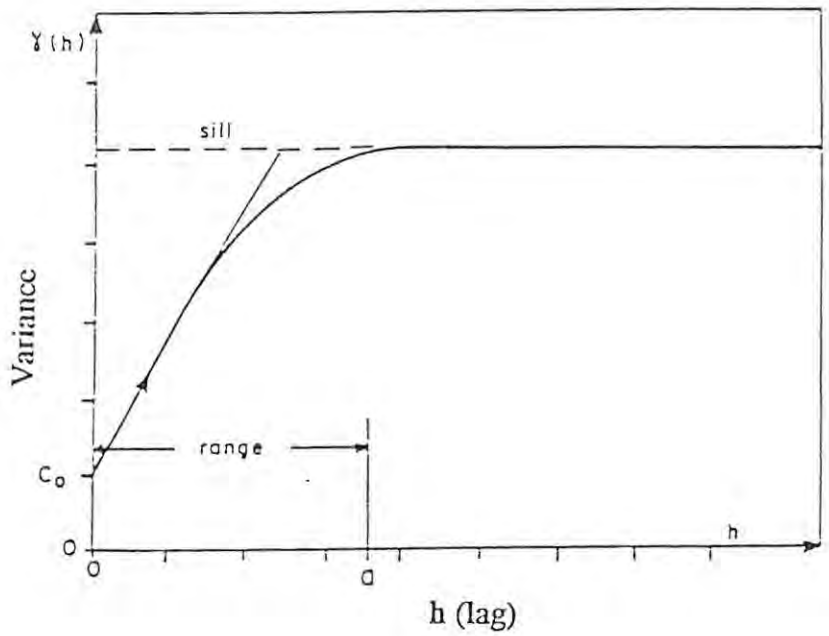

Fig. 44 ; The spherical model variogram, from David (1977).

In conclusion it should be noted that the semivariogram assists in planning an effective sampling pattern from data of a small number of orientation drillhole ore samples. It is an important procedure in the evaluation stage of any kimberlite deposit.

2.10.4.2. Kimberlite diamond grade distributions.

The grade distribution of samples from diamond deposits are positively skewed, often with a peak of barren or poor grade samples. When plotted on lognormal graphs, they show a strong deviation from lognormality, with poor samples having higher frequencies than predicted by the lognormal model. Diamonds are not distributed uniformly, or totally at random, in a deposit. The grade distributions in kimberlites are much more homogeneous than in alluvial deposits. Because stone density distribution is relatively homogeneous in a given facies it often approaches a simple Poisson or normal distribution (Rombouts, 1995).

As kimberlite deposits are characterised by a lognormal grade distribution, the arithmetic mean of sample results can be used as an estimate of the average grade of the deposit provided all the samples are of unit size and taken along a regular grid. However, the average grade of sample results are only meaningful if the confidence limits on the estimated average are known. If the confidence limits are too wide a denser sampling pattern is necessary. The variance of the stone size distribution are combined in the variance of the grade distribution. The average grade and the confidence limits at any level (such as 80% or 90%) can be used to classify reserves, depending on what is considered an acceptable risk. As a rule of thumb proven reserves should have the average grade and its lower confidence limit above the break-even grade. Uneconomic reserves should have their mean and upper confidence limits below the break-even grade. Probable reserves will fall between the above-mentioned grades (David, 1977 ; Rombouts, 1995).

Grade distributions are represented by histograms (Fig.45a), where the data is split into classes or intervals. These classes are usually of equal size with the data grouped into them and can also be represented by a relative frequency curve or a cumulative frequency curve.

According to Till (1974) a distribution is usually described by the following parameters ;

(1) median value - which divides the area under the curve into two equal parts,
(2) mode - the value of the measurement with the greatest frequency and,
(3) mean - (μ) which is the sum of the measurements or observations divided by the number of measurements).

The mean is formulated as ;

$$\mu = \sum_{i=1}^{n} x_i / n$$

where x_i = the value of the i^{th} measurement (i = 1, 2, 3 ..., n-1, n).

To describe the spread or deviation of values about the mean the standard deviation (σ = which is the square root of the variance) is used.

$$\sigma^2 = \sum_{i=1}^{n} (x_i - \mu)^2 / n$$

Fig.45b is a graph of a lognormal distribution showing the relative positions of the median, mode and mean mentioned above. As mentioned before kimberlite deposits show lognormal diamond grade distribution, in other words most diamonds are small compared to the mean but a few are very large. It is called a lognormal distribution because the logarithms of the measurements result in a normal distribution (Fig.45c).

(a)

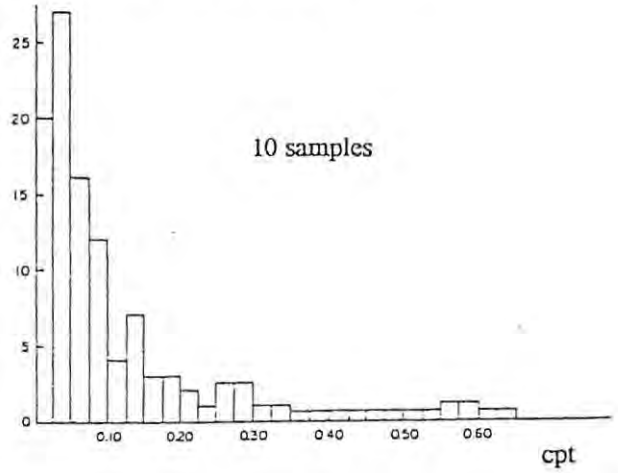

(b)

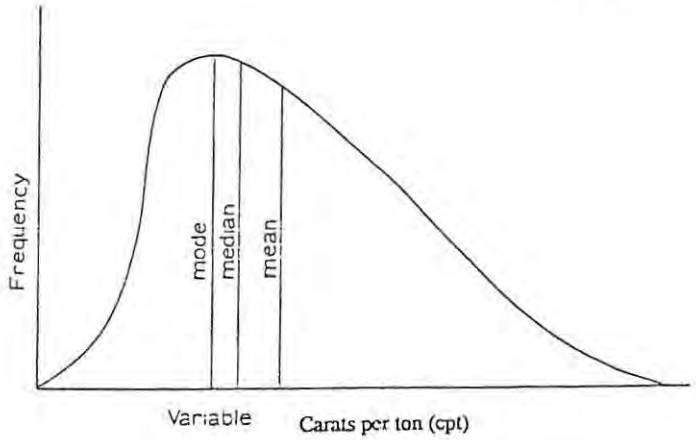

(c)

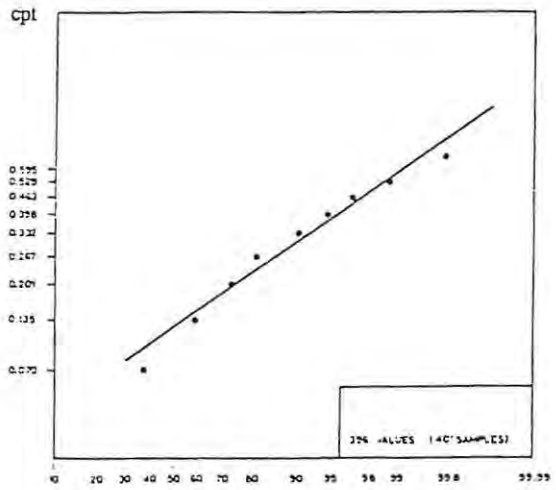

Fig. 45 ; (a) An example of an asymmetrical frequency histogram (or lognormal distribution). (b) The positions of median, mode and mean values. (c) An example of the cumulative distribution of microdiamonds plotted on log-probability paper. From Till (1974) and David (1977).

Mallinson (1997) summarised the characteristics of a lognormal ditribution as follows ;

(1) the curve is skewed to the right,
(2) logarithms of grades are normally distributed about the natural log (*ln*) of the geometric mean,
(3) median = geometric mean (GM) = $e^{(\text{mean of the } ln \text{ values} + B)} - B$, where e is the antilog and B a constant
(4) mean = $\mu = (GM + B) * (e^{\sigma^2/2} - B)$,
(5) mode = $(GM + B)/(e^{\sigma^2/2} - B)$ - these equations hold if σ^2 (logarithmic variance) is known and n is infinite, where σ^2 is the variance of the natural logs of the grades + B,
(6) variance of the actual grades = $(\mu + B)^2 * (\sigma^2 - 1)$

From the sampling the probability distribution of the diamond frequency is calculated to determine the minimum sample size for obtaining a given number of stones, called the Sichel *t*-estimator (Sichel, 1972).

$$\text{Sichels } t \text{ estimator} = (GM + B)\,[\gamma_n\,(v)]$$

where $v = 1/n * \Sigma(x_i - x)^2$ and $x_i = ln\,(x + B)$, x = mean of x_i's,

γ_n (v) has been tabulated by Sichel (1972), as having various confidence limits for the mean.

The intercept with the 50% line gives the average of the logarithms and can be read of a graph, such as Fig.45c. To read the standard deviation of the logarithms, B, one should take the difference of the logarithms of the grades associated with the interval 16% to 50%, and 50% to 84%. The formula $B = 0.5\,[ln\,(x_{84}/x_{50}) + ln\,(x_{50}/x_{16})]$ can also be used (David, 1977).

2.10.4.3. Block definition and local estimation.

It has been mentioned that where samples are of unit size and laid out on a regular grid, the arithmetic mean gives the best estimate of the average grade. The confidence limits around the estimated mean will indicate how adequate the sampling spacing is. Block limits are defined by the geological boundaries established independently from the sampling results, such as facies boundaries in the kimberlite deposit. If sample results are used to define block limits, the samples inside the block needs to be weighted correctly to avoid overestimation (Rombouts, 1995 ; Oldenziel, 1997).

Local grade estimation can be done by geometrical- or distance-weighting methods. Geometrical methods were favoured until the advent of computers and include the polygonal-, triangular- and cross-sectionl techniques. The grade of a portion of a diamond drill hole is assigned to the whole block. Distance-weighting methods assign grades to a block by the linear combination of the grades from surrounding samples (David, 1977).

The correct weighting of samples are based on a reliable variogram, with the weighting commonly done by kriging. The kriging method optimally weighs the grade data segments, taking into account both the spatial location of the data segment with respect to the unknown block and the spatial location of the data segments with respect to each other. A basic assumption in the theoretical development of linear kriging is that the variogram model is independent of location within the area of interest, referred to as stationary. On the scale of an orebody grade trends are evident but local stationarity is adequate for local estimation. Stationary means that the expected mean and variance remains the same over the domain studied (Brooker, 1979).

2.10.5. Stone size distributions.

The extrapolation of the size distribution of microdiamonds recovered from orientation- and bulk sampling is routinely used at present to estimate the grade of the whole orebody.

2.10.5.1. Microdiamond counts for grade estimation.

At the production stage diamonds are usually recovered to a bottom screen-size of 0.5 mm to 2.5 mm. The stone densities of these macrodiamonds can be low and samples of several tons are necessary to recover a few stones. Microdiamonds (< 0.5 mm) are, therefore, used in the early stages of kimberlite evaluation, together with mineral chemistry, as a method for predicting whether a kimberlite is likely to be economic or not.

Large diameter diamond drill- or percussion borehole kimberlite samples are crushed, acid-digested (typically with HCl and HF) and fused (with caustic soda or sodium peroxide) to liberate the microdiamonds. The light fraction of the fusion residue is then floated off in TBE (tetra-bromo-ethane). A shaking table is more practical where a large amount of material needs to be concentrated. A detergent is commonly added to the pulp as the hydrophobic surface characteristic of the microdiamonds means that may be floated off together with the lighter fraction. Drill bits are fitted with synthetic diamonds as they can be distinguished from kimberlitic diamonds by their yellow-green colour and cubo-octahedral crystal form (Rombouts, 1995).

Bulk sample core drilling only recovers a few hundreds of stones within the size range 0.00001 to 0.1 carats from 100 to 1000 kg of material. As the commercial size range of diamonds are > 0.1 carats an extrapolation of the microdiamond size distribution is needed beyond 0.1 carats. If the microdiamond size distribution displays a clear mode on a doubly logarithmic scale, a least squares fit may be used to fit the second degree polynomial. The extrapolation of this curve to the commercial size ranges will give the frequency of occurrence of the larger diamonds (Rombouts, 1995).

To apply the microdiamond technique, a statistical model for the stone size distribution is necessary. The Cullinan diamond from the Premier mine (South Africa) is the largest diamond ever found in nature and weighed 3106 carats. Usually the size distribution of diamonds in a deposit can be expected to spread over a range of 1000 carats down to molecular sized crystals. Mining operations only recover commercial-sized diamonds in the size range 0.1 to few 100's carats. Depending on the value distribution of the diamonds, mining operations set the lower screen size at different levels. The lower screen size usually falls in the size range 0.5 to 2.5 mm. Where hard ore needs to be crushed the primary crusher setting defines the upper size limit (Rombouts, 1995).

Within a homogeneous deposit, the size distribution of the diamonds recovered during evaluation or production is often well approximated by a lognormal distribution. A distribution can be tested for lognormality by plotting the data on a lognormal graph. A straight line indicates a good fit to the two-parameter lognormal model (refer to Fig.45). Deviations from the lognormal model is mostly due to mixing of different stone populations within a deposit as different intrusive phases may be associated with different grades (Jennings, 1995 ; Rombouts, 1995).

In kimberlites the number of diamonds increases exponentially with diminishing size, in other words a loghyperbolic distribution. A lognormal distribution has a mode but does not explain the continuous exponential increase in the number of stones with decreasing size. A loghyperbolic distribution explains both the mode of the weight distribution and the exponential increase of the number distribution with decreasing size (Rombouts, 1995).

2.10.5.2. Value estimation.

Diamonds, unlike metals, do not have a unit value. De Beers uses a standard price list to price their diamonds, which are valued according to 6000 categories. The value of diamonds are dependent on their colour, carat weight (size) and clarity (quality). The commercial value of diamonds varies from deposit to deposit, and depends on the ratio of industrial to gem-quality diamonds. While reserves are usually expressed as carats per cubic meter or per ton, they are only meaningful if the average value of the diamonds is also known (Oldenziel, 1997).

The commercial value of diamonds are usually expressed as an average price per carat. This is obtained by sending a large parcel of several thousand stones from a bulk sample to a diamond valuer. The valuer takes the total value of the parcel and divides it by the total weight and returns the average price per carat, in other words the mean of the stone values are divided by their mean stone size. The size distribution and the stone value distribution usually follows a lognormal distribution. In the case of a lognormal distribution, the arithmetic mean is better replaced by a more efficient estimator of the average, which Sichel (1952) called the *t*-estimator. The *t*-estimator is only slightly more efficient than the arithmetic mean for stone sizes, but three times more efficient for the stone values (Rombouts, 1995 ; Oldenziel, 1997).

3. Conclusions.

All diamondiferous kimberlite occurrences in Southern Africa are confined to areas underlain by Archaean cratons. The kimberlitic source material is derived from Archaean peridotite from the asthenosphere, and lesser amounts of Proterozoic eclogite derived from the continental lithospheric mantle. The kimberlitic source material is produced at depths varying between 150 and 300 km. Diamonds are formed in the above-mentioned source material, are entrained within kimberlite and transported to the surface of the Earth. Diamonds ae liberated into the kimberlite by the disaggregation of kimberlite xenoliths. Kimberlite emplacement is associated with structural controls ranging from large scale, regional tectonic, long-lived deep-crustal lineaments to local crosscutting or conjugate fault- and/or fracture zones.

Kimberlite occurrences are expressed as pipes, dykes or sills. Pipes are subdivided into crater-diatreme- and hypabyssal facies. Mineralogically kimberlites are complex, hybrid rocks with two varieties that are noted in Southern Africa. Group I ilmenite-bearing kimberlites are the most common and occurs over the whole of Southern Africa, whilst Group II micaceous kimberlites have only been noted in South Africa. Both a mineralogical- and textural-genetic classification scheme has been developed for Southern African kimberlites. The differences in Group I and Group II kimberlites are also seen in their geochemical signatures. Group I kimberlites are depleted in LREE and Rb, thought to have been derived from an asthenospheric source, and Group II kimberlites are enriched in LREE and Rb, thought to have a lithospheric source.

Diamonds are only found as a rare constituent of kimberlites. P-type (peridotite) and E-type (eclogitic) mineral inclusions are found in diamonds, with P-type inclusions predominating over E-type inclusions. Resorption of diamonds may occur within the area of formation and during transportation to the surface. Resorption can reduce the initial diamond mass with up to 50%.

A kimberlite exploration programme follows a well established sequence. It is initiated by a literature survey on the known occurrences, their structural controls and a preliminary study of the landscape evolution as well as the surface processes active on the kimberlites after emplacement. Subsequent fieldwork entails indicator mineral sampling, in conjunction with satellite imagery-, aerial photographic-, geophysical-, geochemical-, petrographic-, geobotanical- and geobiological assessments. When a kimberlite is located pit-, trench- or diamond drill sampling and geostatistical evaluation of the deposit is carried out. The Southern African countries with potential for more kimberlite discoveries include Angola, Botswana, Lesotho, South Africa, Swaziland, Tanzania and Zimbabwe.

The geomorphic evolution of the Earth's surface after kimberlite emplacement determines the degree of preservation or erosion, and is assessed by a landscape analysis. Surface processes active on a kimberlite is divided into the physical/mechanical destruction of diamonds and indicator minerals in the fluvial- and/or deflation environment and the chemical destruction of diamonds and indicator minerals, especially in the lateritic weathering environment.

The most successful exploration technique for locating kimberlite occurrences is indicator mineral sampling. Indicator mineral sampling can be carried out by drainage- and/or soil sampling programmes. A heavy mineral concentrate is produced from the sampled material and the indicator minerals extracted by use of a binocular microscope. The distribution of recovered indicator minerals are plotted to delineate areas for detailed exploration.

The geochemistry of indicator minerals is also a useful tool for discriminating between diamondiferous and non-diamondiferous kimberlites.

The common indicator minerals are pyrope garnet, picro-ilmenite, chrome diopside (clinopyroxene), chrome spinel, zircon, olivine and phlogopite. Peridotitic (chrome-rich) garnets are used to discriminate between diamondiferous and barren kimberlites by comparing their CaO against Cr_2O_3 ratios. The sub-calcic garnets are termed G10 and the calcic garnets G9. All known diamondiferous kimberlites have garnets that plot within the sub-calcic (G10) field. Ilmenite geochemistry reflect the redox conditions in the mantle and, therefore, the diamond resorption potential during kimberlite emplacement. Ilmenite suites with low Fe^{3+}/Fe^{2+} ratios have better diamond preservation potential. High MgO chrome diopsides are associated with high Ca/(Ca + MgO) ratios, whilst the Cr_2O_3 contents of kimberlite chrome spinels are amongst the highest ever observed. The chromite compositions high in MgO and Cr_2O_3 are regarded as favourable for diamond occurrence. Zircons from kimberlites have very low uranium and thorium contents, which differentiates them from granitic zircons. Olivine and phlogopite are not used as indicator minerals in Southern Africa as they weather rapidly.

Remote sensing techniques use the energy from some part of the electromagnetic spectrum to characterise some part of the Earth. Satellite imagery and aerial photographs provide a synoptic view of large areas. Landsat Multi Spectral Scanners (MSS) and the Thematic Mapper (TM) data is most commonly used for satellite imagery interpretation. Unfortunately, their relatively coarse resolution (30 by 30 m picture elements) only provides for large scale structural-, lithological- and other surficial spectral data interpretation.

Aerial photography furnishes higher resolution information and is especially useful for geomorphological features, such as drainage system analysis, as well as vegetational differences and topographic interpretation (stereoscopic photo pairs). Geophysical techniques are routinely used for both reconnaissance and follow-up exploration. Magnetics and electromagnetics are the most commonly used methods. Geophysics is only useful where sufficient physical contrast between the kimberlite and surrounding host rock exists. The electric methods includes electromagnetics, induced polarisation and resistivity. These methods, together with gravity, is commonly used to delineate the kimberlite boundaries once it has been found. The radiometric method is not particularly useful in kimberlite exploration. Refraction seismics is used to establish the characteristics of the soils overlying kimberlites and basement rocks (regolith). Reflection seismics is used for deeper level investigation, such as defining the boundaries between the lithosphere, asthenosphere and mantle interfaces. Heat flow models are only used for delineating the boundaries between cool cratonic and warmer mobile belt areas.

Geochemical techniques are not used for reconnaissance exploration, but may come into effect with follow-up sampling, or where weathering and oxidation of the kimberlite makes petrographic analysis difficult. The suite of elements commonly analysed for includes Mg, Ni, V, Co, Cr, Ti, Nb, La, Sc, Ta, Zr, Hf, P, Ba, Sr, Th, U and the LREE. Petrographic analysis of kimberlites is done by transmitted light thin section petrography, however, only the macroscopic features can be examined. The fine-grained groundmass is best analysed by electron microbeam methods, typically by back-scattered electron imagery and energy dispersive X-ray spectrometry. The clays associated with kimberlite weathering may give vegetational (geobotanical) contrasts, whilst ant and termite activity or burrowing animals (geobiological) may exhume indicator minerals.

The ultimate aim of any exploration programme is to delineate an economic kimberlite deposit. Ore reserve estimation of kimberlites require pit-, trench- or large diameter borehole grid sampling. Samples are crushed or ground, passed over vibrating screens and the heavy fraction seperated by gravity methods, typically rotary pans, jigs or heavy media cyclones. Diamonds are recovered by hand picking, grease belt tables or X-ray sorters. Diamond grade distributions are classified by geostatistical methods based on the grid sampling values.

The geostatistical grade distribution is quantified by the experimental variogram, which establishes the trends and variability of mineralisation in a number of directions through the orebody, and the grade sampling is then extrapolated to block grades using geometrical- or distance-weighting methods. The most commonly used distance-weighting technique is the procedure known as kriging. Due to the small sample size and low grades associated with kimberlites microdiamond counts are routinely used in evaluation. The microdiamond grades are then extrapolated to model the grades of the whole orebody. The value of diamonds recovered from a kimberlite deposit, and the *in situ* value of the deposit in US$ / ton, depends on the diamond colour, carat weight and clarity.

In exploration the empirical model rather than the genetic model is important, and emphasis should be placed on facts rather than theory. Table XV is an attempt to summarise the salient characteristics of Southern African kimberlites and exploration techniques. Indirect methods, such as satellite imagery, aerial photography and geophysics are not very effective in kimberlite exploration. Emphasis should be placed on direct, simpler methods, especially indicator mineral sampling. Sampling (most commonly large diameter drilling) of a kimberlite occurrence must be done as early as possible as it is the only method to give definitive results. The simpler methods only require financial backing, time, application and some perseverance.

Table XV ; Integrated exploration guidelines for Southern African kimberlites.

PHASE	GEOLOGICAL TECHNIQUES	GEOCHEMICAL TECHNIQUES	GEOPHYSICAL TECHNIQUES	REMOTE SENSING TECHNIQUES
TECTONO-METALLOGENIC CRUSTAL FRAMEWORK STUDIES Scale 1 : 1 000 000	PLATE AND CRUSTAL TECTONIC STUDIES Delineation of broad metallogenic provinces ; (1) Archaean cratons associated with thick lithospheric crust and low geothermal gradients, (2) Asthenospheric- and upper mantle lithospheric, peridotitic- and eclogitic source rocks, (3) Regional structural controls, includes landward extensions of oceanic transform faults onto pre-existing basement faults, deep-seated basement shear-, fracture-, and fault zones, linear grabens and aulacogens, (4) Areas of regional uplift due to mantle hot spots, upwelling convection currents, mantle diapirs, rifting of continents, flat-dipping subduction zones and transform faults,	Regional first-pass, indicator mineral drainage and/or soil sampling,	Spaceborne data : (1) MAGSAT (2) GRAVSAT (delineating Archons) Airborne data : (1) Aeromagnetics (structural interpretations) (2) Gravity (negative response from weathered kimberlite) (positive response from fresh kimberlite) Ground data : (1) Reflection seismics (used to delineate the lithosphere-asthenosphere- mantle interfaces) (2) Heat flow models (cratons associated with low geothermal gradients) (3) Seismic tomography (craton roots characterised by high shear wave velocities)	Spaceborne data : (1) Landsat TM & MSS (large scale structural-, lithological- and vegetational interpretation)
TARGET GENERATION - REGIONAL STUDIES Scale 1 : 500 000 1 : 250 000	REGIONAL STRUCTURAL AND GEOLOGICAL EVOLUTION MODELS Selection and application of mineralisation models ; (1) Areas where deep crustal lineaments are intersected by conjugate fracture zones (kimberlite clusters), (2) Kimberlite morphology noted as pipes, dykes and sills (dykes up to 1 m in width and pipes up to 167.5 ha in diameter), (3) Kimberlites consist of ultramafic (mostly forsteritic olivine), potassic, volatile-rich minerals of macrocrysts set in a fine-grained matrix, producing the characteristic inequigranular texture, (4) Deuteric alteration of mostly olivine to serpentine, talc and carbonates are common,	Follow-up indicator mineral drainage and/or soil sampling ;	Airborne data : (1) Aeromagnetics (structural interpretations) (2) Gravity (high for fresh kimberlite) (low for weathered kimberlite) Ground data : (1) Magnetics (structural and lithological interpretations) (2) Gravity (high for fresh kimberlite) (low for weathered kimberlite)	Spaceborne data (1) Landsat TM & MSS (surface weathering absorption features related to iron, hydroxyl and water from the presence of serpentine minerals, or micas) (2) Landsat SMIRR (surface weathering absorption features related to calcite, kaolinite and montmorillonite) Airborne data : (1) Small-scale aerial photographs (1 : 50 000)
TARGET EVALUATION Scale 1 : 100 000 1 : 50 000	ORE TRAP AND ACCUMULATION MODELS Stratigraphic drilling : (1) Kimberlite pipes are subdivided into crater-, diatreme- and hypabyssal facies, (2) Kimberlite classification are based on two schemes ; (a) Mineralogical classification based on the relative proportions of diopside, monticellite, phlogopite, calcite and serpentine of the hypabyssal facies and (b) Textural-genetic classification of the crater-, diatreme- and hypabyssal facies, (3) Two distinct types of kimberlites are noted in Southern Africa ; (a) Group I ilmenite bearing kimberlites are characterised by a monticellite serpentine calcite assemblage and (b) Group II ilmenite poor kimberlites are characterised by phlogopite and diopside, (4) Two types of diamonds are distinguished, based on mineral inclusions within them ; (a) Peridotitic inclusions derived from residual carbon that existed from the Earth's creation (P-type diamonds) and (b) Eclogitic inclusions derived from the Earth's crust (E-type diamonds), (5) Exploration techniques considered ; (a) Literature research and historical/current production information for Angola, Botswana, Lesotho, South Africa, Swaziland, Tanzania and Zimbabwe, (b) Landscape analysis regarding the geomorphological evolution of the Earth's surface, i.e. the degree of erosion or burial, (c) Surface processes active after kimberlite emplacement are divided into mechanical- and chemical destruction of minerals, (d) Structural controls - second and third order brittle-ductile tensile features within a shear-, fault- or fracture zone (a Riedel shear model for conjugate systems has been noted in places), (e) Indicator mineral drainage- or soil sampling programmes to recover pyrope-garnets, picro-ilmenite, chrome-diopside, spinel, zircon, olivine and phlogopite, Garnet ; (i) Peridotitic garnets with low CaO (sub-calcic garnets) are termed G10 and are good indicators for diamondiferous kimberlites, (ii) High Cr2O3 (peridotitic garnets) and low Cr2O3 (eclogitic- or megacrystic garnets), (iii) Diamond-rich kimberlites have a high proportion of garnets with Ni-temperatures in the "diamond window", Ilmenite ; (i) Diamond preservation is associated with ilmenite suites of low Fe3+/Fe2+ ratios, high MgO and Cr2O3, Spinel ; (i) Chrome spinels with high MgO and very high Cr2O3 increases the diamond potential of kimberlites, Zircon ; (i) Low U and Th contents are associated with kimberlitic zircons, (f) Petrographic- and electron beam techniques include ; (i) transmitted light thin section petrography for macrocrystal and phenocrystal mineralogy and textural analysis and, (ii) back-scattered electron images and energy dispersive X-ray spectrometry for resolution and identification of the fine-grained groundmass minerals, (g) Geobotanical (vegetation anomalies)- and geobiological (termite activity) techniques,	Detailed indicator mineral- and multi-element grid soil sampling ; (1) Major- and trace element geochemistry of compatible and incompatible elements show enrichment in Mg, Ni, V, Co, Cr, Ti, Nb, Ca, Fe, B, K, Mo, Pt, Y, Se, Bi, Rb, Pb, Ta, Zr, Hf, P, Ba, Sr, Th, P, U, Nd, Sm, Ti, F, Ca, La, Sc, Ce, HREE and LREE, (2) Radiogenic isotope geochemistry show systematic variation in Sr, Nd and Pb isotopic compositions ; (a) Group I kimberlites are characterised by ; (i) 87Sr/86Sr isotopic ratios varying from 0.703 to 0.705, (ii) 143Nd/144Nd isotopic ratios varying from 0.51271 to 0.51287, (iii) Depletion in Rb, but enriched in Pb, (iv) Relatively low Sm/Nd ratios, (a) Group II kimberlites are characterised by ; (i) 87Sr/86Sr isotopic ratios varying from 0.707 to 0.712, (ii) 143Nd/144Nd isotopic ratios varying from 0.51208 to 0.51228, (iii) Enrichment in Rb, but depleted in Pb, (iv) Relatively high Sm/Nd ratios, (3) Stable isotope geochemistry show that kimberlites have interacted with groundwater (noted in the delta values of O and D), and where kimberlites have intruded carbonates the delta values for C and O are heavier, (4) Infrared mineral analyser spectrometer (has been used to map the occurrence of serpentine and talc in weathered kimberlites)	Airborne data : (1) Aeromagnetics (structural and lithological interpretations) (2) Gravity (high for fresh kimberlite) (low for weathered kimberlite) (3) E-M (low resistivity from conductive clay minerals in weathered portion of kimberlites) (4) I-P (low resistivity from porous, weathered kimberlite) (5) Radiometrics (K, Th, U associated with kimberlite) Ground data : (1) Magnetics (delineation of individual pipe- and dyke occurrences) (2) Gravity (delineation of individual pipe boundaries) (3) E-M (establishing depth of kimberlite weathering) (4) I-P (delineating fresh versus weathered kimberlite boundaries and the resistive versus conductive structure of the overburden) (5) Refraction seismics (establishing the depth of weathering or depth to bedrock in areas of overburden)	Spaceborne data : (1) Landsat TM & MSS (surface weathering and digital topography maps) Airborne data : (1) Aerial photography (structural- and fracture pattern mapping, geomorphology, drainage analysis, stream sediment sampling site planning, vegetation mapping) (2) Stereoscopic aerial photograph pairs (used for structural- and lithological mapping in rugged terrains as well as topographic analysis) (1 : 50 000)
AREA PROSPECTING Scale 1 : 50 000 1 : 5 000	ORE CONCENTRATION MODELS Large diameter diamond and percussion drilling, trenching and pitting ; (1) Establishing the tonnage and value (grade, size and quality of diamonds) of the orebody by ; (a) Establishing the trends and variability of diamond grades within the orebody by experimental variograms in different directions through the orebody (it is also used to define the optimal sampling pattern), (b) Kimberlite diamond grade distribution plotted on frequency histograms and the median, mode and mean is calculated, (c) Kimberlites typically show a log-normal diamond grade distribution and is represented by a straight line on log-probability paper, from which the median, mode, mean, variance and standard deviation can be calculated, median, mode and mean is calculated (microdiamond counts are commonly used), (d) Block limits are defined by geological boundaries such as different facies within the kimberlite or structural boundaries, (e) Local estimation in side blocks are done by geometrical- or distance-weighting (especially kriging) methods	Direct detection of rock and soil anomalies (1) Establish the diamond grade of the ore body	Ground data (downhole geophysics) : (1) Magnetics (delineation of crater-, diatreme- and hypabyssal facies boundaries) (2) E-M (delineation of internal weathering pattern in kimberlites) (3) I-P (delineation of internal weathering pattern in kimberlites) (4) Radiometrics (variation in U, Th and K in different kimberlite or different intrusive phases)	Airborne data : (1) Aerial photography (2) Multi-spectral scanners (3) Digital topographic maps from radar imagery (1 : 10 000)

4. References.

African Mining, 1996 ; *De Beers breathes new life into Williamson Diamonds.* African Mining, Vol. 1. No. 3, pp. 6-7.

African Mining, 1998 ; *Light of day for Angola's diamonds.* African Mining, Vol. 3. No. 1/2, pp. 11-21.

Allen, H.E.K., 1981 ; *Development of Orapa and Lethlakane diamond mines, Botswana.* Trans. Inst. Min. Metall., Sect. A : Min. Ind., Vol. 90, pp. 177-191.

Allsopp, H.L. & Kramers, J.D., 1977 ; *Rb-Sr and U-Pb age determinations on Southern African kimberlite pipes.* Extended Abstracts, Second International Kimberlite Conference, Santa Fe, New Mexico, pp.

Allsopp, H.L., Bristow, J.W. & Skinner, E.M.W., 1985 ; *The Rb-Sr geochronology of the Colossus kimberlite pipe, Zimbabwe.* Trans. of the Geol. Soc. of S. Afr., Vol. 88, pp. 245-248.

Allsopp, H.L., Bristow, J.W., Smith, C.B., Brown, R., Gleadow, A.J.W., Kramers, J.D. & Garvie, O.G., 1989 ; *A summary of radiometric dating methods applicable to kimberlites and related rocks.* In : Kimberlites and related rocks, their composition, occurrence, origin and emplacement. Vol. I, Ross, J. (Ed.). Proceedings of the Fourth International Kimberlite Conference, Perth, 1986, Geol. Soc. of Austr., Spec. Publ., No. 14, pp. 343-357.

Allsopp, H.L., Smith, C.B., Seggie, A.G., Skinner, E.M.W. & Colgan, E.A., 1995 ; *The emplacement age and geochemical character of the Venetia kimberlite bodies, Limpopo Belt, northern Transvaal.* S. Afr. Journ. of Geol., Vol. 98, pp. 239-244.

Atkinson, W.J., 1989 ; *Diamond exploration philosophy, practice and promises : a review.* In : Kimberlites and related rocks, their mantle/crust setting, diamonds and diamond exploration. Vol. II, Ross, J. (Ed.). Proceedings of the Fourth International Kimberlite Conference, Perth, 1986, Geol. Soc. of Austr., Spec. Publ., No. 14, pp. 1075-1107.

Baldock, J.W., 1977 ; *Resource inventory of Botswana : Metallic minerals, mineral fuels and diamonds.* Geol. Surv. of Botswana, Mineral Resources Report, No. 4, pp. 49-57.

Baldock, J.W., Hepworth, J.V & Marengwa, B.S., 1976 ; *Gold, base metals and diamonds in Botswana.* Econ. Geol., Vol. 71, pp. 139-156.

Ballard, S. & Pollack, H.N., 1987 ; *Diversion of heat by Archaean cratons : a model for Southern Africa.* Earth Planet. Sci. Lett., Vol. 85, pp. 253-264.

Bates, R.L. & Jackson, J.A., 1987 ; *Glossary of Geology.* 3rd Edition, American Geological Institute, Alexandria : Virginia, p. 788.

Bliss, J.D., 1992 ; *Grade-tonnage and other models for diamond kimberlite pipes.* U.S. Geol. Surv., Nonrenewable Resources, Vol. 1, No. 3, pp. 214-230.

Boyd, F.R. & Danchin, R.V., 1980 ; *Lherzolites, eclogites and megacrysts from some kimberlites of Angola.* Amer. Journ. of Science, Vol. 280a, pp. 528-549.

Boyd, F.R. & Gurney, J.J., 1986 ; *Diamonds and the African lithosphere.* Science, Vol. 232, pp. 472-47.

Boyd, F.R. & Gurney, J.J. & Richardson, S.H., 1985 ; *Evidence for a 150-200 km thick Archaean lithosphere from diamond inclusion therbarometry.* Nature, Vol. 315, pp. 387-389.

Brooker, P.I., 1979 ; *Kriging.* Engineering & Mining Journal, Vol. 180, No. 9, pp. 148-153.

Business Day, 1998 ; *Black business to get stake in Marsfontein.* Business Day, 20 November 1998, pp. 4.

Chadwick, J.R., 1983 ; *Jwaneng and Botswana : at height of diamond production.* World Mining, January 1983, pp. 64-68.

Clement, C.R., 1982 ; *A comparative geological study of some major kimberlite pipes in the Northern Cape and Orange Free State.* PhD Thesis (2 volumes, unpubl.), University of Cape Town, p. 286.

Clement, C.R. & Reid, A.M., 1989 ; *The origin of kimberlite pipes.* In : Kimberlites and related rocks, their composition, occurrence, origin and emplacement. Vol. I, Ross, J. (Ed.). Proceedings of the Fourth International Kimberlite Conference, Perth, 1986, Geol. Soc. of Austr., Spec. Publ., No. 14, pp. 632-646.

Clement, C.R. & Skinner, E.M.W., 1985 ; *A textural-genetic classification of kimberlites.* Trans. Geol. Soc. of S. Afr., Vol. 88, pp. 403-409.

Clement, C.R., Skinner, E.M.W. & Scott-Smith, B.H., 1984 ; *Kimberlite redefined.* Journ. of Geol., Vol. 92, pp. 223-228.

Clendenin, C.W., Charlesworth, E.G., Maske, S. & de Gesparis, A.A., 1988 ; *Normal simple shear model for the structural evolution of the early Proterozoic Ventersdorp Supergroup, Southern Africa.* Econ. Geol. Research Unit, Inform. Circular, No. 201, p. 20.

Clifford, T.N., 1966 ; *Tectono-metallogenic units and metallogenic provinces of Africa.* Earth. Plan. Sci. Lett., Vol. 1, pp. 421-434.

Cole, D.I., 1998 ; *Diamonds in the SADC region.* Mining Sector Coordinating Unit, Mineral Resources Survey Programme, No. 3, Project AAA 1.2, p. 36.

Corner, B., 1998 ; *Geophysical techniques in exploration geology.* MSc. Course Notes, Rhodes University : Grahamstown, p. 300.

Cox, K.G., 1978 ; *Kimberlite pipes.* Scientific American, Vol. 238, No. 4, p. 120-132.

Da Costa, A.J.M., 1989 ; *Palmietfontein kimberlite pipe, South Africa - a case history.* Geophysics, Vol. 54, No. 6, pp. 689-700.

Damarupurshad, A., 1998 ; *Preliminary rough diamond production, 1997.* Bulletin Minerals Bureau, Vol. 11, No. 1, pp. 1.

Daniels, L.R.M., 1991 ; *Diamonds and related minerals from the Dokolwayo kimberlite, Kingdom of Swaziland.* Unpubl. Ph.D thesis, Univ. of Cape Town, p. 109.

Daniels, L.R.M. & Gurney, J.J., 1989 ; *The chemistry of the garnets, chromites and diamond inclusions from the Dokolwayo kimberlite, Kingdom of Swaziland.* In : Kimberlites and related rocks, their mantle/crust setting, diamonds and diamond exploration. Vol. II, Ross, J. (Ed.). Proceedings of the Fourth International Kimberlite Conference, Perth, 1986, Geol. Soc. of Austr., Spec. Publ., No. 14, pp. 1012-1021.

David, M., 1977 ; *Geostatistical ore reserve estimation.* Elsevier Scientific Publishing : Amsterdam, p. 364.

Dawson, J.B., 1962 ; *Basutoland kimberlites.* Bull. of the Geol. Soc. of Amer., Vol. 73, pp. 545-560.

Dawson, J.B., 1967 ; *A review of the geology of kimberlite.* In : Ultramafic and related rocks, Wyllie P.J. (Ed.), Wiley & Sons : New York, pp. 241-251.

Dawson, J.B., 1970 ; *The structural setting of African kimberlites.* In : African magmatism and tectonics. Clifford, T.N. & Gass, I.G. (Eds.), Oliver & Boyd : Edinburgh, pp. 321-335.

Dawson, J.B., 1971 ; *Advances in kimberlite geology.* Earth Sci. Review, Vol. 7, pp. 187-214.

Dawson, J.B., 1972 ; *Kimberlites and their relation to the Mantle.* Phil. Trans. R. Soc. of London, Ser. A, Vol. 271, pp. 297-311.

Dawson, J.B., 1989 ; *Geographic and time distribution of kimberlites and lamproites : relationships to tectonic processes.* In : Kimberlites and related rocks, their composition, occurrence, origin and emplacement. Vol. I, Ross, J. (Ed.). Proceedings of the Fourth International Kimberlite Conference, Perth, 1986, Geol. Soc. of Austr., Spec. Publ., No. 14, pp. 323-342.

Dawson, J.B. & Hawthorne, J.B., 1973 ; *Magmatic sedimentation and carbonatitic differentiation in kimberlite sills at Benfontein, South Africa.* Geol. Soc. of London, Vol. 129, pp. 61-85.

Dawson, J.B. & Stephens, W.E., 1976 ; *Statistical classification of garnets from kimberlite and associated xenoliths.* Addendum. J. of Geol., Vol. 84, pp. 495-496.

De Boorder, H., 1982 ; *Deep-reaching fracture zones in the crystalline basement surrounding the West Congo System and their control on mineralisation in Angola and Gabon.* Geo-exploration, Vol. 20, pp. 259-273.

Dirlam, D.M., Misiorowski, E.B., Tozer, R., Stark, K.B.and Bassett, A.M., 1992 ; *Gem wealth of Tanzania.* Gems & Gemology, Summer 1992, pp. 80-102.

Edwards, C.B. & Howkins, J.B., 1966 ; *Kimberlites in Tanganyika with special reference to the Mwadui occurrence.* Econo. Geol., Vol. 61, pp. 537-554.

Eggler, D.H., 1989 ; *Kimberlites : how do they form ?.* In : Kimberlites and related rocks, their composition, occurrence, origin and emplacement. Vol. I, Ross, J. (Ed.). Proceedings of the Fourth International Kimberlite Conference, Perth, 1986, Geol. Soc. of Austr., Spec. Publ., No. 14, pp. 489-504.

Fipke, C.E., Gurney, J.J. & Moore, R.O., 1995 ; *Diamond exploration techniques emphasising indicator mineral geochemistry and Canadian examples.* Geol. Surv. of Canada, Bulletin 423, pp. 1-86.

Friese, A.E.W., 1998 ; *Structural control on kimberlite genesis and crustal emplacement within South Africa and the Kaapvaal Craton during the Cretaceous.* Abstracts, Seventh International Kimberlite Conference, Univ. of Cape Town, pp. 224-226.

Gerryts, E., 1967 ; *Diamond prospecting by geophysical methods - a review of current practice.* Proceedings of the International Conference, Mining & Groundwater Geophysics, pp. 439- 446.

Gerryts, E., 1970 ; *Diamond prospecting by geophysical methods : a review of current practice.* Geol. Surv. of Canada, Econ. Geol. Report 26, pp. 439-446.

Gobba, J.M., 1989 ; *Kimberlite exploration in Tanzania.* Journ. of African Earth Sciences, Vol. 9, No. 3/4, pp. 565-578.

Goetz, A.F.H, Rowan, L.C. & Kingston, M.J., 1982 ; *Mineral isdentification from orbit : Initial results from the shuttle multispectral infrared radiometer.* Science, Vol. 218, pp. 1020-1024.

Grand, S.P., 1987 ; *Tomographic inversion for shear velocity beneath the North American plate.* J. of Geophys. Res., Vol. 92, pp. 14065-14090.

Gregory, G.P. & White, D.R., 1989 ; *Collection and treatment of diamond exploration samples.* In : Kimberlites and related rocks, their mantle/crust setting, diamonds and diamond exploration. Vol. II, Ross, J. (Ed.). Proceedings of the Fourth International Kimberlite Conference, Perth, 1986, Geol. Soc. of Austr., Spec. Publ., No. 14, pp. 1123-1134.

Griffin, W.L., Cousens, D.R., Ryan, C.G., Sie, S.H. & Suter, G.F., 1989 ; *Ni in chrome pyrope garnets : a new thermometer.* Contrib. Mineral. Petrol., Vol. 103, pp. 199-203.

Griffin, W.L. & Ryan, C.G., 1992 ; *Trace elements in garnets and chromites : their use in diamond exploration.* International Round Table Conference on Diamond Exploration & Mining : New Delhi, pp. 24-57.

Griffin, W.L. & Ryan, C.G., 1993 ; *Trace elements in garnets and chromites : evaluation of diamond exploration targets.* In : Diamonds : exploration, sampling and evaluation. Prospectors and Developers Assoc. of Canada, Short Course Notes, pp. 187-211.

Griffin, W.L. & Ryan, C.G., 1995 ; *Trace elements in indicator minerals : area selection and target evaluation in diamond exploration.* In : Diamond Exploration : Into the 21st Century. Griffin, W.L. (Ed.). J. of Geochem. Explor., Vol. 53, pp. 311-337.

Griffin, W.L., Ryan, C.G., Gurney, J.J., Sobolev, N.V. & Win, T.T., 1994 ; *Chromite macrocrysts in kimberlites and lamproites : geochemistry, and origin.* In : Kimberlites, related rocks and mantle xenoliths. Meyer, H.O.A. & Leonardos, O.H. (Eds.), CPRM Spec. Publ., 1A/93, pp. 366-377.

Gurney, J.J., 1985 ; *A correlation between garnets and diamonds in kimberlites.* In : Kimberlite occurrence and origin : A basis for conceptual models in exploration. Glover, J.E. & Harris, P.G. (Eds.). Geol. Dept./Univ. Ext., Univ. of W.A., Publ. No. 8, pp. 143-166.

Gurney, J.J., 1989 ; *Diamonds.* In : Kimberlites and related rocks, their mantle/crust setting, diamonds and diamond exploration. Vol. II, Ross, J. (Ed.). Proceedings of the Fourth International Kimberlite Conference, Perth, 1986, Geol. Soc. of Austr., Spec. Publ., No. 14, pp. 935-965.

Gurney, J.J., 1990 ; *The diamondiferous roots of our wandering continent.* Trans. of the Geol. Soc. of S. Afr., Vol. 93, No. 3, pp. 423-437.

Gurney, J.J., 1998 ; *Terrac diamond classification notes.* M.Sc. Exploration Geology, Course Notes, Rhodes Univ. : Grahamstown, p. 7.

Gurney, J.J. & Ebrahim, S., 1973 ; *Chemical composition of Lesotho kimberlites.* In : Lesotho kimberlites, Nixon, P.H. (Ed.), Lesotho National Development Corporation, pp. 280-293.

Gurney, J.J., Moore, R.O., Otter, M.L., Kirkley, M.B., Hops, J.J. & McCandless, T.E., 1991 ; *Southern African kimberlites and their xenoliths.* In : Magmatism in extensional structural settings - the Phanerozoic African Plate. Kampunzu, A.B. & Lubala, R.T. (Eds.), Springer-Verlag : Berlin Heidelberg, pp. 495-536.

Gurney, J.J. & Switzer, G.S., 1973 ; *The discovery of garnets closely related to diamonds in the Finsch pipe, South Africa.* Contrib. Mineral. Petrol., Vol. 39, pp. 103-116.

Gurney, J.J. & Zweistra, P., 1995 ; *The interpretation of the major element compositions of mantle minerals in diamond exploration.* In : Diamond Exploration : Into the 21st Century. Griffin, W.L. (Ed.). J. of Geochem. Explor., Vol. 53, pp. 293-309.

Haggerty, S.E., 1986 ; *Diamond genesis in a multiple-constrained model.* Nature, Vol. 320, pp. 34-38.

Haggerty, S.E. & Tompkins, L.A., 1983 ; *Redox state of the Earth's upper mantle from kimberlitic ilmenites.* Nature, Vol. 303, pp. 295-300.

Harris, R.W., 1998 ; *An introduction to remote sensing and image processing for geologists.* M.Sc. Exploration Geology, Course Notes, Rhodes Univ. : Grahamstown, p. 81.

Harte, B., Gurney, J.J. & Harris, J.W., 1980 ; *The formation of peridotitic suite inclusions in diamonds.* Contrib. Mineral. Petrol., Vol. 72, pp. 181-190.

Hawthorne, J.B., 1975 ; *Model of a kimberlite pipe.* Physics and chemistry of the earth, Vol. 9, pp. 1-15.

Hawthorne, J.B., 1968 ; *Kimberlite sills.* Trans. of the Geol. Soc. of S. Afr., Vol. 71, pp. 291-311.

Helmore, R., 1984 ; *Diamond mining in Angola.* Mining Magazine, June, pp. 530-537.

Helmstaedt, H.H. & Gurney, J.J., 1995 ; *Geotectonic controls of primary diamond deposits : implications for area selection.* In : Diamond Exploration : Into the 21st Century. Griffin, W.L. (Ed.). J. of Geochem. Explor., Vol. 53, pp. 125-144.

Henckel, J., 1992 ; *Garnets in ferricrete : a case study on the Goedgevonden kimberlite.* Internal Report, Gold Fields of South Africa, p. 5.

Holloway, J. & Associates, 1997 ; *Setbacks in Zimbabwe.* Supplement to Mining Journal, London, 12 September 1997, p. 110.

Janse, A.J.A., 1985 ; *Kimberlites - where and when.* In : Kimberlite occurrence and origin : A basis for conceptual models in exploration. Glover, J.E. & Harris, P.G. (Eds.). Geol. Dept./Univ. Ext., Univ. of W.A., Publ. No. 8, pp. 19-61.

Janse, A.J.A., 1995 ; *A history of diamond sources in Africa.* Gems & Gemology, Part. I, Winter 1995, pp. 288-255.

Janse, A.J.A., 1996 ; *A history of diamond sources in Africa.* Gems & Gemology, Part. II, Spring 1995, pp. 2-30.

Janse, A.J.A. & Sheahan, P.A., 1995 ; *Catalogue of world wide diamond and kimberlite occurrences : a selective and annotative approach.* In : Diamond Exploration : Into the 21st Century. Griffin, W.L. (Ed.). J. of Geochem. Explor., Vol. 53, pp. 73-111.

Jennings, C.M.W., 1995 ; *The exploration context for diamonds.* In : Diamond Exploration : Into the 21st Century. Griffin, W.L. (Ed.). J. of Geochem. Explor., Vol. 53, pp. 113-124.

Jordan, T.H., 1988 ; *Structure and formation of the continental lithosphere.* J. Petrol., Spec. Lithosphere Issue, pp. 11-37.

Kashabano, J.B., 1989 ; *Ion probe U-Pb perovskite dating of the Bubiki kimberlite, Tanzania.* Report Geol. Surv. of Tanzania, pp.

Keating, P., 1995 ; *A simple technique to identify magnetic anomalies due to kimberlite pipes.* Explor. Mining Geol., Vol. 4, No. 2, pp. 121-125.

Kingston, M.J., 1989 ; *Spectral reflectance features of kimberlites and carbonatites : implications for remote sensing for exploration.* In : Kimberlites and related rocks, their mantle/crust setting, diamonds and diamond exploration. Vol. II, Ross, J. (Ed.). Proceedings of the Fourth International Kimberlite Conference, Perth, 1986, Geol. Soc. of Austr., Spec. Publ., No. 14, pp. 1135-1145.

Kirkley, M.B., Gurney, J.J. & Levinson, A.A., 1991 ; *Age, origin and emplacement of diamonds : Scientific advances in the last decade.* In : Gems & Gemology, Vol. 27, No.1, pp. 2-25.

Kirkley, M.B., Smith, H.S. & Gurney, J.J., 1988 ; *Kimberlite carbonates : a carbon-oxygen stable isotope study. In : Kimberlites and related rocks, their composition, occurrence, origin and emplacement.* Vol. I, Ross, J. (Ed.). Proceedings of the Fourth International Kimberlite Conference, Perth, 1986, Geol. Soc. of Austr., Spec. Publ., No. 14, pp. 264-281.

Klump, J. & Gurney, J.J., 1998 ; *A pilot study of the Swartruggens kimberlite dyke.* Abstracts, Seventh International Kimberlite Conference, Univ. of Cape Town, pp. 441-442

Kobelski, B.J., Gold, D.P. & Deneis, P., 1979 ; *Variations in stable isotope compositions for carbon and oxygen in some South African and Lesothan kimberlites.* In : Kimberlites, diatremes and diamonds : their geology, petrology and geochemistry. Boyd, F.R. & Meyer, H.O.A. (Eds.), American Geophysical Union : Washington D.C., pp. 129-139.

Levinson, A.A., Gurney, J.J. & Kirkley, M.B., 1992 ; *Diamond sources and production : past, present and future.* Gems & Gemology, Vol. 28, No.4, pp. 234-254.

Light, M.P.R., 1982 ; *The Limpopo Mobile Belt : a result of continental collision.* Tectonics, Vol. 1, pp. 325-342.

Lynn, M.D., Wipplinger, P.E. & Wilson, M.G.C. 1998 ; *Diamonds.* In : The Mineral Resources of South Africa, Wilson, M.G.C. & Anhaeusser, C.R. (Eds.), Handbook 16, 6th Edition, Council for Geoscience : Pretoria, pp. 232-258.

Macnae, J., 1995 ; *Applications of geophysics for the detection and exploration of kimberlites and lamproites.* In : Diamond Exploration : Into the 21st Century. Griffin, W.L. (Ed.). J. of Geochem. Explor., Vol. 53, pp. 213-243.

Mallinson, C., 1997 ; *An introduction to ore reserve estimation.* M.Sc. Exploration Geology, Course Notes, Rhodes Univ. : Grahamstown, p. 61.

Marsh, J.S., 1973 ; *Relationships between transform directions and alkaline igneous rock lineaments in Africa and South America.* Earth Planet. Sci. Lett., Vol. 18, pp. 317-323.

Mason-Smith, D.J., 1960 ; *Gravity traverses over kimberlite pipes in Tanganyika.* Unpubl. Report, O.G.S. of G.B., p. 30.

McNae, J.C., 1979 ; *Kimberlites and exploration geophysics.* Geophysics, Vol. 44, pp. 1395-1416.

Meyer, H.O.A. & Boyd, F.R., 1972 ; *Composition and origin of crystalline inclusions in natural diamonds.* Geochim. Cosmochim. Acta., Vol. 36, pp. 1255-1274.

Meyer, H.O.A. & Tsai, H.M., 1976 ; *Mineral inclusion in diamond temperature and pressure of equilibration.* Science, Vol. 181, pp. 849-851.

Miller, P., 1995 ; *Diamonds : commencing the countdown to market renaissance.* Yorkton Securities Inc., Lindsay Ross Publishing Ltd. : London, p. 230.

Mining Journal, 1997 ; *Diamond supplement.* Mining Journal Supplement, Vol. 329, No. 8452, 24 October 1998, p. 15.

Mining Journal, 1998 ; *Diamond supplement.* Mining Journal Supplement, Vol. 331, No. 8505, 6 November 1998, p. 11.

Mining Weekly, 1996 ; *Aussies set to explore Limpopo.* Mining Weekly, Vol. 2, No. 44, pp. 15.

Mining Weekly, 1997a ; *Diamond giant's Angolan surveys nears completion.* Mining Weekly, Vol. 3, No. 34, 5 September 1997, pp. 1.

Mining Weekly, 1997b ; *Debswana Orapa and Letlhakane mines, Botswana.* Mining Weekly, Vol. 3, No. 8, 7 March 1997, pp. 8.

Mining Weekly, 1997c ; *Renewed diamond prospecting along Limpopo River.* Mining Weekly, Vol. 3, No. 31, 15 August 1997, pp. 6.

Mining Weekly, 1997d ; *SA diamond industry on track for this year.* Mining Weekly, Vol. 3, No. 41, 24 October 1997, pp. 10.

Mining Weekly, 1998 ; *Angolan diamond talks open.* Mining Weekly, Vol. 4, No. 5, 13 February 1998, pp. 9.

Mitchell, R.H., 1986 ; *Kimberlites :mineralogy, geochemistry and petrology.* Plenum Press : New York, p. 442.

Mitchell, R.H., 1989 ; *Aspects of the petrology of kimberlites and lamproites : some definitions and distinctions.* In : Kimberlites and related rocks, their composition, occurrence, origin and emplacement. Vol. I, Ross, J. (Ed.). Proceedings of the Fourth International Kimberlite Conference, Perth, 1986, Geol. Soc. of Austr., Spec. Publ., No. 14, pp. 7-45.

Mitchell, R.H., 1991 ; *Kimberlites and lamproites : primary sources of diamond.* Geoscience Canada, Vol. 18, No. 1, pp.1 -16.

Mitchell, R.H., 1994 ; *Suggestions for revisions to the terminology of kimberlites and lamprophyres from a genetic viewpoint.* In : Proceedings of the Sixth Int. Kimberlite Conference. Meyer, H.O.A. & Leonardos, O., (Eds.), Vol. 1, pp. 15-26.

Mitchell, R.H., 1995 ; *Kimberlites, orangeites and related rocks.* Plenum Press : New York, p. 410.

Mitchell, R.H., 1995 ; *The role of petrography and lithogeochemistry in exploration for diamondiferous rocks.* In : Diamond Exploration : Into the 21st Century. Griffin, W.L. (Ed.). J. of Geochem. Explor., Vol. 53, pp. 339-350.

Moore, R.O. & Gurney, J.J., 1985 ; *Pyroxene solid-solution in garnets included in diamonds.* Nature, Vol. 318, pp. 553-555.

Muggeridge, M.T., 1995 ; *Pathfinder sampling techniques for locating primary sources of diamond : recovery of indicator minerals, diamonds and geochemical signatures.* In : Diamond Exploration : Into the 21st Century. Griffin, W.L. (Ed.). J. of Geochem. Explor., Vol. 53, pp. 183-204.

Nixon, P.H., 1973 ; *Lesotho kimberlites.* In : Nixon, P.H. (Ed.), Lesotho National Development Corporation, Cape and Transvaal Printers Ltd., Cape Town : South Africa, pp. 300-312.

Nixon, P.H., 1980 ; *Regional diamond exploration - theory and practice.* In : Kimberlites and diamonds. Glover, J.E. & Groves, D.I. (Eds.). Geol. Dept./Univ. Ext., Univ. of W.A., Publ. No. 5, pp. 65-80.

Nixon, P.H., 1995 ; *The morphology and nature of primary diamondiferous occurrences.* In : Diamond Exploration : Into the 21st Century. Griffin, W.L. (Ed.). J. of Geochem. Explor., Vol. 53, pp. 41-71.

Nixon, P.H., 1995 ; *A review of mantle xenoliths and their role in diamond exploration.* J. of Geodynamics, Vol. 20, No. 4, pp. 305-329.

Nixon, P.H. & Condliffe, E., 1989 ; *Tanzanian kimberlites : a preliminary heavy mineral study.* In : Kimberlites and related rocks, their composition, occurrence, origin and emplacement. Vol. I, Ross, J. (Ed.). Proceedings of the Fourth International Kimberlite Conference, Perth, 1986, Geol. Soc. of Austr., Spec. Publ., No. 14, pp. 407-418.

Oldenziel, C.E., 1997 ; *Financing diamond mines : a review of the risks and parties involved.* Internal Report, ABN-AMRO Bank, Amsterdam : Netherlands, p. 92.

O'Reilly, S., 1985 ; *The mantle environment.* In : Kimberlite occurrence and origin : A basis for conceptual models in exploration. Glover, J.E. & Harris, P.G. (Eds.). Geol. Dept./Univ. Ext., Univ. of W.A., Publ. No. 8, pp. 1-18.

Paterson, N.R., MacFadyen, D.A. & Turkeli, A., 1977 ; *Geophysical exploration for kimberlites with special reference to Lesotho.* Geophysics, Vol. 42, No. 7, pp. 1531.

Peters, W.C., 1978 ; *Exploration and mining geology.* Wiley & Sons : New York, p. 696.

Pretorius, W. & Leahy, K., 1998 ; *Implications for diamond prospectivity from comparisons of diamond-bearing lithosphere in two Proterozoic orogenic belts.* Abstracts, Seventh International Kimberlite Conference, Univ. of Cape Town, pp. 713-715.

Pybus, G.Q.J., Hussey, M.C. and Lipton, P.L., 1998 ; *Spectral investigation of a variety of magnesium-bearing rock types : implications for kimberlite exploration.* Abstracts, Seventh International Kimberlite Conference, Univ. of Cape Town, pp. 717-719.

Reis, B. 1972 ; *Preliminary note on the distribution and tectonic control of kimberlites in Angola.* 24th International Geological Congress, Section 4, pp. 276-281.

Richardson, S.H., Gurney, J.J., Erlank, A.J. & Harris, J.W., 1984 ; *Origin of diamond in old enriched mantle.* Nature, Vol. 310, pp. 198-202.

Richardson, S.H., Erlank, A.J., Harris, J.W. & Hart, S.R., 1990 ; *Eclogitic diamonds of Proterozoic age from Cretaceous kimberlites.* Nature, Vol. 346, pp. 54-56.

Robinson, D.N., 1975 ; *Magnetite-serpentine-calcite dykes at Premier Mine and aspects of their relationship to kimberlite and to carbonatite of alkalic carbonatite complexes.* Physics and Chemistry of the Earth, pp. 61-70.

Robinson, D.N., 1978 ; *The characteristics of natural diamond and their interpretation.* Min. Sci. Eng., Vol. 10, pp. 55-72.

Rolfe, D.G., 1973 ; *The geology of the Kao kimberlite pipes.* Lesotho National Development Corporation, Cape and Transvaal Printers Ltd., Cape Town : South Africa, pp. 101-106.

Rombouts, L., 1995 ; *Sampling and statistical evaluation of diamond deposits.* In : Diamond Exploration : Into the 21st Century. Griffin, W.L. (Ed.). J. of Geochem. Explor., Vol. 53, pp. 351-367.

Scott-Smith, B.H., 1992 ; *Contrasting kimberlites and lamproites.* Explor. Mining Geol., Vol. 1, pp. 371-381.

Scott-Smith, B.H., 1996 ; *Kimberlites.* In : Undersaturated alkaline rocks : mineralogy, petrogenesis and economic potential. Mitchell, R.H. (Ed.). Mineral. Assoc. of Canada, Vol. 24, pp. 217-243.

Scott-Smith, B.H., Skinner, E.M.W. & Loncy, P.E., 1989 ; *The Kapamba lamproites of the Luangwa Valley, eastern Zambia.* In : Kimberlites and related rocks, their composition, occurrence, origin and emplacement. Vol. I, Ross, J. (Ed.). Proceedings of the Fourth International Kimberlite Conference, Perth, 1986, Geol. Soc. of Austr., Spec. Publ., No. 14, pp. 189-205.

Shee, S.R., Bristow, J.W., Bell, D.R., Smith, C.B., Allsopp, H.L. & Shee, P.B., 1989 ; *The petrology of kimberlites, related rocks and associated mantle xenoliths from the Kuruman Province, South Africa.* Geol. Soc. of Austr., Spec. Publ., Vol. 1, No. 14, pp. 60-82.

Sheppard, S.M.F. & Dawson, J.B., 1975 ; *Hydrogen, carbon and oxygen isotope studies of megacryst and matrix minerals from Lesothan and South African kimberlites.* Phys. Chem.of the Earth, Vol. 9, pp. 747-763.

Sichel, H.S., 1952 ; *New methods in the statistical evaluation of mine sampling data.* Trans. Inst. Min. Metall. (London), Vol. 61, pp. 261-288.

Sichel, H.S., 1972 ; *Statistical valuation of diamondiferous deposits.* J. of. S. Afr. Inst. Min. Metall., Vol. 73, pp. 235-243.

Skinner, E.M.W., 1998 ; *The geochemistry of kimberlites.*. M.Sc. Exploration Geology, Course Notes, Rhodes Univ. : Grahamstown, p. 7.

Skinner, E.M.W., 1989 ; *Towards a genetic model for kimberlites.* In : Kimberlites and related rocks, their composition, occurrence, origin and emplacement. Vol. I, Ross, J. (Ed.). Proceedings of the Fourth International Kimberlite Conference, Perth, 1986, Geol. Soc. of Austr., Spec. Publ., No. 14, pp. 528-544.

Skinner, E.M.W. & Clement, C.R., 1979 ; *Mineralogical classification of Southern African kimberlites.* In : Kimberlites, diatremes and diamonds : their geology, petrology and geochemistry. Boyd, F.R. & Meyer, H.O.A. (Eds.), American Geophysical Union : Washington D.C., pp. 129-139.

Skinner, E.M.W., Clement, C.R., Gurney, J.J., Apter, D.B. & Hatton, C.J., 1992 ; *The distribution and tectonic setting of South African kimberlites.* Russ. Geol. Geophys., Vol. 33, pp. 26-31.

Smith, C.B., 1983 ; *Pb, Sr and Nd isotopic evidence for sources of Southern African Cretaceous kimberlites.* Nature, Vol. 304, pp. 51-54.

Smith, C.B., 1985 ; *What is a kimberlite ?* In : Kimberlite occurrence and origin : A basis for conceptual models in exploration. Glover, J.E. & Harris, P.G. (Eds.). Geol. Dept./Univ. Ext., Univ. of W.A., Publ. No. 8, pp. 1-18.

Smith, C.B. & Barton, E.S., 1995 ; *The timing of kimberlite emplacement in Southern Africa.* Geol. Soc. of South Africa, Extended Abstracts, Randse Afrikaanse Univ. : Johannesburg, pp. 107-110.

Smith, C.B., Gurney, J.J., Skinner, E.M.W., Clement, C.R. and Ebrahim, N., 1985 ; *Geochemical character of southern African kimberlites : a new approach based upon isotopic constraints.* Trans. Geol. Soc. S. Afr., Vol. 88, pp. 267-280.

Sobolev, N.V., 1977 ; *Deep-seated inclusions in kimberlites and the problems of the composition of the upper mantle.* Amer. Geophysical Union, Washington, p. 279.

Stocklemayer, V.R., 1981 ; *Diamonds in Zimbabwe.* Annals of the Zimbabwe Geol. Surv., Vol. 6, pp. 27-34.

Sykes, L., 1978 ; *Intraplate seismicity, reactivation of pre-existing zones of weakness, alkaline magmatism, and other tectonism postdating continental fragmentation.* Rev. Geophys. Space Phys., Vol. 16, pp. 621-688.

Till, R., 1974 ; *Statistical methods for the Earth Scientist - an introduction.* The MacMillan Press : London, p. 154.

Towie, N.J. & Seet, L.H., 1995 ; *Diamond laboratory techniques.* In : Diamond Exploration : Into the 21st Century. Griffin, W.L. (Ed.). J. of Geochem. Explor., Vol. 53, pp. 205-212.

Turner, B.R. & Minter, W.E.L., 1985 ; *Diamond-bearing upper Karoo fluvial sediments in NE Swaziland.* Journ. of the Geol. Soc. of London, Vol. 142, pp. 765-776.

Unrug, R., 1996 ; *Geodynamic map of Gondwana Supercontinent assembly.* Publication by the Council for Geoscience, Pretoria.

Wedepohl, K.H. & Muramatsu, Y., 1979 ; *The chemical compositions of kimberlites compared with the average composition of three basaltic magma types.* In : Kimberlites, diatremes and diamonds : their geology, petrology and geochemistry. In : Boyd, F.R. & Meyer, H.O.A. (Eds.), American Geophysical Union : Washington D.C., pp. 300-312.

White, S.H., Boorder, H. & Smith, C.B., 1995 ; *Structural controls of kimberlite and lamproite emplacement.* In : Diamond Exploration : Into the 21st Century. Griffin, W.L. (Ed.). J. of Geochem. Explor., Vol. 53, pp. 245-264.

Zweistra, P., Jarvis, W. & McGeorge, I.B., 1998 ; *The geology of micaceous kimberlite intrusives, Khutse, Botswana.* Abstracts, Seventh International Kimberlite Conference, Univ. of Cape Town, pp. 1037-1038.

APPENDICES

Appendix I ; Diamond descriptions.

1. Crystal state.

(a) Whole (w)

(b) Broken (b)

(c) Chipped (c)

2. Crystal regularity (shape).

(a) Equidimensional (q), e.g. single well developed crystals

(b) Elongated (e), e.g. macles, twins and aggregates

(c) Distorted (d), e.g. distorted single crystals

(d) Flattened (f), e.g. very flat macles

(e) Cleaved (c), e.g. cleaved fragments

(f) Chipped (u), e.g. broken diamonds of unknown (u) shape

3. Crystal morphology (form) and modifiers.

Morphology (form).

(a) Octahedra (o)

(b) Dodecahedra (d)

(c) Hexahedra (h)

(d) Tetrahedra (e)

(e) Cube (c)

(f) Tetrahexahedra (th)

(g) Macle (m)

(h) Fragment (x)

(i) Cleaved fragment (v)

(j) Resorbed (r)

(k) Irregular/complex (i)

(l) Twinned (t)

Modifiers.

(a) Round (r)

(b) Elongate (e)

(c) Flattened (f)

(d) Chipped (c)

(e) Percussed

(f) Abbraided (a)

(g) Frosted (f)

Classification ; e.g. resorbed flat macle (r, f), macle described in (2)

e.g. flattened and chipped octahedron (f, c), octahedron described in (2)

APPENDICES

4. Resorption morphology.

(a) Class 1 ; 1 to 55% preservation (1)

(b) Class 2 ; >55 to 65% preservation (2)

(c) Class 3 ; > 65 to 75% preservation (3)

(d) Class 4 ; > 75 to 85% preservation (4)

(e) Class 5 ; >85 to 95% preservation (5)

(f) Class 6 ; Unknown preservation (6)

Refer to accompanying chart.

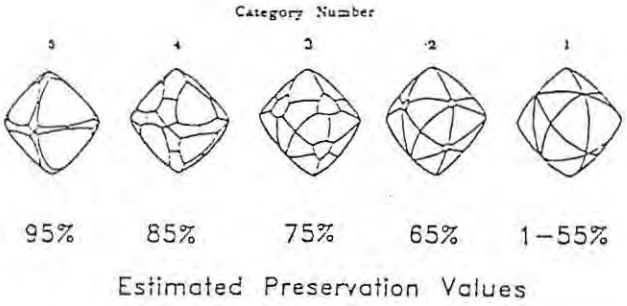

5. Colour.

(a) Colourless (c)

(b) Yellow (y)

(c) Green (g)

(d) Grey (e)

(e) Brown (b)

(f) Black (l)

(g) Amber/orange (a)

(h) Pink/mauve (p)

(i) Blue (h)

(j) Other (o)

APPENDICES

6. Colour intensity.

(a) No colour (0)

(b) Colour visible as a faint hue (1)

(c) Colour is easily visible (2)

(d) Colour is strong (3)

(e) Colour is very strong/opaque (4)

7. Clarity (inclusions).

(a) No inclusions (0)

(b) Inclusions between 0 and 2% (1)

(c) Inclusions between 2 and 5% (2)

(d) Inclusions between 5 and 10% (3)

(e) Inclusions between 10 and 20% (4)

(f) Inclusions between 20 and 30% (5)

(g) Inclusions between 30 and 50% (6)

(h) Inclusions more than 50% (7)

Refer to accompanying chart.

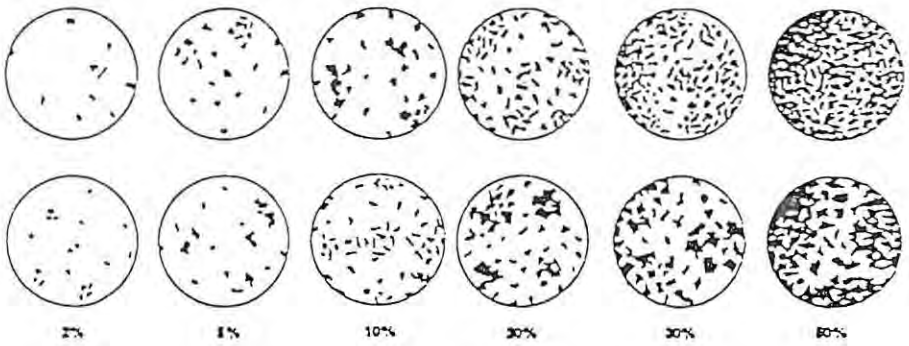

8. Mechanical abrasion.

(a) No abrasion on four-fold axis (A)

(b) Abrasion localised at four-fold axial corners (B)

(c) Abrasion at four-fold axial corners and at the sharpest parts of "A" edges (C)

(d) Continuously abraded "A" edges but with "C" edges intact (D)

(e) Abrasion at "A" and "C" edges (E)

(f) Abrasion has rounded all edges (F).

Appendix I : Diamond descriptions.

Date ;
Farm name ;
X-coordinate ;
Y-coordinate ;
$ / carat ;

Mean size (carats) ;
Diamond size range (carats) ;
Largest diamond (carats) ;

CRYSTAL STATE	CRYSTAL REGULARITY (SHAPE)	CRYSTAL MORPHOLOGY (FORM)	RESORPTION MORPHOLOGY	COLOUR	COLOUR INTENSITY	CLARITY (INCLUSIONS)	ABRASION	COMMENTS

APPENDICES

Appendix II ; Indicator mineral descriptions.

1. Mineral identification.

(a) G10 garnet

(b) G9 garnet

(c) Eclogitic garnet

(d) Megacrystic garnet

(e) Chrome diopside

(f) Olivine

(g) Orthopyroxene

(h) Ilmenite

(i) Chromite

(j) Zircon

(k) Other

2. Colour.

(a) Pink - metamorphic (1)

(b) Pale pink to brown - metamorphic (2)

(c) Brown to orange - metamorphic (3)

(d) Brown - metamorphic (4)

(e) Orange - eclogitic (5)

(f) Dark orange - eclogitic (6)

(g) Red to orange - peridotitic (7)

(h) Purple red to red - peridotitic (8)

(i) Dark purple red - peridotitic/lherzolitic (9)

(j) Purple - peridotitic/lherzolitic (10)

(k) Lilac - peridotitic/harzburgitic (11)

(l) Dark purple/green - peridotitic/alexandritic (12)

3. Crystal state.

(a) Whole (w)

(b) Broken (b), < 50% broken faces with fresh, clean breaks due to fluvial action

(c) Fragments (f), > 50% broken faces

APPENDICES

4. Crystal shape.

(a) Equidimensional (eq)

(b) Elongate (el)

(c) Very angular (va)

(d) Angular (an)

(e) Sub-angular (sa)

(f) Sub-rounded (sr)

(g) Rounded (r)

(h) Very rounded (vr)

5. Crystal form.

(a) Euhedral

(i) Cubic (c)

(ii) Octahedral (o)

(iii) Rhombohedral (r)

(b) Anhedral

(iv) No crystal form (u)

6. Primary surface features.

(a) Kelyphite (k)

(b) Sub-kelyphitic orange peel pitting (opp)

7. Sculptured surface features.

(a) Hillocks (sh)

(b) Etch pits (sep)

(c) Reaction surfaces (sr)

(d) Conchoidal breaks (sc)

(e) Blocky surfaces (sb)

(f) Etch channels (sch)

(g) Sculptured surfaces (ss)

(h) Cavernous surfaces (sca)

8. Chemical decomposition features.

(a) Dislocation features

(i) Trichitic cavities (dct)

(ii) Chattermark trails (dcc)

(iii) Solution pits (dsp)

(iv) Honeycomb texture (dh)

(v) Anastomosing grooves (dag)

APPENDICES

8. Chemical decomposition features. (continued).

(b) Incipient stippling, i.e. tarnishing of conchoidal breaks (cb)

(c) Solution cavities, i.e. fluted surfaces (cc)

(d) Cubic surfaces
- (i) Cubic faces (cf)
- (ii) Smooth, curved botryoidal surfaces (cm)

(e) Cracking (cr)

(f) Etch channels (ce)

(g) Cavernous relief (ca)

(h) Sculpturing due to hydrothermal or dyke activity (ch)

(i) Alteration (cl)

(j) Imbricate wedge marks (ci)

(k) Cockscomb clinopyroxene (cocpx)

(l) Stress fractures (csf)

9. Mechanical abrasion surface features.

(a) Abrasion features
- (i) Pitting (mp)
- (ii) Frosting (mf)

(b) Conchoidal breaks
- (i) Mechanically abraided (ma)
- (ii) Fresh, clean surfaces (mc)

10. % Chemical/Mechanical surface features.

(a) Percentage of chemical to mechanical surface features, e.g. if no mechanical features = 100%

Appendix II : Indicator mineral descriptions.

Date ;
Farm name ;
X-coordinate ;
Y-coordinate ;

SAMPLE NO.	MINERAL IDENTIFICATION	SIZE (mm)	COLOUR	CRYSTAL STATE	CRYSTAL SHAPE	CRYSTAL FORM	PRIMARY SURFACE FEATURES	SCULPTURED SURFACE FEATURES	CHEMICAL DECOMPOSITION SURFACE FEATURES	MECHANICAL ABRASION SURFACE FEATURES	% CHEMICAL/MECHANICAL SURFACE FEATURES	COMMENTS